

THE ROLE OF BIOFILM FORMATION IN SYSTEMIC
MOVEMENT OF *ERWINIA AMYLOVORA* IN APPLE

By

Jessica Koczan

A DISSERTATION

Submitted to
Michigan State University
in partial fulfillment of the requirements
for the degree of

DOCTOR OF PHILSOPHY

Plant Biology

2011

ABSTRACT

THE ROLE OF BIOFILM FORMATION IN SYSTEMIC MOVEMENT OF *ERWINIA AMYLOVORA* IN APPLE

By

Jessica Koczan

Erwinia amylovora is a highly virulent, necrogenic plant pathogen that causes fire blight disease on apple, pear, and other rosaceous plants. The fire blight pathogen is highly invasive and capable of rapid systemic movement through plants. Current methods of control focus on chemical and antibiotic treatments. The popularity of highly susceptible cultivars and the emergence of antibiotic resistance have driven the need to find other methods to control fire blight. The study of pathogen virulence factors has the potential to identify novel control methods.

Several bacterial virulence factors have been shown to be critical for biofilm formation, the production in a complex aggregated network of bacterial cells, exopolysaccharides, and other macromolecules. In addition, vascular plant pathogens commonly use the ability of biofilm formation to aid in the systemic movement of the pathogen. Research presented here used *in silico* analysis to identify several virulence factors. Biofilm formation and virulence assays determined that virulence factors that contribute to the systemic movement of *E. amylovora* in vascular tissue of apple.

The production of exopolysaccharides amylovoran and levan was determined to be needed for the formation of a mature biofilm. Though cells are motile, amylovoran deficient mutants are unable to move past the site of inoculation. Levan deficient mutants display a

delayed, reduced virulence phenotype. Several putative bacterial surface proteins, or attachment structures, assist in the initial attachment (both reversible and irreversible) of the pathogen to host tissue. Deletions in genes encoding for the production of attachment structures drastically reduce the biofilm capability of *E. amylovora*, and the ability to get into the xylem tissue. In addition, mutation of functional flagellar motor stators demonstrated that motility was important in mediating contact of bacterial cells to surfaces. Motility of the fire blight pathogen is shown to be important in the movement of bacterial cells within host tissue. Additionally, motility seems to be important in the expansion of biofilms. In total, the contribution of the virulence factors to biofilm formation and the localization of the pathogen in host tissue imply that biofilm formation assists in the systemic movement of *E. amylovora* in apple.

DEDICATION

Dad. Love you, miss you. I know you will always be looking over my shoulder.

AKNOWLEDGEMENTS

First and foremost I would like to thank my mom for her unwavering love and support. I also could not have had a better advisor- thanks George. Additionally, I would like to thank everyone who has helped me through including the help of my committee members and my family and friends. And of course, I thank my undergrad, Bryan Lenneman, whose counting of single cells attached to the coverslips helped tremendously.

TABLE OF CONTENTS

List of Tables.....	vii
---------------------	-----

List of Figures.....	ix
----------------------	----

Chapter 1: Literature Review.....	1
I. Contributing factors to the virulence of <i>Erwinia amylovora</i>	1
A. Type II secretion system.....	3
B. Type III secretion system.....	5
C. Exopolysaccharides.....	6
i. Amylovoran.....	6
ii. Levan.....	7
D. Motility.....	8
E. Attachment to surfaces.....	9
II. Disease stages of fire blight.....	10
A. Blossom blight.....	10
B. Shoot blight.....	11
C. Asymptomatic disease progression.....	12
III. Current control of disease.....	12
IV. Identification of host defenses and the ability of the pathogen to overcome them.	14
A. Anatomical defense.....	14
B. Host recognition responses.....	16
i. ROS response.....	16
ii. Production of agglutination factor.....	17
iii. Phytoalexin production.....	18
iv. Activation of defense associated genes.....	18
V. Systemic movement of <i>Erwinia amylovora</i> within the host.....	19
VI. Rationale and project goals.....	21
Figures.....	24
Literature cited.....	30

Chapter 2: The contribution of <i>Erwinia amylovora</i> exopolysaccharides amylovoran and levan to biofilm formation: implications in pathogenicity.....	40
Abstract.....	40
Introduction.....	41
Materials and Methods.....	44
Results.....	49
Discussion.....	53
Tables.....	57
Figures.....	59

Literature Cited.....	67
Chapter 3: Cell surface attachment structures contribute to biofilm formation and xylem colonization of <i>Erwinia amylovora</i>	71
Abstract.....	71
Introduction.....	72
Materials and Methods.....	74
Results.....	78
Discussion.....	81
Tables.....	86
Figures.....	92
Literature Cited.....	101
Chapter 4: Deletion of <i>Erwinia amylovora</i> flagellar motor protein genes alters biofilm formation and virulence in apple	105
Abstract.....	105
Introduction.....	106
Materials and Methods.....	109
Results.....	114
Discussion.....	118
Tables.....	122
Figures.....	127
Literature Cited.....	137
Chapter 5: Conclusions and Future Directions	140
Summary of Work.....	140
Questions for the Future.....	144
Literature cited.....	148
Appendix 1: Investigating mechanisms of fire blight control by prohexadione-calcium	151
Abstract.....	151
Introduction.....	153
Materials and Methods.....	155
Results.....	159
Discussion.....	161
Tables.....	165
Figures.....	167
Literature Cited.....	175

List of Tables

Table 2-1. Bacterial strains, plasmids and primers used in chapter 2.....	57
Table 3-1. Deletion mutants constructed in chapter 3, sequence ID of the respective genes, and putative structure targeted for deletion.....	86
Table 3-2. Plasmids and oligonucleotide primers used in mutagenesis and complementation.....	87
Table 3-3. Time course assay measuring attachment of cells at 2, 4, 6, 8, 16, 24 h to glass coverslips.....	90
Table 3-4. Percent lesion size on immature pear fruit inoculated with <i>E. amylovora</i> Ea1189 or various attachment mutants at 4, 6 and 8 days post inoculation.....	91
Table 4-1. Bacterial strains used in chapter 4.....	122
Table 4-2. Plasmids and primers used in chapter 4.....	123
Table 4-3. Swarming motility of <i>Erwinia amylovora</i> on 0.3% minimal agar medium, 0.3% minimal agar medium plus NaCl, and 0.3% minimal agar medium plus sucrose.....	125
Table 4-4. Attachment of cells to glass coverslips in the presence of Ficoll to limit bacterial motility.....	126
Table A-1. Effect of prohexadione-calcium and paclobutrazol on the width of cell walls widths of the mid-vein cortical parenchyma tissue of apple cv ‘Gala’.....	165

List of Figures

Figure 1-1. Select virulence factors of <i>Erwinia amylovora</i>	24
Figure 1-2. Scanning electron microscope image of the stigmatic surface of apple flower.....	25
Figure 1-3. Cross-section depicting cellular structure of a pear leaf.....	27
Figure 1-4. Biofilm formation process.....	28
Figure 2-1. Symptoms of <i>E. amylovora</i> Ea1189, Ea1189 Δ <i>ams</i> , and Ea1189 Δ <i>lsc</i> in immature pear at seven days post-inoculation.....	59
Figure 2-2. Quantification of the effect of growth medium on biofilm growth on glass by <i>E. amylovora</i> Ea1189.....	60
Figure 2-3. Attachment and aggregation of <i>E. amylovora</i> Ea1189, Ea1189 Δ <i>ams</i> and Ea1189 Δ <i>lsc</i> to glass after 16h.....	61
Figure 2-4. Quantification of biofilm formation of Ea1189, Ea1189 Δ <i>ams</i> , Ea1189 Δ <i>lsc</i> , and Ea1189 Δ <i>lsc</i> /pJMK1 in 0.5x LB after 48 h.....	62
Figure 2-5. Three-dimensional view of flow cell contents through intensity mapping after 24 h growth.....	63
Figure 2-6. Biofilm formation <i>in planta</i> by <i>E. amylovora</i> Ea1189 seven days post-inoculation of 2×10^8 cfu per ml using scissor cut method.....	64
Figure 2-7. Visualization of <i>E. amylovora</i> of <i>ams</i> , <i>lsc</i> deficient mutants in apple shoots..	65
Figure 3-1. Gene maps of genes deleted in this chapter.....	92
Figure 3-2. Images of putative attachment structures of <i>E. amylovora</i>	93

Figure 3-3. Biofilm formation of <i>E. amylovora</i>	95
Figure 3-4. Flow cell imaging after 48 h growth measuring aggregates as brightness in fluorescence, where higher intensity equals larger aggregates.....	96
Figure 3-5. Measurement of necrosis progression in Gala apple tissue at 3 and 7 days post inoculation.....	97
Figure 3-6. Bacterial populations in immature pear fruit over 3 days.....	98
Figure 3-7. SEM images of Ea1189 and a representative deficient mutant in putative attachment structures in xylem and mesophyll tissue of apple.....	99
Figure 4-1. Sequence comparison of <i>E. amylovora motA</i> genes with <i>E. coli</i> , <i>Y. pestis</i> , <i>P. syringae</i> and <i>motB</i> genes of <i>E. amylovora</i> with <i>E. coli</i> , <i>Y. pestis</i> , <i>P. syringae</i>	127
Figure 4-2. Biofilm quantification of flagellar stator mutants.....	129
Figure 4-3. Biofilm quantification of complemented flagellar stator mutants.....	130
Figure 4-4. Brightfield imaging of biofilm formation of flagellar motor stator mutants on glass coverslips.....	131
Figure 4-5. Three-dimensional view of flow-cell contents through intensity mapping after 48 h of growth.....	132
Figure 4-6. Immature pear fruit assay examining virulence of flagellar motor stator mutants at 4 days post inoculation and 8 days post inoculation.....	134
Figure 4-7. Disease progression of Ea1189 and flagellar stator mutants in apple, 3 and 7 dpi.....	135

Figure A-1. Disease incidence on non-treated apple shoots, and shoots treated with prohexadione-Ca, or paclobutrazol..... 167

Figure A-2. Disease severity (with S.E.) on non-treated apple shoots, and shoots treated with prohexadione-Ca, or paclobutrazol..... 168

Figure A-3. Conditional severity (with S.E.) on non-treated apple shoots, and shoots treated with prohexadione-Ca, or paclobutrazol..... 169

Figure A-4. Mean log (x+1) CFU/shoot (with S.E.) on non-treated apple shoots, and shoots treated with prohexadione-Ca or paclobutrazol at 0 d (initial inoculation), and 28 d after inoculation with the virulent strain *Erwinia amylovora* Ea 110 using the scissor dip method 170

Figure A-5. Mean log CFU/g in shoots of cv. ‘McIntosh’ treated with high doses of ProCa (250 mg/l Apogee®), low doses of ProCa (125 mg/l Apogee® applied twice), or shoots left untreated after inoculation with the virulent strain *Erwinia amylovora* Ea 110..... 171

Figure A-6. Apple mid-vein tissue 2 cm from the leaf tip of the 2nd newest unfolded leaves, 13 d after treatment with ProCa, paclobutrazol, or trees left untreated..... 172

Chapter 1: Literature Review

Apple (*Malus x domestica*), is both a popular and agriculturally important crop. Fire blight, caused by the plant pathogen *Erwinia amylovora*, is a common and devastating disease on apple, pear and other pome fruits, and affects crops globally. *E. amylovora* was first determined to be a plant pathogen in the 1880s; however, records of disease can be traced to 1780 in the Hudson valley in the Eastern United States (1). Despite a lengthy history, fire blight is still one of the most prominent diseases on apple worldwide (58). In the southwest growing region of Michigan, in the year 2000, fire blight was responsible for the loss of over four hundred thousand trees (77). Outside the United States, *E. amylovora* has been given quarantine status and poses significant problems in Europe and Asia (100).

Fire blight is recognized by wilting of tissue, necrosis, as well as exudates of ooze from tissue. *E. amylovora* is a vascular invading plant pathogen that is capable of rapid systemic movement within the xylem tissue (11). The pathogen is currently managed through the use of chemical control programs, including the use of antibiotics and copper; however, the emergence of antibiotic resistance has highlighted a need for alternate control methods (77,104). In addition, because current fire blight control programs center on controlling flower infections, if the pathogen can make it to the vascular tissue or inoculum is present when damaging storms occur, there are no means of control for the systemic movement of *E. amylovora* (77).

Identification of host defenses differentially altered in response by the pathogen between resistant and susceptible apple cultivars has been largely unsuccessful (71, 114). These results have steered the majority of fire blight research towards understanding how the pathogen causes disease. Researchers working with closely related bacterial species, such as *Erwinia*

chrysanthemi, have used genetic analysis of virulence factors to design novel control strategies (100). Thus, the understanding of virulence mechanisms of *E. amylovora* may lead to not only the discovery of novel controls but improved design of current control measures. In that hope, a large number of important virulence factors of *E. amylovora* have been identified through a variety of techniques (22, 23, 39, 73, 102, 119). The main purpose of this chapter is to review current knowledge on the systemic movement of *E. amylovora* in apple. However, the systemic movement of *E. amylovora* is largely understudied. Thus, I will address current knowledge on the disease process, host defenses, and the identity and proposed function of several virulence factors, all of which are potentially involved in the systemic movement of *E. amylovora*.

I. Contributing factors to the virulence of *E. amylovora*.

E. amylovora, a Gram negative, rod shaped bacterium, is a member of the Enterobacteriaceae family, which includes the animal pathogens *Escherichia coli* and *Yersinia pestis*, and plant pathogens *Pantoea stewartii*, and *Dickeya dadantii*. The biology of the fire blight pathogen is defined by the virulence factors that are present (Fig. 1-1). Physiological, biochemical and serological studies performed throughout the 1970's and 1980's first identified basic characteristics associated with pathogen virulence, including the production of exopolysaccharides (EPS) (53), and bacterial motility (86). The advent of genetic techniques led to transposon mutagenesis studies, which identified the pathogenicity factors of *E. amylovora*: the EPS amylovoran, the hrp region, and DspA/E (4, 8, 102). Additional transposon mutagenesis studies identified several virulence genes involved in lipopolysaccharide (LPS) production (107) and the production of an additional EPS, levan (46). Over time, development of new screening techniques has led to a long list of additional factors that contribute to the virulence of *E. amylovora* including penicillin-binding proteins, multidrug efflux pumps, autoinducers, and a

siderophore (22, 23, 33, 39, 73, 119). Despite the extensive research put into identifying virulence factors, functional characterization is limited to only that of the pathogenicity factors amylovoran and DspA/E. This may be due to redundant functionality of factors, or virulence factors may act in an additive fashion, similar to the factors in *Xanthomonas oryzae* (84).

Despite a lack of functional characterization, virulence factors can give insight into the lifestyle of the pathogen. For example, a pathogen that utilizes the type II secretion system promotes damage in the host tissue cells, not only providing nutrients but also aiding the expansion of colonization (27). The use of the type III secretion system can be more subtle, but often functions in inhibiting host defenses (45). Other virulence factors such as polysaccharides often contribute to cell structure (LPS) and in protecting the bacterium from the environment (EPS) (34). Recent studies have determined that the role of polysaccharides has multiple functions in the pathogenicity process (34). Bacterial motility has also been determined to be essential in the colonization of surfaces and bacterial surface structures involved in motility have been shown to be important in attachment of cells to surfaces, as well as the development of biofilms, an aggregated network of EPS, bacterial cells, and other macromolecules (47). The ability to use the suite of virulence factors in vascular systemic movement is one of the factors that allows *E. amylovora* to be so devastating. Thus insight into movement of the pathogen will assist in future control.

I A. Type II Secretion System. The type II secretion system is important in the virulence of several plant pathogens including *X. fastidiosa* (25), *X. oryzae* (83), *E. carotovora* (92), and *D. dadantii* (28). Machinery spanning across the cell membranes (Fig. 1-2) is similar to that of the type IV pilus, and consists of at least 12 core components, including pseudopilins (28, 92). The system secretes proteins or extracellular enzymes, such as polygalacturonases, endoglucanases,

cellulases, and proteases, which are involved in the breakdown of cellular material (56). The type II secretion system is often controlled by quorum-sensing or by the environment (92).

Early transposon mutagenesis studies determined that unlike other *Erwinia* species, *E. amylovora* does not use cell wall degrading enzymes to aid in pathogenicity by the breakdown of tissue (95). Though this early work suggests an absence of the type II secretion system, Riekki and others (87) demonstrated that *E. amylovora* encodes for type II secretion machinery, including a functional *celA* gene. More recently, a study examining genes induced during infection of immature pear fruit also identified several genes encoding for, and secreted by, the type II secretion system (119). Though deletion of one of those genes only had a slight effect on virulence (119), the effect of the secreted enzymes could be additive. Similarly, deletion of individual type II secreted proteins of *X. oryzae* does not alter virulence, but multiple deletions results in much greater reductions in virulence (84). *D. dadantii* also produces multiple factors deemed essential for virulence, though changes in virulence are seen when genes encoding multiple virulence factors have been deleted (94).

Secreted proteins are virulence factors that function in the break down tissue; however the role these enzymes play in the disease process is mainly speculative (92). Proposed functions include combating host defenses, provision of nutrients, or the establishment on a surface (92). *X. fastidiosa* secretes enzymes that are suspected to degrade pit membranes, aiding in the movement of the pathogen through xylem vessels (25). Interestingly, further studies into the function for the type II secretion system in *P. aeruginosa* suggests type II secretion pseudopilins have an additional role in the adherence of bacterial cells and an increased ability to form biofilms (56). Though functionality of type II secretion proteins from *E. amylovora* has yet to be

defined, these proteins could assist in the systemic movement of the pathogen through degradation of vascular elements or the adherence of cells.

I B. Type III secretion system. The type III secretion system, spanning both membranes of a bacterial cell (Fig. 1-1), is important in the secretion of effector proteins into intercellular space of host tissue and can be found in enteric and gram negative plant pathogenic bacteria (30, 45, 79). The system is generated by an island that encodes genes that assemble the type III, or Hrp secretion system (30). Pathogens use the system to deliver effector proteins into the host to suppress host defense responses (45).

Early transposon mutagenesis screens in *E. amylovora* identified mutants in the Hrp island as nonpathogenic and no longer able to elicit a hypersensitive response (HR) (79, 102). Biochemical studies identified a limited number of proteins that are secreted by the type III secretion system including the effector protein DspA/E (17). *dspA/E* has been shown to be homologous to *avrE*, whose secretion in *P. syringae* suppresses papilla formation of the host (12, 45). When expressed *in planta*, DspA/E suppresses salicylic acid-mediated cell wall defenses, including callose deposition, and induces necrotic cell death (17, 32). Interestingly, DspA/E is thought to function within the intercellular space of a plant cell (17); however, *E. amylovora* is a vascular invading pathogen, residing primarily in the xylem tissue. It is plausible that DspA/E could function in the movement of *E. amylovora* to the vascular tissue. Additional studies have shown that DspA/E also plays a role in the induction of reactive oxygen species (ROS) *in planta* (112). Induction of ROS has the potential for damaging host tissue, including that of bundle sheath (60), suggesting additional function in the movement of *E. amylovora*.

I C. Exopolysaccharides. Characteristic signs of fire blight include wilted tissue, necrosis, and ooze. Wilted shoots are thought to be a product of vascular tissue clogged with bacterial cells and EPS (68). EPS, which forms a loose capsule around bacterial cells (Fig. 1-1), is a determinant that often contributes to disease in several enteric pathogens (2, 28, 68). There are many roles for EPS including protection of the bacterium from desiccation and rapid changes in environment, adherence to surfaces, and biofilm formation (34, 68). In the 1970's, work in the Goodman and Beer labs determined EPS to be one of the underlying causes of wilt due to *E. amylovora* (42, 98). *E. amylovora* produced a material, initially described as the toxin amylovorin, which caused wilt symptoms in host, but not in nonhost plants (42). Later the toxin was identified as amylovoran, an EPS. Additional transposon mutagenesis studies identified the EPS levan, as a virulence factor, and an unnamed low molecular weight EPS (40).

i. Amylovoran. Amylovoran is a heteropolymer comprised of a branched repeating unit consisting of galactose, glucose, and pyruvate residues (75). Genes encoding the biosynthesis of amylovoran are contained within a 12-gene operon on the *E. amylovora* chromosome (21). Deletion and insertion mutants of critical genes of the operon result in a loss of pathogenicity (8, 120). In plant tissue, bacterial populations are low in concentration, and some single gene deletions cause slight increases in population size (72). In addition, the quantity of amylovoran produced by individual *E. amylovora* strains is correlated with the degree of virulence, with weak producers exhibiting reduced virulence (2). Coinoculation with other avirulent mutants can restore pathogenicity, and cells that lack EPS gain EPS sloughed off from EPS positive cells (7, 81).

The role of amylovoran in causing wilt symptoms was examined by Sjulín and Beer (98) and found to be associated with restriction of water movement through physical blockage of

vascular element. However, the Goodman group later argued that EPS has additional roles in disease, including a possible role in interaction with the host xylem tissue (43, 97). The EPS of *E. amylovora* has also been shown to aid in the survival of the bacteria when exposed to reactive oxygen species *in vitro* (61). Despite the implications for multiple roles for amylovoran, the actual function in pathogenicity for amylovoran has yet to be determined.

Interestingly, the genes encoding for the biosynthesis of amylovoran from *E. amylovora* share a high sequence identity with the genes encoding for the biosynthesis of stewartan from the pathogen *P. stewartii* (29). In addition, cross complementation experiments demonstrated that amylovoran can replace stewartan in *P. stewartii*; however when complementing amylovoran, stewartan is not enough to restore disease to wild type levels, yet disease symptoms can be seen, suggesting partial restoration of function (9). Stewartan has not only been suggested to function in the movement of *P. stewartii* through the rupturing of pit membranes in the xylem tissue (34), but it also has been shown to be an important factor in biofilm formation, which ultimately aids in the colonization and pathogenicity of the pathogen through the vascular tissue (63). High sequence identity and partial restoration of function suggests that amylovoran may function in a similar manner.

ii. Levan. Bacteria often have the ability to produce more than one EPS; however, few secrete two or more EPSs at the same time (35). Nonetheless, *E. amylovora* produces two other EPSs: levan, a homopolymer of fructose residues that is produced following the breakdown of sucrose (46), and an uncharacterized low molecular weight glucan (21). Levan production is controlled by the *lsc* gene encoding the levansucrase enzyme which breaks down sucrose into levan and glucose (46). The low viscosity nature of levan suggests it is highly branched, with properties similar to levan in *P. syringae* (34). The low molecular weight glucan was determined to be

branched with D-glucose residues; however, little is known about this EPS, including its role in virulence, though the glucan is speculated to function in stabilizing the cell structure of *E. amylovora* (21, 99).

Due to an excess of sucrose on floral surfaces, it is speculated that levan functions in the protection of bacteria on the floral surface, as well as altering the floral environment through the reduction of available sucrose (34, 46). It was believed that levan functions primarily on the flower due to a lack of available sucrose *in planta* (34); however, levan has been shown to contribute to virulence and aid in the spread of bacterial cells within the host (14, 46). In addition, sucrose has been demonstrated to not only be produced by photosynthesis, but also be essential in transport of carbohydrates within plants (51). The limited availability of sucrose in the xylem would suggest that levan is not always produced; however, when sucrose is present, levan assists in the spread and ultimately systemic movement of the pathogen.

I D. Motility. Bacteria capable of motility have increased survival and growth, and motility has been demonstrated to be an integral component in the virulence of both closely related enteric (38) and vascular plant pathogens (25, 106). For example, the vascular plant pathogen *Ralstonia solanacearum* requires flagellar driven motility for early colonization of tomato (106). *X. fastidiosa* requires functional pili to aid in movement through the vascular tissue in grape (25). Like many enteric pathogens, motility of *E. amylovora* is driven by temperature and pH dependent peritrichous flagella (Fig. 1-1) (86). Early research demonstrated motility to be required for blossom colonization (5). It was also established that bacterial growth and motility are inversely related (86). In that same study, bacteria cells are nonmotile *in planta*, leading to the conclusion that flagellar driven motility is essential for blossom colonization, but not colonization of the host. Additionally, nonmotile strains can be injected directly into shoots and

disease progresses similar to that of the wild type (5, 24). In contrast, more recent work examining the relationship between motility and virulence demonstrated that elevated swarming motility positively correlated with severity of virulence of *E. amylovora* (115). Virulence studies also demonstrated *E. amylovora* needs motility to enter uninjured tissue (19), further indicating the importance of motility in virulence in apple.

In response to environmental changes, bacterial cells can switch from motile to nonmotile lifestyles, often by way of extracellular or cell-to-cell signals (38). Signals can be sensed through two-component regulatory systems (38). A recent study examining two-component systems of *E. amylovora* identified multiple flagellar regulators (83). An additional study demonstrated a link between the two-component systems and motility (121). *E. amylovora* cells arrested in motility *in planta* can have motility restored; inoculated shoots were immersed in water, after which motile cells emerged from tissue (5). These results further indicate that motility may be multifunctional throughout the pathogenicity process.

I E. Attachment to surfaces. Bacterial attachment is known to facilitate the disease process, both in the initial colonization as well as expansion (88). Cells adhere to a surface either through specific attachment structures such as pili or fimbriae, or by a complex matrix of EPS, proteins and DNA (86). Attachment structures have been thoroughly examined in model pathogens such as *E. coli* and *P. aeruginosa*; however, structures have been shown to be important in the virulence of *X. fastidiosa* (37) and *R. solanacearum* (59). In addition, the type I fimbriae function in the attachment of *E. rhapontici* to rhubarb plant tissue (62), as well as in the *E. herbicola*-cassava interaction (88). Attachment of *E. amylovora* to floral surfaces has been shown to be important in initial colonization of the pathogen (58). Competition from other bacteria such as *E. herbicola* restricts pathogen growth and incidence of disease on the blossom (49, 57). Despite

the importance of attachment in the pathogenicity process, besides the role in virulence on floral tissue, the role of attachment for *E. amylovora* is largely unknown. One of the main functions of attachment is to prevent cells from being removed from a surface (88). The cells within the environment of the xylem are exposed to regular washing of xylem fluids. Thus, attachment of cells would seem to be important in the colonization of xylem tissue, and may aid in the systemic movement of *E. amylovora*.

II. Disease stages of fire blight.

II A. Blossom blight. The fleeting life of floral tissue has made the study of blossom blight challenging. Researchers have found ways around these challenges because flowers are central to controlling the disease cycle of *E. amylovora*. Epiphytic populations of *E. amylovora* develop on floral tissue (108), and are subsequently spread by pollinating insects and rain (77). In addition, the co-occurrence of floral tissue and ideal growing conditions favor a lifestyle preferable for *E. amylovora* (58). However, the presence of epiphytic populations is not enough to cause disease, the fire blight pathogen has to also progress into the tissue (108).

Once *E. amylovora* attaches to the surface of the stigma within the floral tissue, epiphytic growth greatly increases pathogen population size (Fig. 1-2) (108). To maintain a large population the stigma provides nutrients to the pathogen. In addition, surface structures on the stigma, termed papillae (Fig. 1-2), provide protection for bacterial cells against environmental stress (49). The mechanism of the switch from an epiphytic life to a pathogenic lifestyle is unknown, though it could result from bacterial population size, weather conditions, changes in nutrient availability, or floral age. Currently, the thought is that rain facilitates the migration of *E. amylovora* down the stigma of pear to the hypanthium (nectary) (101). Once at the nectary,

bacteria are thought to gain entrance into the host through nectarthodes (20, 101). However, this method of entry cannot be universal for fire blight infection. The anatomy of the apple blossom, though similar to pear in most accounts, does not allow for easy access to the nectarthodes, due to positioning, excess hair, and a ring of stamens (53, 108). Thus, it is also probable that *E. amylovora* is able to enter apple through the stigmatic walls, which tend to be thin celled walls with little or no cuticle, and ruptured papillae (53, 117). This hypothesis is supported by the presence of large populations within the papillae of the stigma (117). Once infection sets in, the blossom displays characteristic symptoms of fire blight: discolored, dehydrated tissue and ooze. Populations grow and press out of the tissue, where they can provide further inoculum for additional infection. Once the pathogen gains entry to nectary tissue, populations should be able to migrate into the vascular tissue.

II B. Shoot blight. Besides entry into the plant through the blossoms, *E. amylovora* enters through wounds in damaged leaves (31). Early summer storms often include wind and hail, which can damage young leaf tissue. This can lead to disease epidemics if populations of epiphytic *E. amylovora* are present (110). The progression of bacteria from the wound to the xylem, or from the blossom to the xylem, is largely unknown. It is assumed that several virulence factors assist in the progression of the cells to the vascular tissue, where *E. amylovora* is known to colonize and develop into shoot blight (103).

Commonly, shoot blight manifests itself as wilted, necrotic tissue, often forming the shape of a shepherd's crook. Exudates of ooze also emerge from tissue. Wilt is presumed to be a product of clogged vascular tissue due to increases in populations of bacteria, as well as exopolysaccharides (34). In Pierce's disease, which is caused by *Xylella fastidiosa*, similar shoot blight symptoms are seen (25). Though entry of the pathogen is altered (*X. fastidiosa* is vectored

directly into xylem vessels), it is presumed that both pathogens act once inside similar fashion within the tissue. Chatterjee and others (25) concluded that wilt in grape is due to water stress caused by blocked xylem vessels, presumably because they are full of bacteria and bacterial by-products. In apple, shoot blight can lead to internal spread of bacteria to other tissue, including the rootstock. New cankers, or overwintering structures, can form and provide a site for survival of the pathogen for the next growing season (77). Alternatively, if shoot infection is severe enough it can lead to the death of a tree.

II C. Asymptomatic disease progression. In a few cases, *E. amylovora* is able to progress in tissue asymptotically (110). Typically, symptomless infection is present in less susceptible cultivars (11). It is hypothesized that in such cases, *E. amylovora* is unable to escape xylem vessels, thus not allowing for a sufficient population to give rise to disease symptoms (11, 110). Studies examining asymptomatic colonization of grape with *X. fastidiosa* have concluded that asymptomatic tissue has small populations of bacteria compared to symptomatic tissue (25). However, smaller populations of bacteria within asymptomatic grape increased over time, giving rise to blocked tissue and ultimately diseased tissue (25). In apple, *E. amylovora* can be recovered from symptomless tissue up to a year after inoculation, but only in small populations (11).

III. Current control of disease

Fire blight is a serious global threat to pome fruit crops every year. In countries outside of the United States, control is extremely restricted: no genetically modified crops and low use of antibiotics are required (77). Control of the disease is dependent on the region, due in part to differing weather conditions, as well as the robustness of bacterial strains, and governmental

regulation on chemicals (58, 77). In Michigan, current management of fire blight is limited to cultural practices, the use of resistant trees, and chemical controls, mostly applied during bloom. Computational prediction models are effective and widely used in determining when to apply the chemical controls (58). However, erratic weather can result in epidemics of disease. Additionally, false positive predictions can cause the application of chemicals when they are not needed (58). The use of biocontrols, or other living organisms to control growth of *E. amylovora*, is a popular control method in the Western U.S., as well as in Europe. Biocontrol species can compete for growth on floral surfaces or suppress the growth of *E. amylovora* (58). However, this method is ineffective in the Eastern U.S. due to inconsistencies in growth of the biocontrol agent on the blossoms and unpredictable weather (57, 104).

Control of fire blight, once the pathogen has progressed past floral tissue, is very limited. However, an emerging area of research has focused on increasing host defenses to induce host resistance (77). Most of these studies have focused on the introduction of transgenes: natural breeding techniques are not feasible because apple is diploid, self-incompatible, and has a generation time of 4-8 years (96). The introduction of the transgene *attacin E* from *Hyalophora cecropia* pupae resulted in stable expression over a 12 year period, along with increased resistance to fire blight in the field (16). However, consumer acceptance is low for fruit produced using transgenic technology. Other methods of inducing host resistance include the use of growth retardants such as Apogee®, which reduces shoot growth by inhibiting gibberellin biosynthesis (77). This chemical has promise as a control; when applied, fire blight incidence and severity is reduced. This chemical is not a bactericide but causes reduced host vigor (77). However, Apogee® must be applied often, treatment is expensive, and control is not always effective, so the benefits do not always outweigh the costs (77). Currently, the use of chemical

controls, such as antibiotics and copper products, is the most effective and popular way to manage fire blight in the eastern United States. However, the emergence of antibiotic resistance and the lack of new chemistries on the market have led to the need for novel control methods (70, 77).

IV. Identification of host defenses and the ability of the pathogen to overcome them.

Host defense mechanisms in apple that result in more resistant cultivars are largely unknown. Even with the recent sequencing of the apple genome (111), the majority of host defenses were identified through the examination of virulence factors of *E. amylovora*. This has led to a bias towards host responses that *E. amylovora* is able to overcome. Fire blight infection has been shown to elicit several host defense responses, including the production of an HR (114), phytoalexins (23), reactive oxygen species (ROS) (61), and induction of pathogenesis related (PR)- proteins (114). Further studies focusing on the role of genetics in apple defense identified additional *PR* genes (69) and putative resistance genes that interact with DspA/E (71). Induced host responses are often manipulated by the pathogen and do not provide sufficient disease control. However, the presence of more resistant varieties of trees suggests additional plant defense responses including the presence of anatomical barriers. The lack of identified host responses emphasizes the importance of knowing how *E. amylovora* is able to move systematically to and within the vascular tissue in susceptible cultivars, so that resistance mechanisms in other cultivars can be identified.

IV A. Anatomical defense. Despite the importance of anatomical defense, little is known about the anatomy of apple. Nonetheless, *E. amylovora* faces several anatomical barriers which potentially could function in preventing the invasion of the pathogen throughout the different

types of tissue it encounters, from the surface of floral or leaf tissue to the inside of xylem tissue (Fig. 1.3). Logically, there are only two ways past a physical barrier: through or around. Because *E. amylovora* does not produce sufficient amounts of cell wall degrading enzymes (95), it would seem that both on the surface of tissue and inside xylem tissue, the pathogen must either enter through natural openings or go around the physical barriers.

It is well documented that on the surface of floral tissue, *E. amylovora* enters through nectarthodes or wounded tissue (53); however, the mechanisms or process of progression of the pathogen to and through the xylem tissue is unknown. Unless directly loaded into the xylem tissue via insect vector, such as the pathogen *X. fastidiosa*, vascular invading bacteria must cross several barriers to enter the xylem tissue (Fig. 1-3). Presumably, once the pathogen is in the intercellular space surrounding the mesophyll tissue, there would be no physical barriers inhibiting the spread and growth of *E. amylovora* within intercellular space. Similar growth after entry of water pores can be seen in rice by the vascular plant pathogen *X. oryzae* pv. *oryzae* (118). However, bacterial cells encounter more barriers in the passage from the intercellular space into either the mesophyll or bundle sheath tissue, which protects the vascular tissue (Fig. 1-3). If entrance occurs through the mesophyll tissue, bacterial cells then have access through the plasmodesmata into the bundle sheaths, which are connected to the xylem vessels (36). Alternatively, *E. amylovora* could enter the vascular tissue through the smallest veins, which are situated within the intercellular spaces of leaf tissue, and are not surrounded by protective bundle sheath or bundle sheath extensions (36). Ultimately, once *E. amylovora* is in xylem tissue, the pathogen still encounters physical barriers that can impede progression from cell-to-cell, including that of pit membranes (36). However, there may be a compensation for the difficulty

for localization to the vascular system: presumably bacterial cells within the xylem have limited exposure to other host defenses (13).

Currently, it is unknown if anatomical defense plays a role in halting the systemic movement of the pathogen. Few studies have examined the anatomy of apple, probably due to the challenges of working with tree tissue. However, recent work with Apogee® the shoot growth regulator, suggests that anatomy has a role in restricting movement through new tissue (77). An alternate study examining host tissue alterations, demonstrates that 48 hours post inoculation a thickening next to the xylem cell wall occurs (78).

IV B. Host recognition responses

i. ROS response. A typical response of plants after exposure to bacteria is a rapid release a of reactive oxygen species (ROS). This response is has been shown to have multiple effects: it has antimicrobial properties (113) and is often associated with the resistance signaling pathway leading to the hypersensitive response (HR) (50). The HR response is a localized programmed cell death that causes dying tissue to rapidly become dehydrated, which in turn limits the supply of nutrients to a pathogen (44). In addition, the ROS has also been demonstrated to be involved in the activation of pathogenesis related (PR) genes (114), promotion of electrolyte leakage (113), and is a substrate for the reinforcement of cell walls (66).

The process of ROS production in response to bacterial exposure has been well studied using the *P. syringae* model system (109). In short, immediately following bacterial exposure, the host produces a nonspecific, short-lived ROS burst, or oxidative burst (109). This short burst produces low levels of ROS, which can act as signaling molecules to activate various host defenses (41). In response to avirulent or incompatible pathogens, the host produces prolonged

ROS, leading to the development of HR (109). Virulent pathogens have developed mechanisms, including the use of effector proteins, which abolish the prolonged ROS in host tissue (109). It has been suggested that the HR, in coordination with other defense responses, is a host resistance mechanism (55).

Interestingly, when challenged with *E. amylovora*, apple responds atypically. Venisse and colleagues (112) demonstrated that *E. amylovora* elicits an incompatible plant/pathogen response within the host; or rather, a prolonged oxidative burst is released, followed by rapid necrosis of tissue. However, this ROS production is similar in both susceptible and more resistant varieties of apple (114), further demonstrating that a positive correlation between ROS production and host defense against *E. amylovora* cannot be made. It is possible that *E. amylovora* not only survives the increased production of ROS, but is able to manipulate the ROS to do damage against the host, ultimately assisting in the systemic movement of the pathogen. Interestingly, an increased tolerance to ROS exposure (10) suggests that *E. amylovora* may use host defenses to kill the host cells (113), which could ultimately aid in the movement of the pathogen through dead cells.

ii. Production of an agglutination factor. Numerous studies in the 1970's identified host defense factors termed agglutination factors (52, 53, 89). Agglutinins, also known as lectins, bind to specific simple sugar, and have been shown to precipitate polysaccharides (80). However, while lectins have been shown to have multiple roles in plant functions, including plant defense, they have not been shown to interact directly with virulent pathogens (80). Conversely, in avirulent plant/pathogen interactions, agglutination factors have been shown to sequester or arrest avirulent bacterial cells (80). An agglutinating factor produced by apple, when challenged with *E. amylovora* EPS minus mutants, did not allow for bacterial cells to

attach to xylem surfaces and caused the aggregation of cells and ultimately bacterial cell death (53). Additional studies determined that the lectin linked to the LPS of *E. amylovora* cells, which are exposed from the absence of EPS (88). Since the initial discovery of the agglutination factor, there has been no new research on the topic. This leads one to believe that unless the agglutination factor has additional, still to be determined, roles in the activation of plant defenses, it is not effective in inhibiting virulent *E. amylovora*.

iii. Phytoalexin production. Despite little being known about the mode of action of phytoalexins, these low molecular metabolites have long been known to play a role in host defense (48). Typically, production of phytoalexins is positively correlated with resistant phenotypes in hosts (48). In apple, the role of phytoalexins in host defense is largely unknown. However, mutants missing the gene for a phytoalexin-inducible multidrug efflux pump in *E. amylovora* are not as virulent on the host as wild type (22), suggesting phytoalexins have an unknown function in apple defense. Although this research is yet another example of circumvented host defense that is not sufficient to defend against the pathogen, all research was performed in susceptible trees. It is possible that phytoalexin production in more resistant varieties of apple have a more direct role in the host defense response against *E. amylovora*. Precursors for phytoalexin production, produced through the phenylpropanoid pathway, have been shown to be repressed in susceptible varieties, and induced in more resistant varieties (114).

iv. Activation of defense associated genes. In addition to anatomical barriers and biochemical protection, hosts under pathogen attack also have increased activation of several defense related genes. In apple, most notably, pathogenesis related (PR)- protein genes (15) and resistance (R) genes encoding DspA/E-interacting proteins of Malus x domestica (DIPM) (71) are induced after inoculation with *E. amylovora*. PR-proteins are suggested to be involved in the induction of

systemic acquired resistance (SAR) in plants. However, examination of several PR proteins in apple demonstrated that PR-proteins are induced after inoculation with *E. amylovora*, but are not induced by treatment with SAR elicitors (15). Additionally, there seems to be no difference in the induction of PR-proteins between resistant and susceptible varieties (3). An alternate study examining the effect of SAR inducers on apple demonstrated that the severity of disease can be reduced; however, SAR induced host resistance in apple was only sustained for a short time period (69). This suggests that PR-proteins may be involved in the recognition of pathogens but may not have a specific role in the defense against *E. amylovora*.

Host defense can also function in a gene-for-gene fashion, where a plant R gene recognizes a gene product produced by a pathogen, often in the form of an elicitor (45). In apple, the search for R genes led to the identification of DIPMs; however, activation of DIPMs occurs in both susceptible and resistant varieties (71). Numerous genomic studies and the release of the apple genome confirmed that there are no gene-for-gene interactions between apple and *E. amylovora* (3, 71, 111). Despite this, subtractive hybridizations performed between susceptible and resistant varieties of apple has identified several ESTs that have different expression profiles (3) so perhaps in the future specific genes involved in apple defense will be identified.

V. Systemic movement of *E. amylovora* within the host.

Early observations that shoot blight symptoms localized to vein tissue after plant injury led to hypothesis that *E. amylovora* is a vascular invading pathogen (31). Since then, multiple groups have confirmed that *E. amylovora* is found in xylem tissue after inoculation (31, 103). These studies indicate that *E. amylovora* probably moves systemically through the vascular

tissue. More recent imaging of *E. amylovora* using a *gfp* reporter system demonstrated that bacterial cells localize to the xylem tissue and migrate against the flow of xylem fluids (13). Bacterial cells also overflow into xylem parenchyma cells. Similarly, O'Brien (78) found *E. amylovora* cells in parenchyma cells; however the pathogen invaded xylem cells first. Interestingly, even in more resistant cultivars of apple, *E. amylovora* is able to move systemically, though initially at a much slower rate than in more susceptible cultivars (74). However, once the pathogen localized to the xylem tissue, *E. amylovora* is able to travel to the root stock faster in more resistant varieties than susceptible cultivars (74). These results suggest that in resistant cultivars, *E. amylovora* may encounter more host defenses in actively growing tissue. However, the lack of a change in known host defenses between cultivars (71, 114) led researchers to question what is halting the movement of the pathogen. It is possible that changes in anatomy between varieties restrict movement of *E. amylovora*.

In a recent review by Billing (11), the route of initial colonization and systemic movement was brought into question: perhaps there are multiple routes from initial site of multiplication to the vascular tissue. In attempts to resolve the mechanism of movement to the xylem tissue, Bogs and others (13) examined the movement of *gfp*-labeled avirulent *E. amylovora*. In their experiments, amylovoran deficient cells did not move past the site of inoculation. An additional study demonstrated that several mutants decreased in virulence have reduced movement to the central vein (14). Their results indicate that important virulence factors may contribute to the movement of the pathogen to the vascular tissue.

Currently, only a limited number of studies have successfully examined the systemic movement of vascular invading pathogens. Probably the best defined is *X. fastidiosa* on grape. Once the pathogen is delivered into xylem tissue by the leaf hopper vector, *X. fastidiosa*

colonizes xylem vessels. To move systemically through the xylem, *X. fastidiosa* utilizes several virulence factors, including the production of EPS, motility, the type II secretion system, and attachment to xylem tissue (25, 37, 76). Most of the virulence factors identified in this pathogen also contribute to biofilm formation (26, 76, 91), and biofilm formation is essential for the systemic movement of *X. fastidiosa* in grape. Similar studies in *P. stewartii* revealed that the EPS stewartan, necessary for pathogenicity in corn, functions in the development of biofilms within corn xylem tissue (63).

VI. Rationale and Project Goals.

In a review of other vascular invading pathosystems, a common theme emerges: most virulence factors involved in pathogenesis also function in biofilm formation (85). Biofilms, or aggregates of bacteria, EPS and other macromolecules, provide a milieu in which single-celled organisms to act in a multicellular fashion (18). Biofilm formation enables several advantages over non-biofilm forming cells, including the protection of bacterial cells from environmental stress, increased nutrient acquisition, an increased rate of gene exchange. Ultimately, biofilm formation has been shown to be critical in the virulence of many pathogens (46). The process of biofilm formation is well defined (80; Fig. 1-4). Bacterial cells transition from a planktonic lifestyle to become attached to a surface (Fig. 1-4.1). Attachment occurs in two stages: reversible and irreversible. Irreversible cells form a microcolony (Fig. 1-4.2) or a monolayer on a surface. Microcolonies develop into macrocolonies (Fig. 1-4.3). Macrocolonies are surrounded by a matrix of EPS, DNA, and proteins. Water channels are formed through macrocolonies that allow for the diffusion of oxygen and nutrients. An unknown signal then triggers the release of cells from the macrocolony, causing colony dissemination to new sites (Fig. 1-4.4).

The purpose of my doctoral research was to examine the systemic movement of *E. amylovora* within apple. We hypothesized that biofilm formation contributes to the systemic movement of *E. amylovora* in apple. The concept that biofilm formation assists in movement is counterintuitive: attachment and aggregation of bacterial cells suggest fixation in one location. However, within the xylem, *E. amylovora* movement is opposite to the flow of xylem fluid. The attachment of cells and subsequent biofilm formation has the potential of preventing the flushing of bacterial cells. Potentially, motile bacteria could progress farther in the xylem tissue. When the flow of xylem fluids reverses, typically during periods of high transpiration (66), bacterial cells could travel down xylem tissue. Changes in directional movement of xylem fluid could potentially signal the pathogen to attach and begin the biofilm formation process. To test whether *E. amylovora* is capable of forming biofilms, I used defined techniques for measuring biofilm formation. I was able to demonstrate that *E. amylovora* forms biofilms both *in vitro* and *in planta* (Chapter 2).

Two key pieces of evidence led us to examine the role of EPS in biofilm formation and systemic movement: 1) a hallmark of biofilm formation is the architectural matrix that surrounds the bacterial cells which contains EPS (105) and other molecules, and 2) Bogs and others (13) determined that amylovoran deficient *E. amylovora* cells are unable to move past the site of inoculation. It is possible that the lack of biofilm formation halts the systemic movement of the pathogen through the inability to form biofilms. In chapter 2, I examine the role of amylovoran in biofilm formation. Also in chapter 2, I examine the role of levan in biofilm formation. These mutants are still capable of causing disease, but colonization is much slower, and virulence is reduced compared to wild type (45).

Chapter 2 demonstrates that biofilm formation correlates with pathogenicity or virulence and systemic movement of the pathogen. To uncouple biofilm formation from EPS production in order to better understand the role of biofilm formation in systemic movement, I used a genetics approach to identify additional key factors in biofilm formation. Research presented in chapter 3 examines mutants with deletions in genes that encode for putative bacterial surface structures that have the potential to be involved in reversible and irreversible attachment of bacterial cells to surfaces, a key stage in biofilm formation. Prior to this chapter, the only bacterial attachment structures known to be produced by *E. amylovora* were the peritrichous flagella (84). In addition, I wanted to determine if altering the key step in biofilm formation would alter the systemic movement of the pathogen. Similarly, in chapter 4, I examined an additional factor demonstrated to function in biofilm formation, bacterial motility. In other pathosystems, including *P. aeruginosa*, functional flagellar motor stators that drive flagellar motility have been implicated in mediating attachment of the biofilm, as well as the expansion of biofilms. I identified and generated deletion mutants in single genes, a single stator set, and both gene sets encoding for the flagellar motor stators to examine how this factor contributes to the biofilm formation and systemic movement of *E. amylovora*.

In closely related work, we examined the mechanism by which prohexadione calcium (ProCa), a shoot growth regulator, inhibits disease. Treatment of trees with Apogee®, containing the active ingredient Pro Ca, results in a reduction of disease incidence in the field. Our research demonstrates a positive correlation between reductions in disease incidence with a thickening of parenchymal cell walls (Appendix I). Presumably, the thickening of cell walls inhibits the pathogen from infecting these cells, which is a prerequisite to entering the vascular tissue, ultimately halting the systemic movement of the pathogen.

Figure 1-1. Select virulence factors of *Erwinia amylovora*. Notice close association with bacterial cell surface. The majority of known virulence factors were identified through transposon mutagenesis studies. The peritrichous flagella are necessary for motility. Exopolysaccharides (EPS) are thought to protect the bacterial cell from harsh environmental conditions. The type II secretion system (T2SS) is needed for the secretion of cell wall degrading enzymes. The type III secretion system (T3SS) is needed for the secretion of effector proteins, particularly DspE. Additional other factors that are involved in pathogen virulence include a siderophore and penicillin binding protein. For interpretation of the references to color in this and all other figures, the reader is referred to the electronic version of this dissertation.

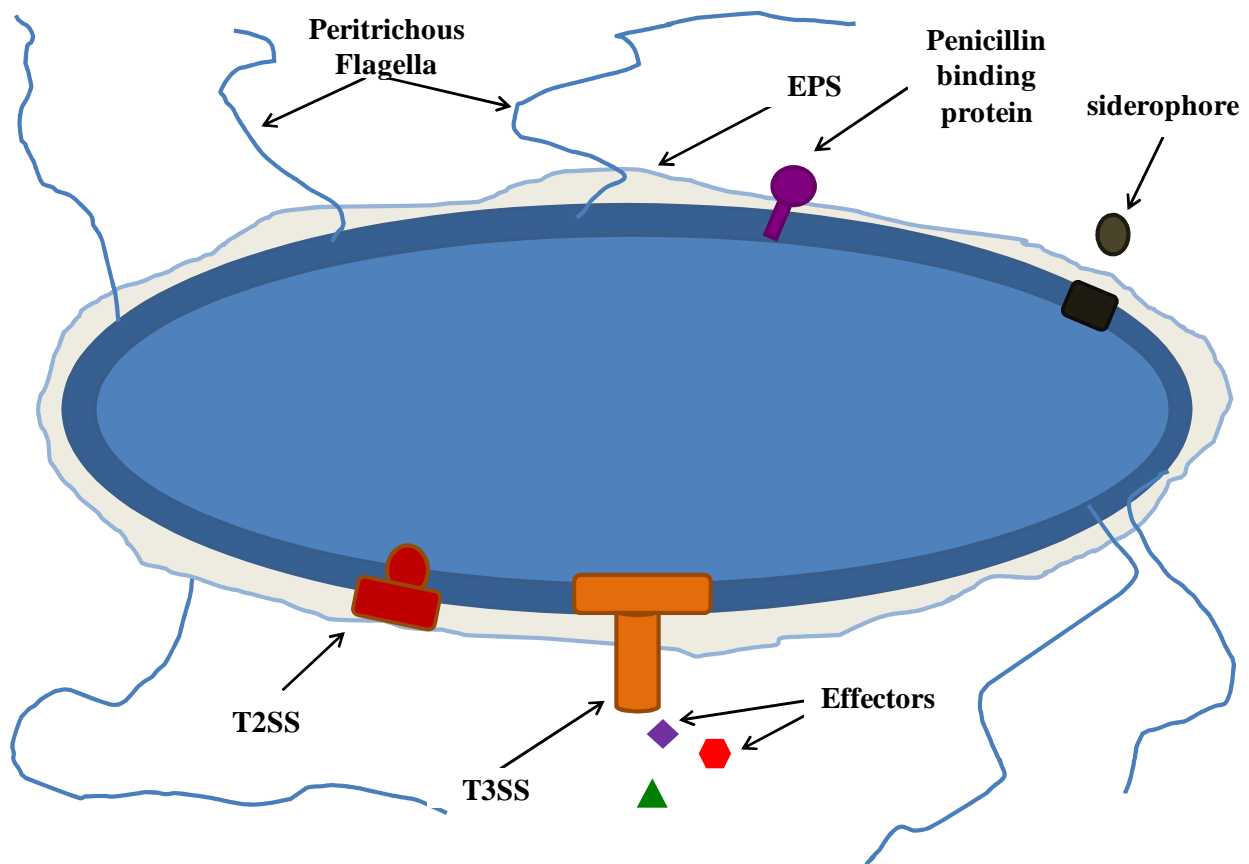


Figure 1-2. Scanning electron microscope image of the stigmatic surface of apple flower. A) The tip of the stigma surface is covered with papillae, which are bulbous-shaped structures indicated by the arrow. The papillae are the location of epiphytic growth during bloom and are the primary source of inoculum for secondary infection. B) Papillae (magnified in image) provide the pathogen protection from environmental stress, while rupture of the papillae provides nutrients and an entry point into the host. *Erwinia amylovora* (indicated by arrows) is able to grow in large populations around the papillae.

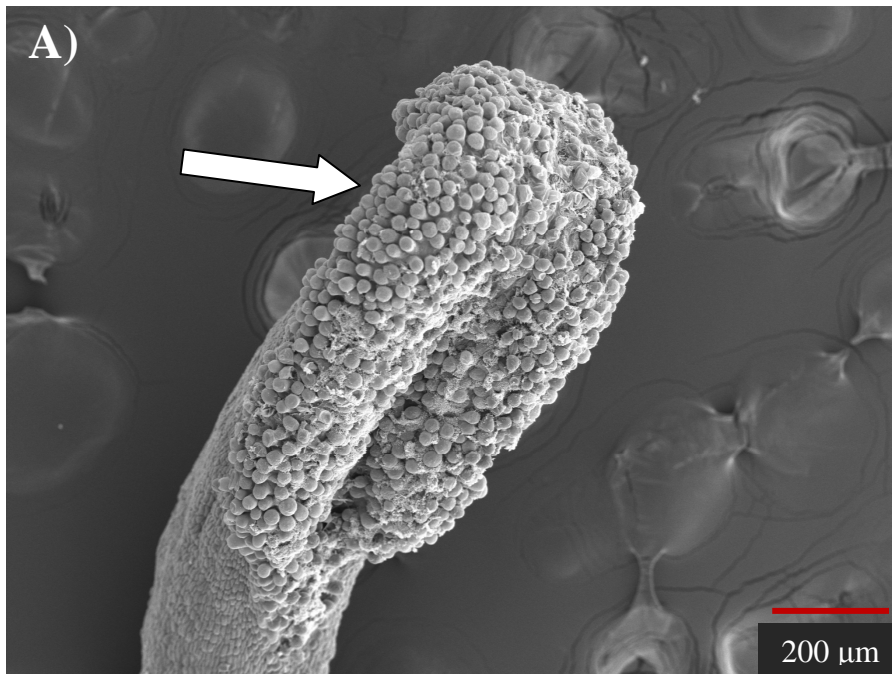


Figure 1-2 (cont'd)

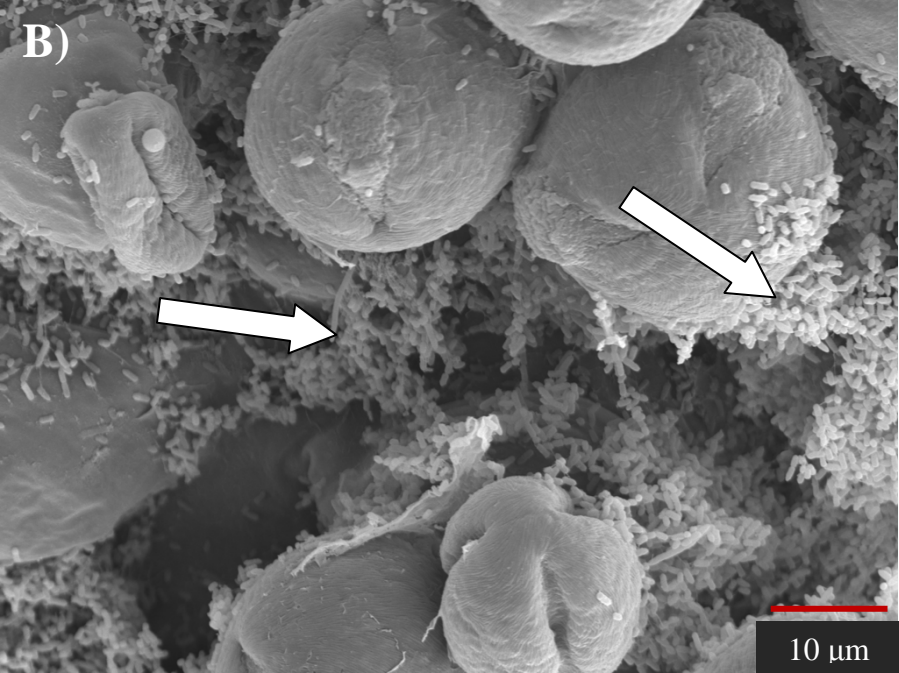


Figure 1-3. Taken from reference 36 with permission. Cross-section depicting cellular structure of a pear leaf. For *E. amylovora* to localize to the xylem tissue, the preferred site of infection, the pathogen must travel through or around many layers of mesophyll and bundle sheath tissue. The bundle sheath is a natural barrier against the pathogen, with no visible access from the intercellular space to the vascular system.

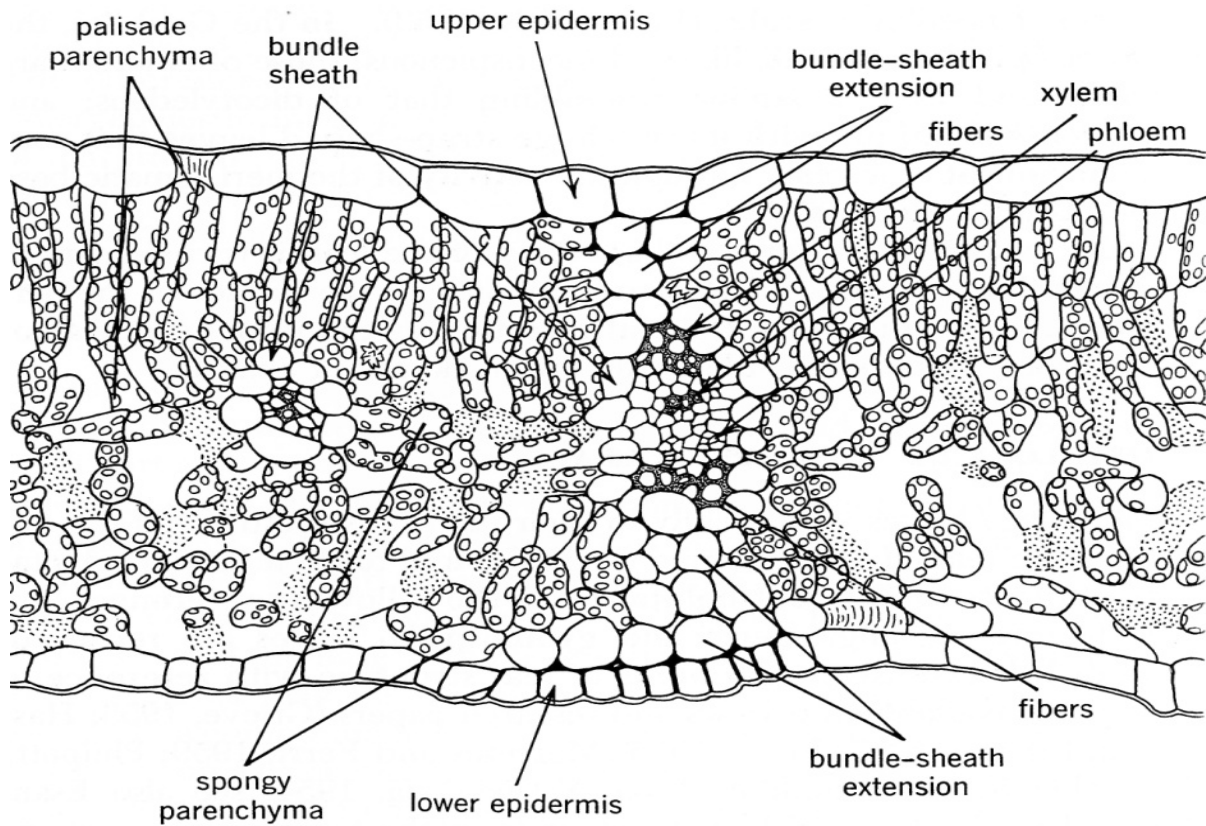
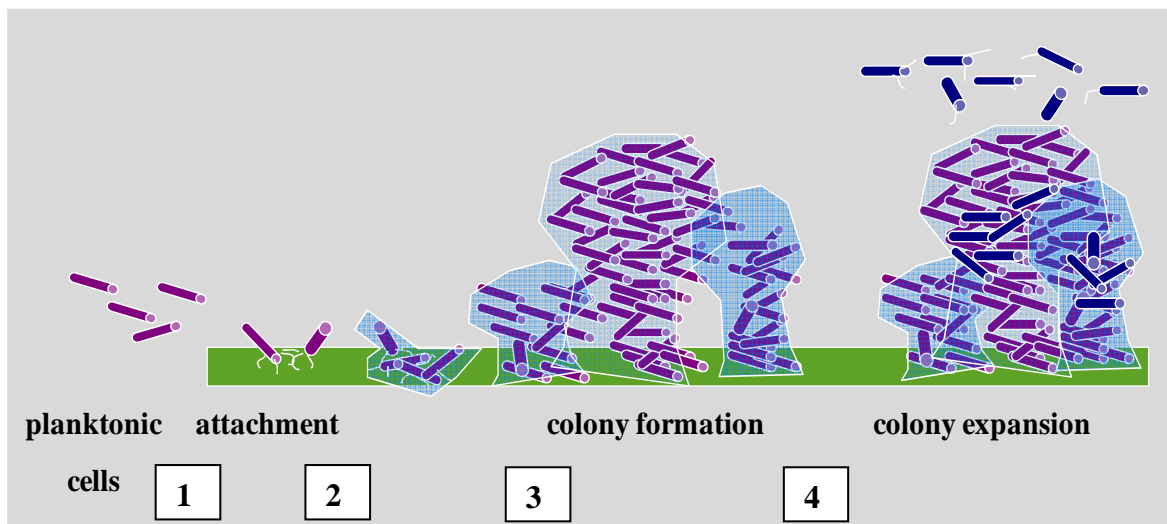


Figure 1-4. Biofilm formation process. 1) Planktonic bacterial cells become attached. Key virulence factors involved in this transition often include bacterial motility and bacterial surface structures that mediate attachment. 2) Microcolony formation. The early stage of a biofilm often includes increased production of exopolysaccharides. 3) Macrocolony formation. A mature biofilm often develops a mushroom-shaped architecture which allows for the flow of fluids within the biofilm. 4) Colony expansion. Bacterial cells are released from the biofilm.



LITERATURE CITED

LITERATURE CITED:

1. Arthur, J.C. 1886. History and biology of pear blight. *Pro. Acad. Nat. Sci. Phil.* 38: 322-341.
2. Ayers, A.R., Ayers, S.B., and Goodman, R.N. 1979. Extracellular polysaccharide of *Erwinia amylovora*: a correlation with virulence. *Appl. Environ. Microbiol.* 38: 659-666.
3. Baldo, A., Norelli, J.L., Farrell Jr., R.E., Bassett, C.L., Aldwinckle, H.S., and Malnoy, M. 2010. Identification of genes differentially expressed during interaction of resistant and susceptible apple cultivars (*Malus x domestica*) with *Erwinia amylovora*. *BMC Plant Biol.* 10: 1.
4. Barny, M.A., Guiriebret, M.H., Marcais, B., Coissac, E., Paulin, J.P., and Laurent, J. 1990. Cloning of a large gene cluster involved in *Erwinia amylovora* CFBP1430 virulence. *Mol. Microbiol.* 4: 777-786.
5. Bayot, R.G., and Ries, S.M. 1987. Role of motility in apple blossom infection by *Erwinia amylovora* and studies of fire blight control with attractant and repellent compounds. *Phytopathology* 76: 441-445.
6. Beer S.V., and Norelli, J.L. 1977. Fire blight epidemiology: factors affecting release of *E. amylovora* by cankers. *Phytopathology* 67: 1119-1125.
7. Bellemann, P., Bereswill, S., Berger, S., and Geider, K. 1994. Visualization of capsule formation by *Erwinia amylovora* and assays to determine amylovoran synthesis. *Int. J. Biol. Macromol.* 16: 290-296.
8. Bellemann, P., and Geider, K. 1992. Localization of transposon insertions in pathogenicity mutants of *Erwinia amylovora* and their biochemical characterization. *J. Gen. Microbiol.* 138: 931-940.
9. Bernhard, F., Schullerus, D., Bellemann, P., Nimtz, M., Coplin, D.L., and Geider, K. 1996. Genetic transfer of amylovoran and stewartan synthesis between *Erwinia amylovora* and *Erwinia stewartii*. *Microbiol.* 142: 1087-1096.
10. Berry, M.C. McGhee, G.C., Zhao, Y., and Sundin, G.W. 2009. Effect of *waaL* mutation on lipopolysaccharide composition, oxidative stress survival and virulence in *Erwinia amylovora*. *FEMS Microbiol. Lett.* 291: 80-87.
11. Billing, E. 2011. Fire blight. Why do views on host invasion by *Erwinia amylovora* differ? *Plant Pathol.* 60: 178-189.
12. Bogdanove, A.J., Kim, J.F., Wei, Z., Kolchinsky, P., Charkowski, A.O., Conlin, A.K., Collmer, A., and Beer, S.V. 1998. Homology and functional similarity of *hrp*-linked

pathogenicity locus, *dpsEF*, of *Erwinia amylovora* and the avirulence locus *avrE* of *Pseudomonas syringae* pathovar tomato. Proc. Natl. Acad. Sci. USA 95: 1325-1330.

13. Bogs, J., Brunchmuller, I., Erbar, C., and Geider, K. 1998. Colonization of host plants by the fire blight pathogen *Erwinia amylovora* marked with genes for bioluminescence and fluorescence. Phytopathology 88: 416-421.
14. Bogs, J., Richter, K., Kim, W.S., Jock, S., and Geider, K. 2004. Alternative methods to describe virulence of *Erwinia amylovora* and host-plant resistance against fireblight. Plant Pathol. 53: 80-89.
15. Bonasera, J.M., Kim, J.F., and Beer, S.V. 2006. PR genes of apple: identification and expression in response to elicitors and inoculation with *Erwinia amylovora*. BMC Plant Biol. 6: 23-45.
16. Borejsza-Wysocka, E., Norelli, J.L., Aldwinckle, H.S., and Malnoy, M. 2010. Stable expression and phenotypic impact of *attacin E* transgene in orchard grown apple trees over a 12 year period. BMC Plant Biol. 10: 41.
17. Boureau, T., El Maarouf-Bouteau, H., Garnier, A., Brisset, M.N., Perino, C., Pucheu, I., and Barny, M.A. 2006. DspA/E, a type III effector essential for *Erwinia amylovora* pathogenicity and growth in planta, induces cell death in host apple and nonhost tobacco plants. Mol. Plant-Microbe Interact. 19: 16-24.
18. Branda, S.S., Vik, A., Friedman, L., and Kolter, R. 2005. Biofilms: the matrix revisited. TRENDS in Microbiol. 13: 20-26.
19. Brisset, M.N., Faize, M., Heintz, C., Cesbron, S., Chartier, R., Thatraud, M., Barny, M.A., and Paulin, J.P. 2002. Competition between the secretion of hrp proteins and flagellins during the infection process by *Erwinia amylovora*. Proc. 9th Int. Workshop on Fire Blight 449-450.
20. Buban, T., Orosz-kovacz, Z., and Farkas, A. 2003. The nectar as the primary site of infection by *Erwinia amylovora* (Burr.) Winslow et al.: a mini review. Plant Syst. Evol. 238: 183-194.
21. Bugert, P. and Geider, K. 1995. Molecular analysis of the *ams* operon required for exopolysaccharide synthesis of *Erwinia amylovora*. Mol. Microbiol. 15: 917-933.
22. Burse, A., Weingart, H., and Ullrich, M.S. 2004. NorM, an *Erwinia amylovora* multidrug efflux pump involved in in vitro competition with other epiphytic bacteria. Appl. Environ. Microbiol. 70: 693-703.
23. Burse, A., Weingart, H., and Ullrich, M.S. 2004. The phytoalexin-inducible multidrug efflux pump AcrAB contributes to virulence in the fire blight pathogen, *Erwinia amylovora*. Mol. Plant-Microbe Interact. 17: 43-54.

24. Cesbron, S., Paulin, J.P., Tharaud, M., Barny, M.A., and Brisset, M.N. 2006. The alternate σ factor HrpL negatively modulates the flagellar system in the phytopathogenic bacterium *Erwinia amylovora* under *hrp*-inducing conditions. *FEMS Microbiol. Lett.* 257: 221-227.
25. Chatterjee, S., Almeida, R.P.P., and Lindow, S. 2008. Living in two worlds: the plant and insect lifestyles of *Xylella fastidiosa*. *Annu. Rev. Phytopathol.* 46: 243-271.
26. Chatterjee, S., Killiny, N., Almeida, R.P.P., and Lindow, S. 2010. Role of cyclic di-GMP in *Xylella fastidiosa* biofilm formation, plant virulence, and insect invasion. *Mol. Plant-Microbe Interact.* 23: 1356-1363.
27. Cianciotto, N.P. 2005. Type II secretion: a protein secretion system for all seasons. *Trends in Microbiol.* 13: 581-588.
28. Condemine, G., Castillo, A., Passeri, F., and Enard, C. 1999. The PecT repressor coregulates synthesis of exopolysaccharides and virulence factors in *Erwinia chrysanthemi*. *Mol. Plant-Microbe Interact.* 12: 45-52.
29. Coplin, D.L., Majerczak, D.R., Bugert, P., and Geider, K. 1996. Nucleotide sequence analysis of the *Erwinia stewartii* *cps* gene cluster for synthesis of stewartan and comparison to the *Erwinia amylovora* *ams* gene cluster for synthesis of amylovoran. *Acta Hort. (ISHS)* 411: 251-258.
30. Cornelis, G.R., and van Gijsegem, F. 2000. Assembly and function of type III secretion systems. *Annu. Rev. Microbiol.* 54: 735-774.
31. Crosse, J.E., Goodman, R.N., and Schaffer, W.H. 1972. Leaf damage as a predisposing factor in the infection of apple shoots by *Erwinia amylovora*. *Phytopathology* 62: 176-182.
32. DebRoy, S., Thilmony, R., Kwack, Y.B., Nomura, K., and He, S.Y. 2004. A family of conserved bacterial effectors inhibits salicylic acid-mediated basal immunity and promotes disease necrosis in plants. *Proc. Natl. Acad. Sci. USA* 101: 9927-9932.
33. Dellagi, A., Brisset, M.N., Paulin, J.P., and Expert, D. 1998. Dual role of desferrioxamine in *Erwinia amylovora* pathogenicity. *Mol. Plant-Microbe Interact.* 11: 734-742.
34. Denny, T.P. 1995. Involvement of bacterial polysaccharides in plant pathogenesis. *Annu. Rev. Phytopathol.* 33: 173-197.
35. Dumitriu, S. 2010. Polysaccharides structural diversity and functional versatility, 2nd Edition. New York, USA: CRC Press.
36. Esau, K. 1967. Plant Anatomy, 2nd Edition. New York, USA: Wiley.

37. Feil, H., Feil, W.S., and Lindow, S.E. 2007. Contribution of fimbrial and afimbrial adhesins of *Xylella fastidiosa* to attachment to surfaces and virulence in grape. *Phytopathology* 97: 318-324.
38. Fraser, G.M., and Hughes, C. 1999. Swarming motility. *Curr. Opin. Microbiol.* 2: 630-635.
39. Gao, Y., Song, J., Hu, B., Zhang, L., Lui, Q., and Liu, F. 2009. The *luxS* gene is involved in AI-2 production, pathogenicity, and some phenotypes in *Erwinia amylovora*. *Curr. Opin. Microbiol.* 58: 1-10.
40. Geier, G. and Geider, K. 1993. Characterization and influences on virulence of the levansucrase gene from the fire blight pathogen *Erwinia amylovora*. *Physiol. Mol. Plant Pathol.* 42: 387-404.
41. Gill, S.S., and Tuteja, N. 2010. Reactive oxygen species and antioxidant machinery in abiotic stress tolerance of crop plants. *Plant Physiol. Biochem.* 48: 909-930.
42. Goodman, R.N., Huang, J.S., and Huang, P.Y. 1974. Host-specific phytotoxic polysaccharide from apple tissue infected by *Erwinia amylovora*. *Science* 183: 1081-1082.
43. Goodman, R.N., and White, J.A. 1981. Xylem parenchyma plasmolysis and vessel wall disorientation caused by *Erwinia amylovora*. *Phytopathology* 71: 844-852.
44. Grant, S.R., Fisher, E.J., Chang, J.H., Mole, B.M., and Dangl, J.L. 2006. Subterfuge and manipulation: type III effector proteins of phytopathogenic bacteria. *Annu. Rev. Microbiol.* 60: 425-449.
45. Greenberg, J.T. 1996. Programmed cell death: a way of life for plants. *Pro. Natl. Acad. Sci. USA* 93: 12094-12097.
46. Gross, M., Geier, G., Rudolph, K., and Geider, K. 1992. Levan and leveansucrase synthesized by the fireblight pathogen *Erwinia amylovora*. *Physiol. Mol. Plant Pathol.* 40: 371-381.
47. Hall-Stoodley, L., Costerton, J.W., and Stoodley, P. 2004. Bacterial biofilms: from the natural environment to infectious disease. *Nature Rev. Microbiol.* 2: 95-109.
48. Hammerschmidt, R. 1999. Phytoalexins: what we have learned after 60 years? *Annu. Rev. Phytopathol.* 37:285-306.
49. Hattings, M.J., Beer, S.V., and Lawson, T.W. 1986. Scanning electron microscopy of apple blossoms colonized by *Erwinia amylovora* and *E. herbicola*. *Phytopathology* 76: 900-904.

50. Heath, M.C. 1998. Apoptosis, programmed cell death and the hypersensitive response. *Eur. J. Plant Pathol.* 104: 117-124.
51. Hitz, W.D., and Giaquinta, R.T. 1987. Sucrose transport in plants. *BioEssays* 6: 217-221.
52. Hsu, S.T., and Goodman, R.N. 1978. Agglutinating activity in apple cell suspension cultures inoculated with a virulent strain of *Erwinia amylovora*. *Phytopathology* 68: 355-360.
53. Huang, J.S. 1986. Ultrastructure of bacterial penetration in plants. *Ann. Rev. Phytopathol.* 24: 141-57.
54. Huang, P.Y., and Goodman, R.N. 1971. Ultrastructure of the cell wall of *Erwinia amylovora*. *J. Bacteriol.* 107: 361-364.
55. Huang, P.Y., Huang, J.S., and Goodman, R.N. 1975. Resistance mechanisms of apple shoots to an avirulent strain of *Erwinia amylovora*. *Physiol. Plant Pathol.* 6: 283-287.
56. Jha, G., Rajeshwari, R., and Sonti, R.V. 2005. Bacterial type two secretion system secreted proteins: double-edged swords for plant pathogens. *Mol. Plant-Microbe Interact.* 18: 891-898.
57. Johnson, K.B., Sawyer, T.L., Stockwell, V.O., and Temple, T.N. 2009. Implications of pathogenesis by *Erwinia amylovora* on rosaceous stigmas to biological control of fire blight. *Phytopathology* 99: 128-138.
58. Johnson, K.B., and Stockwell, V.O. 1998. Management of fire blight: a case study in microbial ecology. *Annu. Rev. Phytopathol.* 36: 227-248.
59. Kang, Y., Liu, H., Genin, S., Schell, M.A., and Denny, T.P. 2002. *Ralstonia solanacearum* requires type 4 pili to adhere to multiple surfaces and for natural transformation and virulence. *Mol. Microbiol.* 46: 427-437.
60. Kingston-Smith, A.H., and Foyer, C.H. 2000. Bundle sheath proteins are more sensitive to oxidative damage than those of the mesophyll in maize leaves exposed to paraquat or low temperatures. *J. Exper. Biol.* 51: 123-130.
61. Kiraly, Z., El-Zahaby, H.M., and Klement, Z. 1997. Role of extracellular polysaccharide (EPS) slime of plant pathogenic bacteria in protecting cells to reactive oxidative species. *J. Phytopathol.* 145: 59-68.
62. Korhonen, T.K., Haahtela, K., Pirkola, A., and Parkkinen, J. 1988. A N-acetyllactosaminic-specific cell-binding activity in a plant pathogen, *Erwinia rhapontici*. *FEBS Lett.* 236: 163-166.

63. Koutsoudis, M.D., Tsaltas, D., Minogue, T.D., and von Bodman, S.B. 2006. Quorum-sensing regulation governs bacterial adhesion, biofilm development, and host colonization in *Pantoea stewartii* subspecies *stewartii*. Proc. Natl. Sci. Acad. USA 103: 5983-5988.
64. Krivanek, A.F., Stevenson, J.F., and Walker, M.A. 2005. Development and comparison of symptom indices for quantifying grapevine resistance to Pierce's disease. Phytopathology 95: 36-43.
65. Krzymowska, M., Konopka-Postupolska, D., Sobczak, M., Macioszek, V., Ellis, B.E., and Hennig, J. 2007. Infection of tobacco with different *Pseudomonas syringae* pathovars leads to distinct morphotypes of programmed cell death. Plant J. 50: 253-264.
66. Lamb, C., and Dixon, R.A. 1997. The oxidative burst in plant disease resistance. Annu. Rev. Plant Physiol. Plant Mol. 48: 251-275.
67. Lang, A. 1990. Xylem, phloem, and transpiration flows in developing apple fruits. J. Exper. Botany 41: 645-651.
68. Leigh, J.A., and Coplin, D.L. 1992. Exopolysaccharides in plant-bacterial interactions. Annu. Rev. Microbiol. 46: 307-346.
69. Maxson-Stein, K., He, S.Y., Hammerschmidt, R., and Jones, A.S. 2002. Effect of treating apple trees with Acibenzolar-S-Methyl on fire blight and expression of pathogenesis-related protein genes. Plant Disease 86: 885-790.
70. McGhee, G.C., Guasco, J. Bellamo, L.M., Blumer-Schuette, S.E., Shane, W.W., Irish-Brown, A., and Sundin, G.W. 2011. Genetic analysis of streptomycin-resistant (Sm^R) strains of *Erwinia amylovora* suggests that dissemination of two genotypes is responsible for the current distribution of Sm^R *E. amylovora* in Michigan. Phytopathology 101: 182-191.
71. Meng, X., Bonasera, J.M., Kim, J.F., Nissinen, R.M., and Beer, S.V. 2006. Apple proteins that interact with DspA/E, a pathogenicity factor of *Erwinia amylovora*, the fire blight pathogen. Mol. Plant-Microbe Interact. 19: 53-61.
72. Menggad, M., and Laurent, J. 1998. Mutations in *ams* genes of *Erwinia amylovora* affect the interactions with host plants. Euro. J. Plant Pathol. 104: 313-322.
73. Milner, J.S., Dymock, D., Cooper, R.M., and Roberts, I.S. 1993. Penicillin-binding proteins from *Erwinia amylovora* mutants lacking PBP2 are avirulent. J. Bacteriol. 175: 6028-6088.
74. Momol, M.T., Norelli, J.L., Piccioni, D.E., Momol, E.A., Gustafson, H.L., Cummins, J.N., and Aldwinkle, H.S. 1998. Internal movement of *Erwinia amylovora* through symptomless apple scion tissue into the rootstock. Plant Dis. 82: 646-650.

75. Nimtz, M., Mort, A., Domke, T., Wray, V., Zhang, Y., Qiu, F., Coplin, D.L., and Geider, K. 1996. Structure of amylovoran, the capsular exopolysaccharide from the fire blight pathogen *Erwinia amylovora*. *Carbohydrate Res.* 287: 59-76.
76. Newman, K.L., Almeida, R.P., Purcell, A.H., and Lindow, S.E. 2004. Cell-cell signaling controls of *Xylella fastidiosa* interactions with both insects and plants. *Proc. Natl. Acad. Sci. USA* 101: 1737-1742.
77. Norelli, J.L., Jones, A.L., and Aldwinkle, H.S. 2003. Fire blight management in the twenty-first century. *Plant Disease* 87: 756-765.
78. O'Brien, I.E.W. 1993. Comparison of *Malus* infection by the pathogen *Erwinia amylovora* and by the colonization by the saprophyte *Erwinia herbicola* by electron microscopy. *New Zealand J. Crop Hort. Sci.* 21: 33-38.
79. Oh, C.S., Kim, J.F., and Beer, S.V. 2005. The Hrp pathogenicity island of *Erwinia amylovora* and identification of three novel genes required for systemic infection. *Mol. Plant Pathol.* 6: 125-138.
80. O'Toole, G., Kaplan, H.B., and Kolter, R. 2000. Biofilm formation as microbial development. *Annu. Rev. Microbiol.* 54:49-79.
81. Peusmans, W.J., and van Damme, E.J.M. 1995. Lectins as plant defense proteins. *Plant Physiol.* 109: 347-352.
82. Politis, D.J., and Goodman, R.N. 1980. Fine structure of extracellular polysaccharide of *Erwinia amylovora*. *Appl. Environ. Microbiol.* 40: 596-607.
83. Qi, M., Sun, F.J., Caetario-Ariolles, G., and Zhao, Y. 2010. Comparative genomics and phylogenetic analyses reveal the evolution of the core two-component signal transduction systems in Enterobacteria. *J. Mol. Evol.* 70: 167-180
84. Rajeshwari, R., Jha, G., and Sonti, R.V. 2005. Role of an in planta expressed xylanase of *Xanthomonas oryzae* pv. *oryzae* in promoting virulence on rice. *Mol. Plant-Microbe Interact.* 18: 830-837.
85. Ramey, B.E., Koutsoudis, M., von Bodman, S.B., and Fuqua, C. 2004. Biofilm formation in plant microbe associations. *Curr. Opin. Microbiol.* 7: 602-609.
86. Raymundo, A.K., and Ries, S.M. 1981. Motility of *Erwinia amylovora*. *Phytopathology* 71: 45-49.
87. Riekki, R., Palomaki, T., Virtaharju, O., Kokko, H., Romantschuk, M., and Saarilahti, H.T. 2000. Members of the amylovora group of *Erwinia* are cellulolytic and possess genes homologous to the type II secretion pathway. *Mol. Gen. Genet.* 263: 1031-1037.

88. Romantschuk, M. 1992. Attachment of plant pathogenic bacteria to plant surfaces. *Annu. Rev. Phytopathol.* 30: 225-243.
89. Romeiro, R.S., Karr, A.I., and Goodman, R.N. 1981. *Erwinia amylovora* cell wall receptor for apple agglutination. *Physiol. Plant Pathol.* 19: 383-390.
90. Romeiro, R.S., Karr, A.I., and Goodman, R.N. 1981. Isolation of a factor from apple that agglutinates *Erwinia amylovora*. *Plant Physiol.* 68: 772-777.
91. Roper, M.C., Greve, L.C., Labavitch, J.M., and Kirkpatrick, B.C. 2007. Detection and visualization of an exopolysaccharide produced by *Xylella fastidiosa* in vitro and in plant. *Appl. Environ. Microbiol.* 73: 7252-7258.
92. Sandkvist, M. 2001. Type II secretion and pathogenesis. *Infect. Immun.* 69: 3523-3535.
93. Schaffer, K., and Wisniewski, M. 1989. Development of the amorphous layer (protective layer) in xylem parenchyma of cv. golden delicious apple, cv. loring peach and willow. *Amer. J. Bot.* 76: 1569-1582.
94. Schneider, D.J., and Collmer, A. 2010. Studying plant-pathogen interactions in the genomics era: beyond molecular Koch's postulates to systems biology. *Annu. Rev. Phytopathol.* 48: 457-479.
95. Seemüller, E.A., and Beer, S.V. 1976. Absence of cell wall polysaccharide degradation by *Erwinia amylovora*. *Phytopathology* 66: 433-436.
96. Shulaev, V., Korban, S.S., Sosinski, B., Abbott, A.G., Aldwinckle, H.S., et. al. 2010. Multiple models for Rosaceae genomics. *Plant Physiol.* 147: 985-1003.
97. Sijam, K., Goodman, R.N., and Karr, A.L. 1985. The effect of salts on the viscosity and wilt-inducing capacity of the capsular polysaccharide of *Erwinia amylovora*. *Physiol. Plant Pathol.* 26: 231-239.
98. Sjulín, T.M., and Beer, S.V. 1978. Mechanism of wilt induction by amylovoran in cotoneaster shoots and its relation to wilting of shoots infected by *Erwinia amylovora*. *Phytopathology* 68: 89-94.
99. Smith, A.R.W, Rastall, R.A., Balke, P., and Hignett, R.C. 1995. Gluco-oligosaccharide production by a strain of *Erwinia amylovora*. *Microbios.* 83: 27-39.
100. Smits, T.H.M., Rezzonico, F., Kamber, T., Blom, J., Goesmann, A., Frey, J.E., and Duffy, B. 2010. Complete genome sequence of the fire blight pathogen *Erwinia amylovora* CFBP 1430 and comparison to other *Erwinia* spp. *Mol. Plant-Microbe Interact.* 23: 384-393.

101. Spinelli, F., Ciampolini, F., Cresti, M., Geider, K., and Costa, G. 2005. Influence of stigmatic morphology on flower colonization by *Erwinia amylovora* and *Pantoea agglomerans*. *Eur. J. Plant Pathol.* 113: 395-405.
102. Steinberger, E.M., and Beer, S.V. 1988. Creation and complementation of pathogenicity mutants of *Erwinia amylovora*. *Mol. Plant-Microbe Inter.* 1:135-144.
103. Suhayda, C.G., and Goodman R.N. 1981. Infection courts and systemic movement of ^{32}P -labeled *Erwinia amylovora* in apple petioles and stems. *Phytopathology* 71: 656-60.
104. Sundin, G.W., Werner, N.A, Yoder, K.S., and Aldwinckle, H.S. 2009. Field evaluation of biological control of fire blight in the eastern United States. *Plant Disease* 93: 386-394.
105. Sutherland, I. 2001. Biofilm exopolysaccharides: a strong and sticky framework. *Microbiology.* 147: 3-9.
106. Tans-Kersten, J., Huang, H., and Allen, C. 2001. *Ralstonia solanacearum* needs motility for invasive virulence on tomato. *J. Bacteriol.* 183: 3597-3605.
107. Tharaud, M., Menggad, M., Paulin, J.P., and Laurent, J. 1994. Virulence, growth and surface characteristics of *Erwinia amylovora* mutants with altered pathogenicity. *Microbiol* 140: 659-669.
108. Thomson, S.V. 1986. The role of the stigma in fire blight infection. *Phytopathology* 76: 476-482.
109. Torres, M.A. 2010. ROS in biotic interactions. *Physiol. Plant.* 138: 414-429.
110. Vanneste, J.L. 2000. Fire Blight: The disease and its causative agent, *Erwinia amylovora*. Oxfordshire, UK: CABI publishing.
111. Velasco, R., Zharkikh, A., Affourtit, J., Dhingra, A., Cestaro, A., et. al. 2010. The genome of the domesticated apple (*Malus x domestica* Borkh.). *Nature Genetics.* 42: 833-841.
112. Venisse, J.S., Barney, M.A., Paulin, J.P., and Brisset, M.N. 2003. Involvement of three pathogenicity factors of *Erwinia amylovora* in the oxidative stress associated with compatible interaction in pear. *FEBS Lett.* 537: 198-202.
113. Venisse, J.S., Gullner, G., and Brisset, M.N. 2001. Evidence for the involvement of an oxidative stress in the initiation of infection of pear by *Erwinia amylovora*. *Plant Physiol.* 125: 2164-2172.
114. Venisse, J.S., Malnoy, M., Faize, M., Paulin, J.P., and Brisset, M.N. 2002. Modulation of defense responses of *Malus* spp. during compatible and incompatible interactions with *Erwinia amylovora*. *Mol. Plant-Microbe Interact.* 15: 1204-1212.

115. Wang, D., Korban, S.S., and Zhao, Y. 2010. Molecular signature of differential virulence in natural isolates of *Erwinia amylovora*. *Phytopathology* 100: 192-198.
116. Wang, L., and Beer, S.V. 2006. Application of signature-tagged mutagenesis to the study of virulence of *Erwinia amylovora*. *FEMS Microbiol. Lett.* 265: 164-171.
117. Wilson, M., Epton, H.A.S., and Sigeo, D.C. 1989. *Erwinia amylovora* infection of the hawthorn blossom II. The stigma. *J. Phytopathol.* 127: 15-28.
118. Young, S.A., Guo, A., Guikema, J.A., White, F.F., and Leach, J.E. 1995. Rice cationic peroxidase accumulates in xylem vessels during incompatible interactions with *Xanthomonas oryzae* pv *oryzae*. *Plant Physiol.* 107: 1333-1341.
119. Zhao, Y., Blumer, S.E., and Sundin, G.W. 2005. Identification of *Erwinia amylovora* genes induced during infection of immature pear tissue. *J. Bacteriol.* 187: 8088-8103.
120. Zhao, Y., Sundin, G.W., and Wang, D. 2009. Construction and analysis of pathogenicity island deletion mutants of *Erwinia amylovora*. *Can. J. Microbiol.* 55: 457-464.
121. Zhao, Y., Wang, D., Nakka, S., Sundin, G.W., and Korban, S.S. 2009. Systems level analysis of two-component signal transduction systems in *Erwinia amylovora*: role in virulence, regulation of amylovoran biosynthesis, and swarming motility. *BMC Genomics* 10: 245-261.

Chapter 2: The contribution of *Erwinia amylovora* exopolysaccharides amylovoran and levan to biofilm formation: implications in pathogenicity.

This chapter has been modified from a publication referenced: Koczan, J.M., McGrath, M.J., Zhao, Y., and Sundin, G.W. 2009. Contribution of *Erwinia amylovora* exopolysaccharides amylovoran and levan to biofilm formation: implications in pathogenicity. *Phytopathology* 99: 1237-1244.

ABSTRACT

Erwinia amylovora is a highly virulent, necrogenic, vascular pathogen of rosaceous species that produces the exopolysaccharide amylovoran, a known pathogenicity factor, and levan, a virulence factor. An *in vitro* crystal violet staining and a bright field microscopy method were used to demonstrate that the *E. amylovora* is capable of forming a biofilm on solid surfaces. Amylovoran and levan production deletion mutants were used to determine that amylovoran was required for biofilm formation and that levan contributed to biofilm formation. An *in vitro* flow cell and confocal microscopy was used to further reveal the architectural detail of a mature biofilm and differences in biofilm formation between *E. amylovora* wild-type (WT), Δ *ams* and Δ *lsc* mutant cells labeled with *gfp* or *cfp*. Scanning electron microscopy analysis of *E. amylovora* WT cells following experimental inoculation in apple indicated that extensive biofilm formation occurs in xylem vessels. However, Δ *ams* mutant cells were nonpathogenic and died rapidly following inoculation, and Δ *lsc* mutant cells were not detected in xylem vessels and were reduced in movement in apple shoots. These results demonstrate that biofilm formation plays a critical role in the pathogenesis of *E. amylovora*.

INTRODUCTION

Erwinia amylovora, a gram-negative plant pathogenic bacterium, is the causal agent of fire blight, a devastating disease on rosaceous species such as apple and pear. The highly-virulent fire blight pathogen moves rapidly both within susceptible plants and between trees in orchards, resulting in significant losses when environmental conditions favor infection. *E. amylovora* is capable of infecting flowers, actively-growing shoots, and rootstock crowns, and successful disease management is difficult because of the lack of effective bactericides and also because most apple varieties are susceptible or highly susceptible to fire blight (25). A hallmark symptom of fire blight is the formation of the shepherd's crook, which is produced by a combination of wilt and necrosis on a shoot. Wilted shoots are typically sources of bacterial ooze, which consists of bacterial cells embedded in a polysaccharide matrix that can be disseminated between hosts by insects and wind-driven rain (39).

In the 1970's, work in the Goodman and Beer labs provided a foundation for the understanding of the causes of host tissue wilting by *E. amylovora* (18, 35). The Goodman group first demonstrated that *E. amylovora* produced a material that caused wilt symptoms in host, but not in nonhost plants (18). This material was initially described as the toxin amylovorin and later identified as the exopolysaccharide (EPS) amylovoran (18). The role of amylovoran in causing wilt symptoms was further examined by Sjulín and Beer (35) and found to be associated with restriction of water movement through physical blockage of vascular elements. Xylem vessel blockage occurred because of the viscosity of amylovoran; this blockage could be eliminated by increasing the salt concentration of amylovoran solutions which reduced viscosity (34).

Amylovoran is a heteropolymer comprised of a branched repeating unit consisting of galactose, glucose, and pyruvate residues (24). Amylovoran is a pathogenicity factor as amylovoran-deficient mutants are avirulent (3, 36). In addition, the quantity of amylovoran produced by individual *E. amylovora* strains is correlated with the degree of virulence, with weak producers exhibiting reduced virulence (1). Genes encoding the biosynthesis of amylovoran are contained within a 12-gene operon on the *E. amylovora* chromosome, and insertional mutants of critical genes of the operon result in a loss of pathogenicity (3). *E. amylovora* also produces levan, a homopolymer of fructose residues that is produced following the breakdown of sucrose. Levan production is controlled by the *lsc* gene encoding the levansucrase enzyme, and also contributes to virulence (17).

A common developmental strategy for microbes in nature is the formation of biofilms, which can be composed of bacterial cells, EPS, protein, and DNA (39). Biofilm formation enables unicellular organisms to interact with other unicellular organisms, resulting in a multicellular assemblage (30). Bacteria inhabiting biofilms exhibit distinct behaviors compared to free-living planktonic cells, and gene expression patterns of bacteria in these two growth modes can be markedly different. A biofilm has the ability to act as a buffer, protecting associated bacterial cells from rapid fluctuations in environmental conditions. Biofilms also enable an accelerated rate of horizontal genetic exchange, and bacteria in biofilms may be protected from both antibiotics and host defenses (30, 38). The classic definition of a biofilm is an aggregation that forms a mushroom-like shape (11). More recently, it has been revealed that there is greater diversity in the structure of biofilms, ranging from flat aggregations to the classical mushroom-shaped aggregation (30, 38). Structural diversity can arise from differences

in environmental conditions or from the individual bacterial components that comprise the biofilm.

The realization that biofilm formation is a critical aspect of pathogenesis in plant and animal bacterial pathogens has increased the scope and significance of biofilm research (30). For example, the biofilm mode of growth is utilized by organisms such as *Pseudomonas aeruginosa* and *Staphylococcus aureus* in the establishment of chronic human infections (29). The vascular tissue of plants is an additional site of biofilm formation by plant pathogens such as *Pantoea stewartii* subsp. *stewartii*, *Xanthomonas campestris* pv. *campestris*, and *Xylella fastidiosa* (20, 31, 32). The interrelationship between EPS production, biofilm formation, and pathogenesis is also an area of emerging interest. EPS is essential for most biofilms, with a number of studies demonstrating that an inability to produce EPS eliminates biofilm formation, but not initial attachment to surfaces (38). EPS is also an essential pathogenicity factor for many plant-pathogenic bacteria (22).

While amylovoran has long been known as a pathogenicity factor in *E. amylovora*, the connection between amylovoran production, biofilm formation, and pathogenesis has not yet been established. We hypothesized that *E. amylovora* would form biofilms on surfaces, that amylovoran and possibly levan production would be necessary for biofilm formation, and that the biofilm mode of growth would contribute to pathogenesis and xylem vessel colonization and migration. In this study, we demonstrate that *E. amylovora* Ea1189 forms a biofilm *in vitro* and *in planta*. Furthermore, we used genetically-defined mutants to show that amylovoran is necessary for biofilm formation, but not levan. This work also implies that biofilm formation may play a significant role in the pathogenesis of *E. amylovora* and in the movement of *E. amylovora* cells via apple xylem.

MATERIALS AND METHODS

Bacterial strains, plasmids, and growth conditions. The bacterial strains, plasmids, and oligonucleotide primers used in this study are listed in Table 2-1. All strains were grown in Luria Broth (LB) medium at 28°C, unless noted. For biofilm formation assays, strains were also grown in 0.5x LB medium and in minimal medium (MM) (14) and in minimal medium supplemented with 2% sucrose. Growth media were supplemented with the antibiotics ampicillin (Amp) ($50 \mu\text{g ml}^{-1}$); chloramphenicol (Cm) ($20 \mu\text{g ml}^{-1}$); gentamicin (Gm) ($15 \mu\text{g ml}^{-1}$); kanamycin (Km) ($30 \mu\text{g ml}^{-1}$); streptomycin (Sm) ($30 \mu\text{g ml}^{-1}$), and tetracycline (Tc) ($12 \mu\text{g ml}^{-1}$) as necessary.

Insertional and deletion mutagenesis and complementation. We generated a deletion mutant of the levansucrase gene *lsc* of *E. amylovora* by using the λ phage recombinases as previously described for *E. coli* (10). Briefly, we transformed *E. amylovora* strain Ea1189 with plasmid pKD46 encoding recombinases *red* β , γ and *exo*. The transformant Ea1189 (pKD46) was grown overnight in LB broth at 28°C, transferred into fresh LB broth medium containing 0.1% arabinose, and grown to exponential phase. The cells were then made electrocompetent (33) and stored at -80°C. Recombination fragments consisting of a Cm resistance gene (Cm^{R}) with its own promoter, flanked by 50-nucleotide (nt) homology arms of the *lsc* gene were generated by PCR using the plasmid pKD3 as a template. The primers Lsc F and Lsc R were used for construction of a *lsc* deletion mutant (Table 2-1). Another primer pair flanking the target gene and an internal primer pair Cm1 and Cm2 of the Cm^{R} resistance gene was used to confirm the mutant by PCR. The PCR products were gel-purified using a gel purification kit (Qiagen,

Valencia, CA). Following electroporation, transformants were plated on LB medium amended with Amp and Cm. Construction and validation of Ea1189 Δ *ams*, in which a 15.8-kb region including the *ams* biosynthetic operon was deleted, is described elsewhere (41). In the resulting mutants, the majority of the coding region(s) of the *ams* operon or *lsc* gene was replaced by the Km^R or Cm^R marker, respectively. The Ea1189 Δ *lsc* mutant was complemented with plasmid pJMK1, a clone containing the *lsc* gene from *E. amylovora* Ea1189 along with its native promoter ligated into pBBR1MCS-3. The *lsc* gene and upstream sequence was amplified from Ea1189 using the primers *lsc* compF and *lsc* compR (Table 2-1)

Pathogenicity assays. Strains were assayed for virulence using a standard immature pear fruit assay and apple shoot assay as previously described (26, 40). Briefly, for immature pear fruit assays, bacterial suspensions of strains were grown overnight in LB broth, harvested by centrifugation, and resuspended in 0.5x sterile phosphate-buffered saline (PBS) with cells adjusted to approximately 1×10^4 cfu/ml. Immature pears (*Pyrus communis* L. cv. 'Bartlett') were surface sterilized with 10% bleach, dried in a laminar flow hood, and wounded with a sterile needle. Wounded pears were inoculated with 2 μ l of cell suspension and incubated in a humidified chamber at 28°C. Symptoms were recorded at 2, 4, 6, 7, and 8 days post inoculation. For bacterial population studies, the pear tissue surrounding the inoculation site was excised using a no. 4 cork borer and homogenized in 0.5 ml of 0.5x PBS. Bacterial growth within the pear tissue was monitored at 0, 1, 2, and 3 days post inoculation by dilution plating of the ground material on LB medium. Fruits were assayed in triplicate, and each experiment was repeated three times.

For shoot assays, overnight cultures were washed and resuspended in 0.5x PBS at a density of approximately 2×10^8 cfu/ml. We used 2 yr.-old potted apple trees (cv. 'Gala' on M9 rootstock) obtained from Hilltop Nursery (Hartford, MI) in all experiments. The two youngest leaves of the central shoot were cut perpendicularly to mid-vein approximately 2.5 cm from the tip of the leaf using scissors dipped in the bacterial suspension. Symptoms were recorded at 7 and 14 days post inoculation. Samples for population studies were taken at 14 days post inoculation, with the first three cm of the inoculated leaf weighed and then ground in chilled PBS using a Polytron® PT 10-35 blender (Brinkmann Instruments Inc.). Bacterial growth was monitored by dilution plating of ground material on LB medium. Shoot assays were done in triplicate and each experiment was repeated three times.

***In vitro* crystal violet assay for biofilm formation.** We used an *in vitro* biofilm formation assay that was modified from a previously established crystal violet staining assay (27). Briefly, Ea1189, Ea1189 Δ *ams*, Ea1189 Δ *lsc*, and Ea1189 Δ *lsc*/pJMK1 strains were each grown overnight in LB broth to a concentration of 2×10^8 cfu/ml. Five μ l of this overnight culture was then added to 125 μ l of sterile LB medium in individual wells of a 96-well polyvinyl chloride (PVC) plate (Corning, New York). The bacteria were incubated in the plates for 16 h at 28°C using minimal agitation. Suspensions from PVC plates were discarded and a 10% crystal violet stain was added to the wells. To ensure that biofilm rings formed were from *E. amylovora* and not due to excess crystal violet stain, the culture volume was added to half the volume of the well, while the stain completely filled wells. After 1 h, the crystal violet stain was decanted and the wells were gently washed three times with water. Individual wells in the plates were examined visually for the

presence of a crystal violet-stained ring which was indicative of biofilm formation on the walls of the well. This assay was repeated three times for each strain tested.

Biofilm formation was quantified following development on glass coverslips. After overnight growth in LB broth to a density of approximately 2×10^8 cfu/ml, 25 μ l of the culture was added to 2 ml of either LB, 0.5x LB, MM, or MM medium amended with 2% sucrose in individual wells of a 24-well plate (Corning). A glass cover slip was placed at an approximately 30° angle in each well to maximize surface exposure to the growing culture. The plates were incubated overnight at 28°C. After 48 h, the suspension was removed and a 10% crystal violet solution was added for 1 h, after which the glass cover slip was rinsed three times with sterile water. The glass cover slips were air dried for 1 h, and then 200 μ l of 40% methanol, 10% glacial acetic acid was added to wells to resolubilized the crystal violet stain. The solubilized crystal violet was quantified through spectrophotometry at an absorbance of 600 nm using a safire microplate reader (Tecan, Research Triangle Park, NC). Each experiment included 24 replicates, and experiments were repeated three times.

Bright field microscopy was also used to visualize biofilm formation and cell aggregation on the glass cover slips. Cover slips were processed as described above, except the crystal violet stain was not resolubilized following the sterile rinses. Cover slips were then examined using bright field microscopy [Olympus IX71 inverted microscope (Olympus America Inc., N.Y.)] and images of cellular aggregation and biofilm formation were captured.

Confocal laser scanning microscopy visualization of *E. amylovora* biofilms. Biofilm formation was further examined using a flow cell apparatus (Stovall Life Sciences, Greensboro N.C.). *E. amylovora* Ea1189, Ea1189 Δ ams, Ea1189 Δ lsc, and Ea1189 Δ lsc/pJMK1 strains were

labeled with *gfp* or *yfp* by introduction of the appropriate plasmid (pMP2444 or pMP4518) via electroporation. Cell suspensions were established in LB medium in the flow cell and fresh medium was passed through the flow cell chamber for up to 48 h at 25°C, using a configuration detailed in the manufacturer's instructions (Stovall Life Sciences). Chambers were examined using the Zeiss 510 Meta ConfoCor3 LSM confocal laser scanning microscope (CLSM; Carl Zeiss Microimaging, GmbH) and images were captured at 10x and 20x using the LSM image browsing software (Carl Zeiss Microimaging, GmbH). Z-stacks were compiled and a three dimensional image that measured intensity was produced by using the '2.5 dimensions' with the LSM browser.

Visualization of *E. amylovora* in shoot tissue using scanning electron microscopy. The two youngest leaves of three independent apple shoots (cv. 'Gala') were inoculated with Ea1189, Ea1189 Δ *ams*, Ea1189 Δ *lsc*, Ea1189 Δ *lsc*/pJMK1, or sterile 0.5xPBS buffer using the scissor cut method described above, except an additional treatment of Ea1189 Δ *lsc* was conducted at 1×10^{10} so bacterial could be visualized in tissue. Leaves were collected at 0, 2, 4 and 10 days post inoculation, sectioned into 1 cm sections and fixed in paraformaldehyde/glutaraldehyde ([2.5% of each compound in 0.1M sodium cacodylate buffer] Electron Microscopy Sciences, Hatfield PA) at 25°C overnight. The tissue was dehydrated successively in 25%, 50%, 75% and 90% ethanol for 30 min each, and in 100% ethanol three times for 15 min. Samples were then critical point dried using a critical point drier (Balzers CPD, Lichtenstein). Dried petiole tissue was sectioned into 1 mm latitudinal slices after critical point drying to reduce artifacts from fixation process and mounted on aluminum mounting stubs (Electron Microscopy Sciences, Hatfield PA), and then coated with gold using a gold sputter coater (EMSCOPE SC500 Sputter coater, Ashford, Kent, Great Britain) for leaf tissue or osmium using a pure osmium coater (Neoc-an,

Meiwa Shoji Co. LTD, Japan) for tissue inoculated with bacteria allowing for greater resolution. Images were captured on the scanning electron microscope (SEM), JEOL 6400V (Japan Electron Optics Laboratories) with a LaB6 emitter (Noran EDS) using analySIS software (Soft Imaging system, GmbH).

RESULTS

Construction and analysis of amylovoran and levansucrase mutants. We used a modified one-step PCR deletion method (10) to construct a mutant of *E. amylovora* Ea1189 with a deletion of the levansucrase gene *lsc*. In addition, we used Ea1189 Δ *ams*, a strain in which a total of 15.8 kb was deleted from the Ea1189 chromosome encompassing all 12 genes between *amsG* and *amsL* (41). Amylovoran production was completely abolished in this strain (41).

Pathogenicity assays were conducted using Ea1189 Δ *ams* and Ea1189 Δ *lsc* and, similar to findings by others (3, 17, 36), the *ams* operon deletion mutant was completely nonpathogenic in the immature pear assay and the *lsc* mutant exhibited a reduction in virulence (Fig. 2-1).

Complementation of Ea1189 Δ *lsc* with the *lsc* gene encoded on pJMK1, restored pathogenicity to Ea1189 levels in immature pear fruit assay (data not shown). In addition, Ea1189 Δ *lsc*/pJMK1 but not Ea1189 Δ *lsc* produced elevated, domed colonies on MM agar medium amended with 2% sucrose, indicative of levansucrase activity. Results with mutants in apple shoot inoculation assays were consistent with those in the immature pear assays (data not shown).

***In vitro* analysis of biofilm formation.** We initially used the crystal violet staining assay with modification (27) to examine biofilm formation *in vitro*. This common technique has been used with a wide variety of bacteria to assess biofilm formation on a surface at the air-liquid interface. After 16 h of growth in a PVC 96-well assay plate, Ea1189 demonstrated visual evidence of

biofilm formation, while there was an absence of biofilm formation within the wells where Ea1189 Δ *ams* was grown (data not shown). Ea1189 Δ *lsc* retained the ability to form a biofilm, but at a reduced rate as evidenced by rings in the wells that were neither as dark nor as thick as Ea1189 (data not shown).

Quantification of biofilm formation was measured, similar to other biofilm studies (19), to assess the effect of growth media and the role of the *ams* and *lsc* mutations on biofilm formation. Biofilm formation by the strain Ea1189 on glass following growth in LB or 0.5x LB was similar in each of three experiments (Fig. 2-2). We also assessed biofilm formation of cells grown in MM medium, a medium which has been used previously for evaluation of exopolysaccharide production in *E. amylovora* (2, 4). Biofilm formation by Ea1189 in MM amended with 2% sucrose was only slightly greater than that in MM alone (Fig. 2-2). However, the biofilms formed by Ea1189 after growth in MM amended with 2% sucrose or MM were significantly reduced compared to biofilms formed by Ea1189 after growth in LB or 0.5x LB (Fig. 2-2).

Based on the growth media results, we used 0.5x LB as the growth medium for subsequent experiments. In the next set of experiments, we visualized biofilm formation on glass cover slips using bright field microscopy and quantified biofilm formation by Ea1189, Ea1189 Δ *ams*, Ea1189 Δ *lsc*, and Ea1189 Δ *lsc*/pJMK1. Similar to the assay results using the 96-well assay plate, cells of strain Ea1189 readily formed large aggregates (Fig. 2-3A) which is a hallmark of biofilm formation, while Ea1189 Δ *ams* cells did not aggregate (Fig. 2-3B). Strain Ea1189 Δ *lsc* also showed a decrease in overall aggregation compared to Ea1189, but aggregates were present on the glass cover slip (Fig. 2-3C). Complementation of Ea1189 Δ *lsc* with pJMK1 restored aggregation on cover slip to wild-type levels (data not shown). Strain Ea1189 Δ *ams*

exhibited a significant reduction in biofilm formation of greater than 80% compared to Ea1189 in the glass cover slips (Fig. 2-4). Biofilm formation by Ea1189 Δ *lsc* was intermediate to that of Ea1189 and Ea1189 Δ *ams* and was complemented with pJMK1, but not to wild-type levels, although not significantly different from wild-type levels (Fig. 2-4).

Confocal laser scanning microscopy visualization of *E. amylovora* biofilms. We also analyzed biofilm formation *in vitro* using a flow cell apparatus. This method enabled a non-invasive observation of biofilm formation under a continuous flow of fresh 0.5x LB medium into an enclosed chamber that was inoculated with either Ea1189/pMP2444 (*gfp*+), Ea1189 Δ *ams*/pMP4518 (*yfp*+), Ea1189 Δ *lsc*/pMP2444 (*gfp*+), or Ea1189 Δ *lsc*/pJMK1/pMP2444 (*gfp*+). After 24 h, we visualized cultures grown in the flow cells using CLSM, and generated a three dimensional view of the confocal image through the measurement of signal intensity. An intensity map with arbitrary values was established which measured the amount of fluorescence emitted from the *gfp*- or *yfp*-labeled cells, where the intensity of the signal reports the density of cells in a particular location. In this assay, Ea1189/pMP2444 demonstrated hallmark signs of biofilm formation including the formation of large spatial cellular aggregates identified through high signal intensity of *gfp* fluorescence after 24 h of growth (Fig. 2-5A). Aggregates were observed throughout the entire chamber attached to the surface of the chamber and exhibiting vertical growth (Fig. 2-5A). In contrast, the Ea1189 Δ *ams*/pMP4518 culture was uniform and had a very low signal intensity of *yfp* fluorescence, showing no signs of aggregation after 24 h (Fig. 2-5B). Growth of Ea1189 Δ *lsc*/pMP2444 in the flow cell resulted in the production of biofilms that were intermediate to the signal intensity of Ea1189/pMP2444 (Fig. 2-5C). The complemented strain Ea1189 Δ *lsc*/pJMK1 + pMP2444 (*gfp*+) exhibited large spacial aggregates

and vertical growth similar to the wild-type strain after 24 h growth (data not shown). Flow cell experiments with each strain were repeated at least three times with similar results.

***in planta* biofilm formation analysis.** Latitudinal sections of petiole tissue from the youngest leaves sampled from shoot tips inoculated with *E. amylovora* Ea1189 and mutant strains were examined using SEM, with the sectioning occurring after the fixation process so material examined had as little artifact as possible. Extensive cell growth was evident within the vascular system, and characteristics of biofilm formation were observed in all samples from Ea1189-inoculated tissue. We first observed multicellular aggregates that appeared to be attached to the xylem wall with cell growth inward into the xylem vessel (Fig. 2-6A). We further observed multicellular aggregates encased within a matrix of fibrillar material that traversed the diameter of xylem vessels, linking cells on either end that were attached to the xylem wall (Fig. 2-6B). Biofilms in more advanced stages of development were comprised of greater numbers of cells and associated fibrillar material retaining linkages to wall-attached cells (Fig. 2-6C). In some cases, the xylem vessels were completely filled with the bacterial biofilm which also included the apparent extrusion of cells outside of individual vessels (Fig. 2-6D). Each stage of biofilm development in xylem vessels (Fig. 2-6A-D) could be visualized within one sample.

It was very difficult to visualize cells of Ea1189 Δ *ams* in petiole tissue after inoculation, and this was confirmed by cell count data that indicated a 10^6 -fold reduction in population within 2 days after inoculation (data not shown). We were only able to visualize Ea1189 Δ *ams* cells near the inoculation site in a few samples; these cells differed from cells of the wild-type Ea1189 in that the cells were elongated and there was no evidence of aggregation or of the production of a fibrillar matrix (Fig. 2-7A). Observation of Ea1189 Δ *lsc* *in planta* revealed that

cells were mostly associated with leaf parenchymal tissue (Fig. 2-7B). We did also observe biofilm formation by Ea1189 Δ *lsc* in xylem tissue similar to that of Ea1189; however, there appeared to be a reduction of the fibrillar matrix materials. Inoculations with Ea1189 Δ *lsc* using higher doses (10^{10} cfu/ml) were also done to determine if higher cell doses would facilitate xylem colonization; however, we did not observe any cells within xylem vessels using the concentrated inoculum.

DISCUSSION

The results of our *in vitro* and *in planta* results demonstrated that *E. amylovora* cells form biofilms and that biofilm growth may play an important role in host plant colonization. The production of biofilms *in planta* is a characteristic shared among several vascular plant pathogens including *P. stewartii* subsp. *stewartii*, *X. campestris* pv. *vesicatoria*, and *X. fastidiosa* (20, 31, 320). Biofilm formation is an important developmental growth feature of a range of bacterial pathogens of plants and animals, and the biofilm growth habit represents an ecological survival strategy in which cells present in the biofilm are more resistant to external stress (29). The transcriptome of biofilm-associated cells differs from that of free-living planktonic cells and biofilm-associated cells are also more resistant to antibiotics and potentially less susceptible to detection by host surveillance mechanisms (23). Thus, the importance of biofilms to pathogenesis is an emerging concept in both animal and plant pathology.

The amylovoran EPS was required for biofilm formation by *E. amylovora*, and the absence of amylovoran production was accompanied by reductions in both attachment to surfaces and cell-to-cell aggregation. EPS and other ligands such as pili or fimbriae facilitate anchoring of bacterial cells to surfaces (13). Attachment is a critical first step in biofilm

development, and surface attachment apparently provides a strong selective advantage to diverse bacteria as surface-associated organisms outnumber free-living cells in most ecosystems (8). Surface association may promote access to nutrients; for example, nutrients in aqueous environments tend to concentrate near solid surfaces (13). Attachment to surfaces may also protect bacterial pathogens from host defense responses (28). In xylem, surface anchoring is of additional importance for bacterial establishment because of sap flow. Cell-to-cell aggregation promotes the next phase of biofilm growth and requires determinants such as type IV pili that enable cells to migrate across a surface and form microcolonies. In *X. fastidiosa*, type I and type IV pili and fimbrial adhesins are involved in aggregation, and a fimbrial adhesin mutant was decreased in virulence, possibly due to the production of a reduced biofilm in host xylem elements (12, 15). Biofilm production by *E. amylovora* within xylem vessels of apple appears to be similar to that of *P. stewartii* subsp. *stewartii* in xylem vessels of corn (20) in that the adherence of cells to xylem walls and aggregation is accompanied by growth extending into the lumen of the xylem vessel. Developing biofilms from various locations on vessel walls can then fuse together, resulting in vessel blockage and the wilting symptoms characteristic of fire blight and Stewart's wilt diseases. Thus, the inability to produce amylovoran cripples the *E. amylovora* mutant cells in all aspects of biofilm formation resulting in cells that are nonpathogenic, possibly due to increased susceptibility to host defense responses (16), but also due to an inability to effectively establish a biofilm within the host.

We found that levan played a role in biofilm formation in *E. amylovora* as a levansucrase-deficient mutant was reduced in biofilm formation and in cell-to-cell aggregation *in vitro*. In addition, secretion of levansucrase is thought to contribute to the colonization of sucrose-containing tissue by *E. amylovora* (17). Plants in the Rosaceae family contain sorbitol

and sucrose as the major storage and transport carbohydrates (7). Levansucrase is utilized by *E. amylovora* to cleave sucrose to fructose which is polymerized into levan with the additional release of glucose (17). Sucrose can also be transported into *E. amylovora* cells and metabolized, and sucrose utilization is a virulence factor that is required for successful leaf colonization (5). An *lsc* mutant would retain the ability to metabolize sucrose suggesting that the energy status of the pathogen is not affected. Instead, our results imply that a reduction in biofilm development *in planta* by the *E. amylovora* Δlsc mutant would result in the observed reduction in virulence, and the virulence defect was restored by complementation. Levan has also been hypothesized to contribute to protection of *E. amylovora* cells against host defenses (17), and could play this role by contributing to biofilm development. Visualization of *E. amylovora* Δlsc *in planta* also revealed that the mutant was localized to the mesophyll tissue, a location where we did not detect the wild type cells in abundance. A misorientation of cells might also contribute to a reduction in virulence and reduced xylem colonization. Localization to the correct tissue appears to be critical to the proper development of fire blight. Localization to incorrect tissue may expose the cell to host defenses or may not provide the proper environment for further disease development.

In summary, we demonstrated that *E. amylovora* forms a biofilm and the importance of biofilm formation to the fire blight infection. We were also able to provide evidence that amylovoran, the main EPS component, is necessary for biofilm formation, and that levan, a minor EPS component, also plays a role in biofilm formation. Our results imply that biofilm formation and pathogenesis are linked; however, further experimentation is needed to confirm this hypothesis. We are currently identifying genes encoding traits necessary for biofilms that

are independent of EPS production. Mutational analysis of those genes would enable determination of the mechanistic role of biofilm formation in *E. amylovora* pathogenesis.

Table 2-1. Bacterial strains, plasmids and primers used in chapter 2.

Strains, plasmids, and primers	Relevant Characteristics ^a	Source or reference
Strains		
<i>E. amylovora</i>		
Ea1189	Wild type	6
Ea1189 Δ <i>ams</i>	Deletion mutant of the <i>ams</i> operon	41
Ea1189 Δ <i>lsc</i>	Deletion mutant of <i>lsc</i> encoding levansucrase	This study
Plasmids		
pBBR1MC-3	Broad-host-range cloning vector, Tc ^R	19
pJMK1	<i>Lsc</i> gene and native promoter in pBBR1MCS-3	This study
pKD3	Plasmid utilized in λ phage recombinase mutagenesis method	10
pKD46	Expresses recombinases red, β , λ , and exo for the construction of deletion mutants	10
pMP2444	pBBR1MCS-5 backbone; <i>gfp</i> expressed from <i>lac</i> promoter; Gm ^R	37
pMP4518	pBBR1MCS-5 backbone; <i>yfp</i> expressed from <i>lac</i> promoter; Gm ^R	37
Primers		
Lsc F	5'-ATGTCAGATTATAATTATAAACC AACGCTGTGGACTCGTGCCGATGC ATTGTGTAGGCTGGAGCTGCTTC-3'	This study

Table 2-1
(cont'd)

Lsc R	5'-AATAAAATTTTCATTACAGAA AGTAACGGCCTTATATAGGTATTAG CTTCGCATATGAATATCCTCCTTA-3'	This study
Comp F	5'GGTACCAAACGTACAG GAACACCTTATATTCTG-3'	This study
Comp R	5'-GAGCTCATGACTATC ATAGCGATATCAGCC-3'	This study

^a Abbreviations: Gm, gentamicin; Sm, streptomycin; Tc, tetracycline

Figure 2-1. Symptoms of *E. amylovora* Ea1189, Ea1189 Δ *ams*, and Ea1189 Δ *lsc* in immature pear at seven days post-inoculation. Ea1189 Δ *ams* is nonpathogenic and Ea1189 Δ *lsc* is reduced in virulence. Representative pears shown from three individual experiments, five pears per trial, inoculated with culture of 1×10^4 cfu/ml.

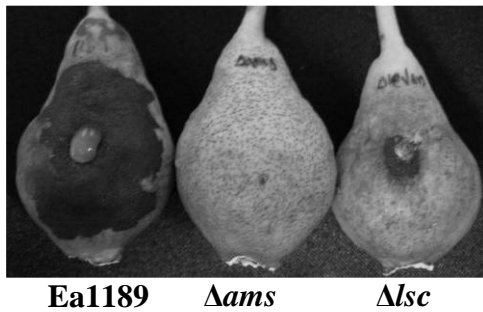


Figure 2-2. Quantification of the effect of growth medium on biofilm growth on glass by *E. amylovora* Ea1189. Biofilm formation is significantly greater in Luria Broth (LB) and 0.5x LB than in Minimal Media (MM), or MM plus 2% sucrose. Measurements were taken after 48 h growth in each medium. Values represent the mean of 24 sample replicates from one representative experiment. Sample means were compared by analysis of variance and separated using the Student's t-test. The presence of different letters above sample mean values indicates the means were significantly different at $P < 0.05$.

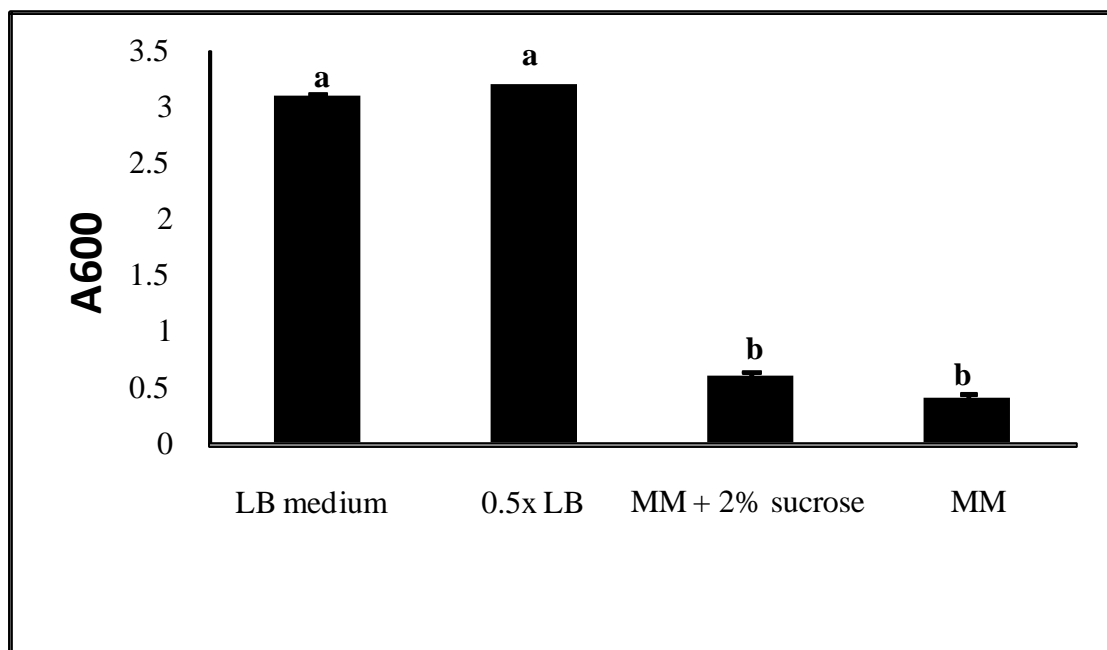


Figure 2-3. Attachment and aggregation of *E. amylovora* Ea1189, Ea1189 Δ *ams* and Ea1189 Δ *lsc* to glass after 16 h. A) *E. amylovora* Ea1189 has large aggregates, B) Ea1189 Δ *ams* has only single cells, and C) Ea1189 Δ *lsc* has reduced aggregate size on the glass surface. Cells were visualized using bright field microscopy following staining with a violet solution. Note: cells appear on both sides of the glass surface with lighter gray cell aggregates on the reverse side.

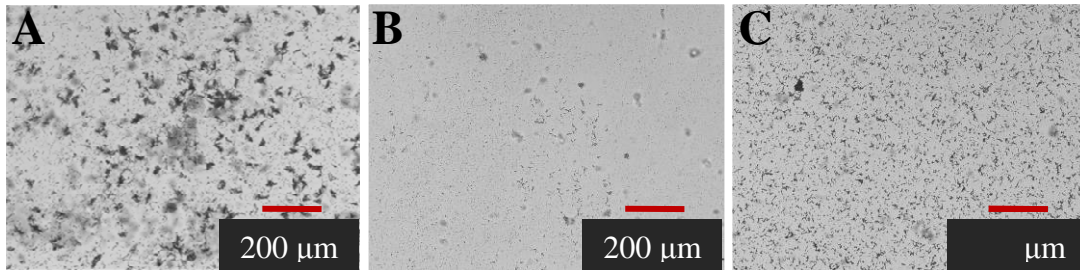


Figure 2-4. Quantification of biofilm formation of Ea1189, Ea1189 Δ ams, Ea1189 Δ lsc, and Ea1189 Δ lsc/pJMK1 in 0.5x LB after 48 h. Values represent mean of three replicates, 24 sample replicates from one representative experiment. Sample means were compared by an analysis of variance and separated using the Student t-test. The presence of different letters above sample mean values indicates the means were significantly different at $P < 0.05$.

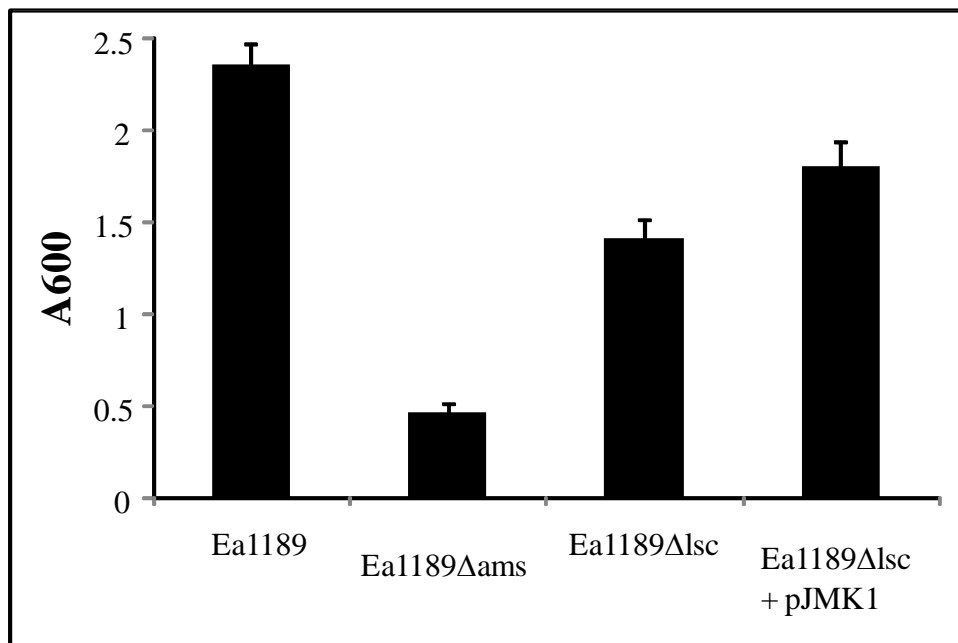


Figure 2-5. Three-dimensional view of flow cell contents through intensity mapping after 24 h growth. A) *E. amylovora* Ea1189, B) Ea1189 Δ ams, C) Ea1189 Δ lsc. Aggregate size is indicated by intensity. The more bacterial cells present in one location (an aggregate), the more intense the color. Note: intensity mapping has set max value at 250 and maps are developed with five color layers. Additional layers of color indicate greater intensity of signal. Representative of three separate trials.

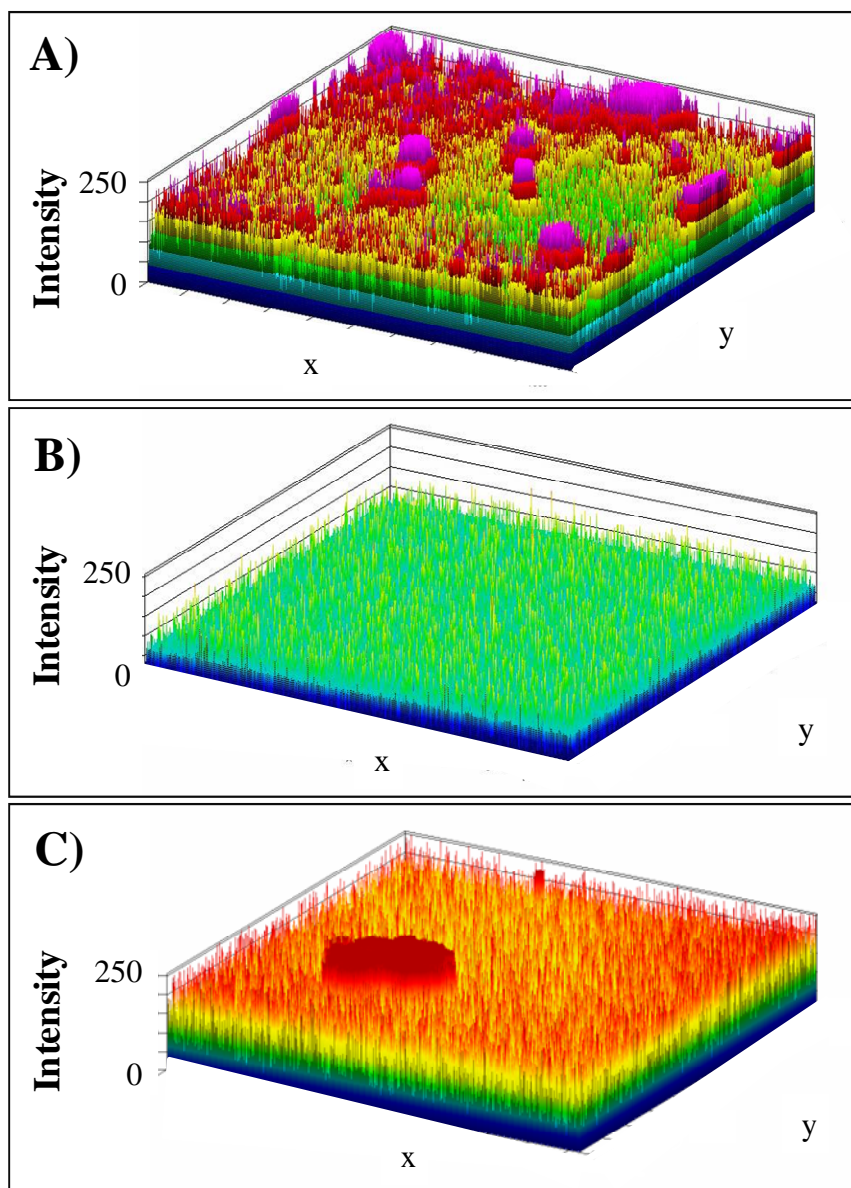


Figure 2-6. Biofilm formation *in planta* by *E. amylovora* Ea1189 seven days post-inoculation of 2×10^8 cfu per ml using the scissor cut method. A) Attachment of cells to inner walls of xylem vessels, aggregation, and initial growth into the lumen of the vessel. B) Fusion of developing biofilms across the expanse of xylem vessels. The fibrillar matrix in which cells are embedded is prominent. C) Further development of biofilms following additional cell growth, and D) complete filling of xylem vessel by the *E. amylovora* biofilm.

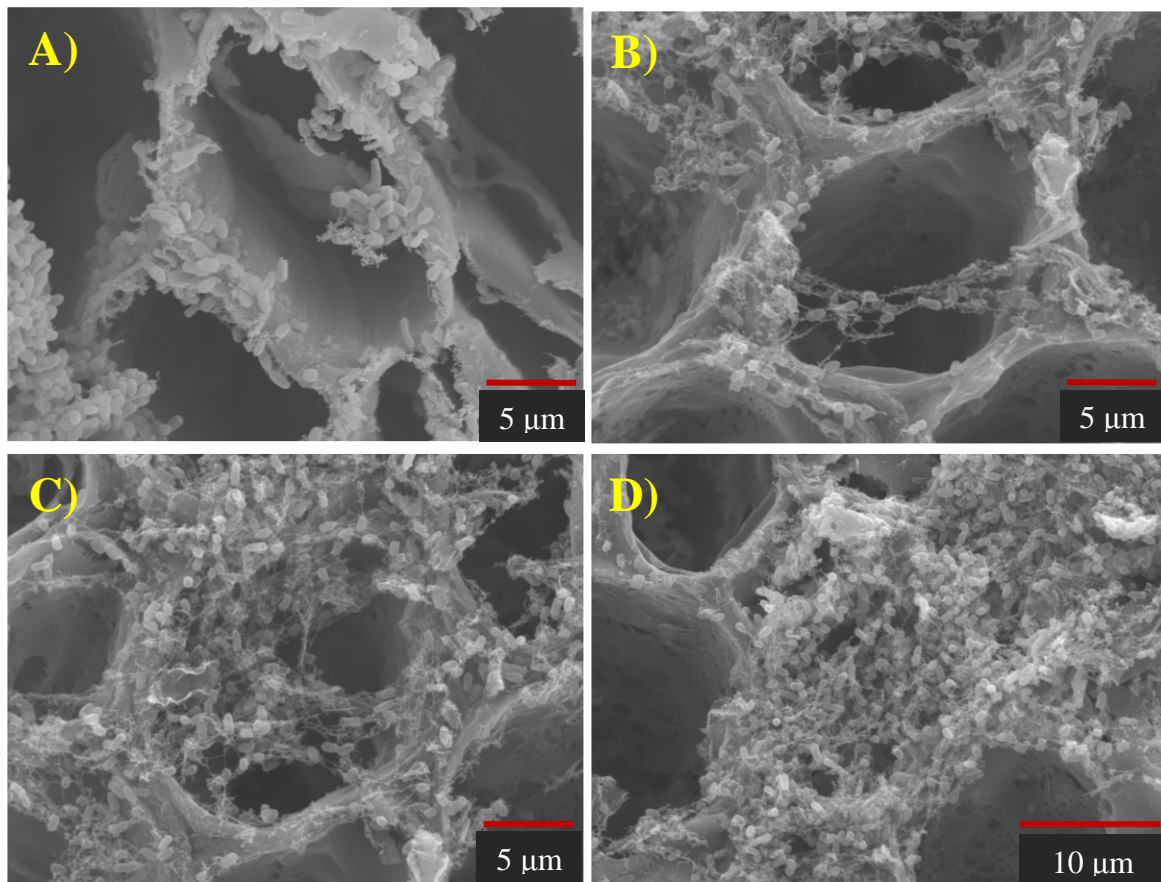
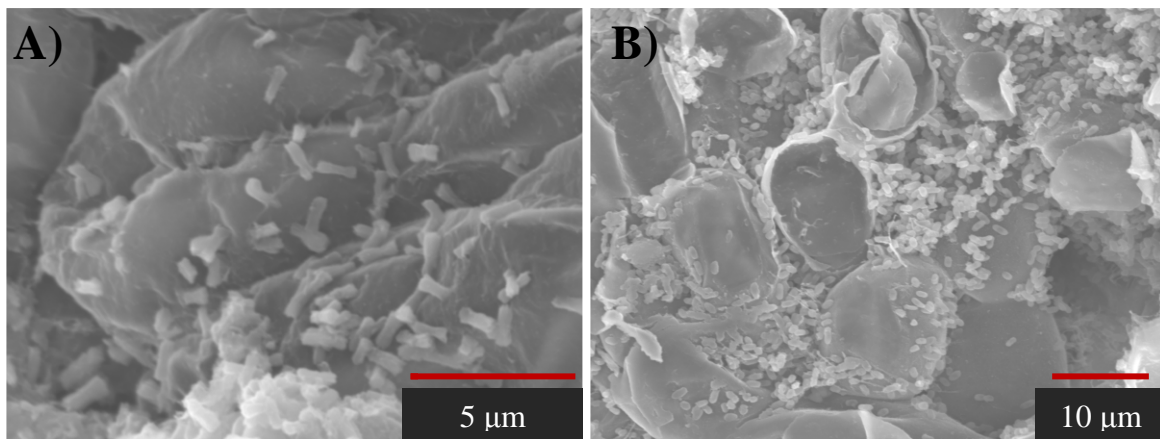


Figure 2-7. A) Visualization of *E. amylovora* Ea1189 Δ ams 48 h post-inoculation with 2×10^8 cells into apple shoots. Cells appear misshapen with no evidence of aggregation or the presence of extracellular fibrillar material. B) Visualization of Ea1189 Δ sc in apple leaf tissue, inoculated with cell concentration of 1×10^{10} . Bacterial cells are localized to plant parenchymal cells with reduced colonization of xylem vessels.



LITERATURE CITED

LITERATURE CITED

1. Ayers, A.R., Ayers, S.B., and Goodman, R.N. 1979. Extracellular polysaccharide of *Erwinia amylovora*: a correlation with virulence. *Appl. Environ. Microbiol.* 38: 659-666.
2. Bellemann, P., Bereswill, S., Berger, S., and Geider, K. 1994. Visualization of capsule formation by *Erwinia amylovora* and assays to determine amylovoran synthesis. *Int. J. Biol. Macromol.* 16: 290-296.
3. Bellemann, P., and Geider, K. 1992. Localization of transposon insertions in pathogenicity mutants of *Erwinia amylovora* and their biochemical characterization. *J. Gen. Microbiol.* 138: 931-940.
4. Bennett, R.A., and Billing, E. 1978. Capsulation and virulence in *Erwinia amylovora*. *Ann. Appl. Biol.* 89: 41-45.
5. Bogs, J., and Geider, K. 2000. Molecular analysis of sucrose metabolism of *Erwinia amylovora* and influence on bacterial virulence. *J. Bacteriol.* 182: 5351-5358.
6. Burse, A., Weingar, H., and Ullrich, M.S. 2004. NorM, an *Erwinia amylovora* multidrug efflux pump involved in *in vitro* competition with other epiphytic bacteria. *Appl. Environ. Microbiol.* 70:693-703.
7. Chong, C. 1971. Study of seasonal and daily distribution of sorbitol and related carbohydrates within apple seedlings by analysis of selected tissue and organs. *Can. J. Plant Sci.* 51: 519-525.
8. Costerton, J.W., Cheng, K.-J., Geesey, G.G., Ladd, T.I., Nickel, J.C., Dasgupta, M., and Marrie, T.J. 1987. Bacterial biofilms in nature and disease. *Annu. Rev. Microbiol.* 41: 435-464.
9. Danhorn, T., and Fuqua, C. 2007. Biofilm formation by plant-associated bacteria. *Annu. Rev. Microbiol.* 61: 401-422.
10. Datsenko, K.A., and Wanner, B.L. 2000. One step inactivation of chromosomal genes in *Escherichia coli* K-12 using PCR products. *Proc. Natl. Acad. Sci. USA* 97: 6640-6645.
11. Davey, M.E., and O'Toole, G.A. 2000. Microbial biofilms: from ecology to molecular genetics. *Microbiol. Mol. Biol. Rev.* 64: 847-867.
12. De La Fuente, L., Burr, T.J., and Hoch, H.C. 2008. Autoaggregation of *Xylella fastidiosa* cells is influenced by type I and type IV pili. *Appl. Environ. Microbiol.* 74: 5579-5582.
13. Dunne, W.M. Jr. 2002. Bacterial adhesion: seen any good biofilms lately? *Clin. Microbiol. Rev.* 15: 155-166.

14. Falkenstein, H., Zeller, W., and Geider, K. 1989. The 29 kb plasmid, common in strains of *Erwinia amylovora*, modulates development of fireblight symptoms. *J. Gen. Microbiol.* 135: 2643-2650.
15. Feil, H., Feil, W.S., and Lindow, S.E. 2007. Contribution of fimbrial and afimbrial adhesins of *Xylella fastidiosa* to attachments to surfaces and virulence to grape. *Phytopathology* 97: 318-324.
16. Geider, K. 2006. Twenty years of molecular genetics with *Erwinia amylovora*: answers and new questions about EPS-synthesis and other virulence factors. *Acta Hort.* 704: 397-402.
17. Geier G., and Geider, K. 1993. Characterization and influence on virulence of the levansucrase gene from the fireblight pathogen *Erwinia amylovora*. *Physiol. and Mol Plant Pathol.* 42: 387-404.
18. Goodman, R.N., Huang, J.S., and Huang, P.Y. 1974. Host-specific phytotoxic polysaccharide from apple tissue infected by *Erwinia amylovora*. *Science.* 183: 1081-1082.
19. Hossain, M.M., and Tsuyumu, S. 2006. Flagella-mediated motility is required for biofilm formation by *Erwinia carotovora* subsp. *carotovora*. *J. Gen. Plant Pathol.* 72: 34-39.
20. Koutsoudis, M.D., Tsaltas, D., Minogue, T.D., and von Bodman, S.B. 2006. Quorum-sensing regulation governs bacterial adhesion, biofilm development, and host colonization in *Pantoea stewartii* subspecies *stewartii*. *Proc. Natl. Acad. Sci. USA.* 103: 5983-5988.
21. Kovach, M.E., Elzer, P.H., Hill, D.S., Robertson, G.T., Farris, M.A., Roop, R.M., and Peterson, K.M. 1995. Four new derivatives of the broad-host-range cloning vector pBBR1MCS, carrying different antibiotic-resistant cassettes. *Gene* 166: 175-176.
22. Leigh, J., and Coplin, D. 1992. Exopolysaccharides in plant-bacterial interactions. *Annu. Rev. Microbiol.* 46: 307-346.
23. Mah, T.C., and O'Toole, G.A. 2001. Mechanisms of biofilm resistance to antimicrobial agents. *Trends Microbiol.* 9: 34-39.
24. Nimtz, M., Mort, A., Domke, T., Wray, V., Zhang, Y., Qiu, F., Coplin, D., and Geider, K. 1996. Structure of amylovoran, the capsular exopolysaccharide from the fire blight pathogen *Erwinia amylovora*. *Carbohydr. Res.* 287: 59-76.
25. Norelli, J., Jones, A.L., and Aldwinkle, H.S. 2003. Fire blight management in the twenty-first century: using new technologies that embrace host resistance in apple. *Plant Disease.* 87: 756-765.

26. Oh, C.H., Kim, J.F., and Beer, S.V. 2005. The Hrp pathogenicity island of *Erwinia amylovora* and identification of three novel genes required for systemic infection. *Mol Plant Pathol.* 6: 125-138.
27. O'Toole, G., Pratt, L., Watnick, P., Newman, D., Weaver, V., and Kolter, R. 1999. Genetic approaches to study of biofilms. *Methods Enzymol.* 310: 91-107.
28. Palmer, J., Flint, S., and Brooks, J. 2007. Bacterial cell attachment, the beginning of a biofilm. *J. Ind. Microbiol. Biotechnol.* 34:577-588.
29. Parsek, M.R., and Singh, P.K. 2003. Bacterial biofilms: an emerging link in disease pathogenesis. *Annu. Rev. Microbiol.* 57: 677-701.
30. Ramey, B.E., Koutsoudis, M., von Bodman, S.B., and Fuqua, C. 2004. Biofilm formation in plant-microbe associations. *Curr. Opin Microbiol.* 7: 602-609.
31. Rigano, L.A., Siciliano, F., Enrique, R., Sendin, L., Filippone, P., Torres, P.S., Questa, J., Dow, J.M., Castagnaro, A.P., Vojnov, A.A., and Marano, M.R. 2007. Biofilm formation, epiphytic fitness, and canker development in *Xanthomonas axonopodis* pv. *citri*. *Mol. Plant-Microbe Interact.* 20: 1222-1230.
32. Roper, M.C., Greve, L.C., Labavitch, J.M., and Kirkpatrick, B.C. 2007. Detection and visualization of an exopolysaccharide produced by *Xylella fastidiosa* *in vitro* and *in planta*. *Appl. Environ. Microbiol.* 73: 7252-7258.
33. Sambrook, J., Fritsch, E.F., and Maniatis, T. 1989. *Molecular cloning- a laboratory manual* 2nd edition. Cold Spring Harbour Laboratory Press, New York.
34. Sijam, K., Goodman, R.N., and Karr, A.L. 1985. The effect of salts on the viscosity and wilt-inducing capacity of the capsular polysaccharide of *Erwinia amylovora*. *Physiol. Plant Pathol.* 26: 231-239.
35. Sjulín, T.M., and Beer, S.V. 1978. Mechanism of wilt induction by amylovorin in cotoneaster shoots and its relation to wilting of shoots infected by *Erwinia amylovora*. *Phytopathology* 68: 89-94.
36. Steinberger, E.M., and Beer S.V. 1988. Creation and complementation of pathogenicity mutants of *Erwinia amylovora*. *Mol. Plant-Microbe Interact.* 1: 135-144.
37. Stuurman, N., Pacios Bras, C., Schlaman, H.R.M., Wijfjes, A.H.M., Bloemberg, G., and Spaink, H.P. 2000. Use of green fluorescent protein color variants expressed on stable broad-host-range vectors to visualize *Rhizobia* interacting with plants. *Mol. Plant-Microbe Interact.* 13: 1163-1169.

38. Sutherland, I.W. 2001. Biofilm exopolysaccharides: a strong and sticky framework. *Microbiology*. 147: 3-9.
39. Van der Zwet, T., and Keil, H.L. 1979. Fire Blight: a bacterial disease of rosaceous species. *USDA Agriculture Handbook* 510.
40. Zhao, Y., Blumer, S.E., and Sundin, G.W. 2005. Identification of *Erwinia amylovora* genes induced during infection of immature pear tissue. *J. Bacteriol.* 187: 8088-8103.
41. Zhao, Y., Sundin, G.W., and Wang, D. 2009. Construction and analysis of pathogenicity island deletion mutants of *Erwinia amylovora*. *Can. J. Microbiol.* 55: 457-464.

Chapter 3: Cell surface attachment structures contribute to biofilm formation and xylem colonization of *Erwinia amylovora*.

This chapter has been modified from work submitted for publication: Koczan, J.M., Lenneman, B.R., McGrath, M.J., and Sundin, G.W. Applied Environmental Microbiology.

ABSTRACT

Biofilm formation plays a critical role in the pathogenesis of *Erwinia amylovora* and the systemic invasion of plant hosts. The functional role of the exopolysaccharides amylovoran and levan in pathogenesis and biofilm formation has been evaluated. However, the role of biofilm formation, independent of exopolysaccharide production, in pathogenesis and movement within plants, has not been studied previously. Evaluation of the role of attachment in *E. amylovora* biofilm formation and virulence was examined through the analysis of deletion mutants of genes encoding structures postulated to function in attachment to surfaces or in cellular aggregation. The genes and gene clusters studied were selected based on bioinformatics. Microscopic analyses and quantitative assays demonstrated that attachment structures such as fimbriae and pili are involved in the attachment of *E. amylovora* to surfaces and are necessary for the production of mature biofilms. A time course assay indicated that type I fimbriae function earlier in attachment, while type IV pilus structures appear to function later in attachment. Our results indicate that multiple attachment structures are needed for mature biofilm formation and full virulence, and that biofilm formation facilitates entry and is necessary for the buildup of large populations of *E. amylovora* cells into xylem tissue.

INTRODUCTION

Biofilm development is often utilized by bacterial pathogens to aid in host establishment, population expansion, and ultimately in disease proliferation (7, 27). The biofilm matrix protects cells from stressful environmental conditions, and enables increased nutrient acquisition. The formation of biofilms is a coordinated and highly regulated process that exhibits distinct transitions between phases. These developmental phases include planktonic (free swimming), attachment (reversible and irreversible), mature biofilm, and detachment (30). The specific regulatory triggers governing the transition between phases are largely unknown; however, it has been shown that mechanical signals, nutritional and metabolic signals, quorum sensing signals, and host derived signals can shift biofilm development through the different phases (7, 16). By understanding the functional mechanisms of distinct biofilm phases in pathogenesis, potential novel targets for disease control can be discovered.

Bacteria produce numerous proteinaceous structures that can be used in cell adhesion and attachment to surfaces. These structures range from monomeric proteins to protein complexes (24) and include the pili and fimbriae, which consist of multiple different appendages, and other structures such as curli, adhesins, intimins, and invasins (16, 17, 24). An understanding of the roles these structures play in attachment, overall biofilm formation, as well as pathogenesis is still at the early stages; however, it has been shown that *Escherichia coli* and *Pseudomonas aeruginosa* both utilize pili and fimbriae in biofilm formation (7). Recently, the roles of afimbrial and fimbrial adhesins of *Xylella fastidiosa* and pili of *Ralstonia solanacearum* and *Acidovorax avenae* have been explored, further demonstrating that biofilm formation within vascular plant pathogens is an important factor in virulence (1, 9, 14). However, though cell

surface structures have been implicated in biofilm formation and attachment, the roles of the structures can vary greatly among different species (7).

The gram-negative plant pathogen *Erwinia amylovora* is the causal agent of fire blight. This organism is highly virulent and capable of rapid systemic movement within plant hosts and of rapid dissemination among Rosaceous species, including apple and pear, when environmental conditions are favorable. The internal movement of the pathogen through the vascular system of plants, and the ability of the pathogen to infect flowers, actively growing shoots, and roots, makes the management of fire blight difficult (21). Previous work has demonstrated that the exopolysaccharides amylovoran and levan are important elements in the biofilm formation of *E. amylovora* (18). Amylovoran is a pathogenicity factor that is also thought to function as a shield that protects cells from host-elicited antimicrobial responses from plants (3). Levan is a known virulence factor (10), though its specific role in pathogenesis is unknown. We were interested in determining the specific role of biofilm formation in *E. amylovora* pathogenesis. We hypothesized that we could use a genetic approach to uncouple biofilm formation from exopolysaccharide biosynthesis thus enabling an evaluation of the importance of biofilm formation in virulence without compromising the pathogen due to a defect in exopolysaccharide biosynthesis. However, to separate biofilm formation from pathogenicity factors, other determinants of biofilm formation are needed. We further hypothesized that *E. amylovora* encodes for surface structures that are necessary for the first critical step of biofilm formation, attachment. *E. amylovora* is known to produce peritrichous flagella and a type III secretion apparatus (13, 27); however, the role of these and other surface appendages in attachment is not known.

In this study, we utilized a bioinformatics approach and the recently sequenced genome of *E. amylovora* (32, 33) to identify genes encoding putative cell surface attachment structures. Individual genes and gene clusters were deleted, and we used a combination of in vitro attachment assays and plant virulence assays to demonstrate that multiple attachment structures are present in *E. amylovora* and play a role in biofilm formation, which is critical to pathogenesis and systemic movement in the host.

MATERIALS AND METHODS

Bacterial strains, plasmids, and growth conditions. The bacterial strains, plasmids, and oligonucleotide primers used in this study are listed in Table 3-1. All strains were grown in Luria Broth (LB) medium at 28°C. For biofilm formation assays, strains were grown in 0.5 x LB. Growth media were supplemented with the antibiotics ampicillin (Amp) (50 $\mu\text{g ml}^{-1}$); chloramphenicol (Cm) (20 $\mu\text{g ml}^{-1}$); gentamicin (Gm) (15 $\mu\text{g ml}^{-1}$); and tetracycline (Tc) (12 $\mu\text{g ml}^{-1}$) as necessary. For PCR amplification, Invitrogen reagents, protocol, and settings were used (Invitrogen Corp.; Carlsbad CA), unless otherwise noted.

Deletion mutagenesis and complementation. Deletion mutants within individual genes or of gene clusters were generated using the λ phage recombinase as previously described (41). Gene names, putative function, annotated gene ID numbers, and maps for *E. amylovora* genes and gene clusters mutated in this study are listed in Table 3-2 and shown in Fig. 3-1. The following deletions were constructed: $\Delta flhCD$, $\Delta fliADST$, ΔEAM_{2544} , $\Delta flgABCDEFGHIJKLMN$ to generate the mutant designated $\Delta flg 3$; $\Delta fliEFGHIJKLMNOPQ$ to generate the mutant designated $\Delta flg 4$; $\Delta hofBCppdD$ to generate the designated mutant Δhof ; $\Delta hofC$; $\Delta fimADclpEFfimACfaeHI$ to generate the mutant designated Δfim ; $\Delta fimD$; Δcrl ; and Δeae . The

deletion mutants Δhof , $\Delta hofC$, Δfim , $\Delta fimD$, Δcrl , and Δeae were complemented with plasmid clones containing the corresponding gene amplified from *E. amylovora* Ea1189 along with its native promoter, digested at restriction sites KpnI and SacI, then ligated into the cloning vector pBBR1MCS-3 (Table 3-1). For complementation of Δfim , gene products were amplified using Roche Expand Long Range, dNTPack, according to the manufacturer's recommendations (Roche Diagnostics GmbH; Mannheim Germany). Mutants Δflg 3 (deletion of 18 kb) and Δflg 4 (deletion of 10 kb) were not complemented due to the larger size of the deletions.

Pathogenicity assays. Strains were assayed for virulence using an immature pear fruit assay and apple shoot assay as previously described (18, 40). For immature pear fruit assays, we used a cell dose of $\sim 1 \times 10^4$ CFU/ml and measured the surface area of lesion size on fruit at 0, 2, 4, 6, and 8 days post inoculation. Bacterial populations within immature pear fruit were quantified at 0, 1, 2, and 3 days post inoculation. Apple shoots were inoculated by cutting the youngest leaves using scissors dipped in a suspension of *E. amylovora*, and tissue was bagged overnight to maintain high humidity conditions. For shoot assays we used a cell dose of $\sim 2 \times 10^8$ CFU/ml and measured symptom progression at 3, 7, and 14 days post inoculation. Trees were maintained in growth chambers at 25°C and a light duration of 16 h. All assays were repeated in triplicate, with at least four independent representatives in each experiment.

***In vitro* crystal violet assays for biofilm formation.** We used an *in vitro* biofilm formation assay that was modified from an established crystal violet staining assay (22), as previously described (18). For brightfield imaging, cellular aggregation on glass coverslips was observed after 48 h growth in static culture following staining with 10% crystal violet and examination using an Olympus IX71 inverted microscope (Olympus America Inc.; New York).

Quantification measured absorbance values (A_{600}) of resolubilized crystal violet stain after 48 h, as previously described (18).

***In vitro* attachment time course assay.** We modified a standard *in vitro* biofilm assay (22) to develop an attachment assay to measure the timing of attachment of bacterial cells to glass coverslips. Strains were each grown overnight in LB broth to a concentration of 2×10^8 cfu/ml. Twenty microliters of this overnight culture was then added to 2 ml of sterile LB medium in individual wells of a 24-well culture plate (Corning; New York), and glass coverslips (Thermo Fisher Scientific; Waltham MA) were angled within the wells. The coverslips were removed following incubation of 2, 4, 6, 8, 16, and 24 h, stained with 10% crystal violet for one hour, rinsed, and air dried. Bacterial cells attached to coverslips within the microscope field of view were enumerated. Ten random field-of-view images of each sample from each time point were taken at 100X using an Olympus IX71 inverted microscope (Olympus America Inc.; New York). Each experiment was repeated at least four times.

Confocal laser-scanning microscopy visualization of *E. amylovora* biofilms. Three-dimensional aspects of biofilm formation were examined using a flow-cell apparatus (Stovall Life Sciences; Greensboro NC) as described previously (18). Strains were labeled with green fluorescent protein (*gfp*) through introduction of the plasmid pMP2444 via electroporation. Flow cell chambers were examined using the Zeiss 510 Meta ConfoCor3 LSM confocal laser-scanning microscope (CLSM; Carl Zeiss Microimaging; GmbH) and images were captured at $10\times$ using LSM image browsing software (Carl Zeiss Microimaging; GmbH). Z-stacks were compiled and a three-dimensional image that measured intensity was produced by using the “2.5 dimensions” with the LSM browser.

Visualization of *E. amylovora* and deletion mutants in shoot tissue using scanning electron microscopy. The two youngest leaves of three independent apple shoots (cv. Gala) were inoculated with bacterial strains by cutting leaves perpendicular to major vein with scissors dipped in an *E. amylovora* suspension (1×10^{10} CFU/ml). Leaves were collected at 3, 7, and 14 days post inoculation, sectioned into 1-cm sections, and fixed in paraformaldehyde/glutaraldehyde (2.5% of each compound in 0.1 M sodium cacodylate buffer) (Electron Microscopy Sciences; Hatfield, PA). The tissue was dehydrated successively, and then critical point dried using a critical point drier (Balzers CPD; Lichtenstein). Dried petiole tissue was sectioned from slices after critical point drying to reduce potential artifacts from the fixation process, mounted on aluminum mounting stubs (Electron Microscopy Sciences), and coated with gold using a gold sputter coater (EMSCOPE SC500 Sputter Coater; Ashford, Kent, Great Britain). Images were captured on the scanning electron microscope (SEM) JEOL 6400V (Japan Electron Optics Laboratories; Tokyo Japan) with a LaB6 emitter (Noran EDS, Thermo Fisher; Waltham MA) using analySIS software (Soft Imaging System; GmbH).

Visualization of *E. amylovora* *in vitro* and *in planta* using transmission electron microscopy.

For *in vitro* examination of Ea1189, cells were grown in LB overnight, and diluted to $\sim 1 \times 10^4$ CFU/ml in sterile water. The cell suspension was negatively stained with 0.25% uranyl acetate, and a 2 μ l sample was placed on a transmission electron microscope (TEM) grid. Samples were examined on the JEOL100 CXII microscope (Japan Electron Optics Laboratories). For *in planta* samples, the two youngest leaves of three independent apple shoots (cv. Gala) were inoculated with Ea1189 by cutting leaves perpendicular to the major vein with scissors dipped in a cell suspension (1×10^{10} CFU/ml). Samples were fixed overnight in

paraformaldehyde/glutaraldehyde. Petiole tissue was embedded in 2% agarose, then thin sectioned with a razor blade and stored in 0.1 M sodium cacodylate buffer (Electron Microscopy Sciences). Post-fix occurred in 2% osmium tetroxide in 0.1 M cacodylate buffer. Samples were dehydrated successively in graded acetone series, then infiltrated and embedded in Poly/Bed 812 (Polysciences; Warrington, PA). Sections were obtained with an ultra microtome, PowerTome XL (Boeckeler Instruments; Tucson, AZ). Thin sections were placed on TEM grids and samples were examined on the JEOL100 CXII microscope (Japan Electron Optics Laboratories).

RESULTS

Visualization of attachment structures of *E. amylovora*. TEM images of individual bacterial cells grown in broth culture, after negative staining, revealed the presence of peritrichous flagella but no other obvious surface appendages (Fig. 3-2A). TEM images of xylem tube cross-sections from petioles of leaves inoculated with wild type *E. amylovora* Ea1189 revealed additional appendages anchoring bacterial cells to the host cell wall (Fig. 3-2B). SEM imaging revealed apparently similar structures of Ea1189 that appeared to attach cells to the interior of xylem tubes of Gala apple tissue (Fig. 3-2C), apparently anchoring cells to the inner xylem wall. SEM images also revealed cellular aggregation, a process that is also presumably mediated by surface attachment structures in initiating biofilms that stretched into the interior space of a xylem vessel (Fig. 3-2C).

Biofilm formation *in vitro* visualization and quantification. Using a previously published, modified *in vitro* crystal violet staining method (18), we determined that, in general, mutants with deletions of cell surface attachment structures exhibited significant reductions in biofilm formation. Absorbance values of resolubilized stain indicated a significant reduction in biofilm formation on glass coverslips after 48 h in Δhof , $\Delta hofC$, Δfim , Δcrl , Δeae , and Δflg 4 (Fig. 3-

3A). In only a few cases, biofilm formation by the mutants was not significantly different than that of Ea1189 (Fig. 3-3A). Brightfield images of bacterial cells on glass coverslips, stained with crystal violet, captured at 48 h, demonstrated a lack of large aggregates, indicative of a lack of biofilm formation in almost all mutants (Fig. 3-3B). Complementation of deletion mutants restored biofilm formation to wild type levels (data not shown).

Examination of biofilm formation after 48 h within a flow cell system yielded similar results, with Δhof , $\Delta hofC$, Δfim , Δcrl , Δeae , and $\Delta flg 4$ all showing little to no aggregation within the chamber, compared to large aggregates formed by the wild type Ea1189 (Fig. 3-4A, B, and data not shown). Although $\Delta fimD$ formed large aggregates on glass coverslips under static conditions, we observed smaller aggregates within the flow cell chamber that did not transition to a mature biofilm (Fig. 3-4C).

***In vitro* biofilm attachment time course assay.** The attachment of wild type Ea1189 and mutant bacterial cells to glass coverslips under static conditions at time points of 2, 4, 6, 8, 16 and 24 h, was assessed. All attachment mutants examined show significant differences compared to the wild type Ea1189 throughout the experiment (Table 3-3). At 2 h, only Δfim exhibited any significant reduction in attachment compared to Ea1189. However, at 4 h, all except Δfim were significantly reduced in attachment. Attachment at 6 h was significantly reduced in all mutants except $\Delta fimD$ and Δcrl . Only Δhof and $\Delta flg 3$ had significant reductions at 8 h. At 16 h, all except $\Delta flg 3$, Δcrl , and Δeae exhibited significant decreases, and finally at 24 h, Δfim , $\Delta flg 4$, Δcrl , and Δeae all were significantly reduced in attachment, while $\Delta fimD$ exhibited a significant increase in attachment compared to Ea1189 (Table 3-3).

Virulence assays in immature pear fruit and apple shoots tissue after inoculation with *E. amylovora* and deletion mutants. All mutants exhibited reductions in lesion size at day 4 and

day 6 post inoculation in immature pear fruit (Table 3-4). However, by 8 days post inoculation, only the Δhof , $\Delta hofC$, $\Delta fimD$, and Δcrl were significantly reduced in lesion size compared to Ea1189. The Δams mutant was non-pathogenic in immature pear fruit as previously noted (3; 39)

Significant differences in bacterial population size in immature pear fruit were observed over the time course of three days following inoculation, including shifts in the timing of population growth, as well as decreases in population size (Fig. 3-5). Significant decreases in population compared to the wild type at day 3 were observed for Δfim , Δflg 3, and Δflg 4. Mutants in the type IV pilus, Δhof and $\Delta hofC$ both have a significant increase in population size compared to the wild type at day 2 post inoculation, however populations at day 3 were similar to that of the wild type, suggesting a shift in population growth.

Virulence of *E. amylovora* in apple shoots is evaluated by measuring the length of wilt symptoms as disease progresses into shoot tissue. We observed a significant reduction in disease progression in shoots inoculated with the $\Delta hofC$, $\Delta fimD$, Δfim , and Δflg 4 mutants compared to Ea1189, while the length of wilt symptoms in shoots inoculated with Δhof and Δflg 3 were not significantly different than the wild type (Fig. 3-6). In all virulence assays, complementation restored virulence to wild type levels (data not shown).

Visualization of *E. amylovora* and deletion mutants in shoot tissue using SEM. Ea1189 cells initially attach to the internal surfaces of the host xylem cell wall and produce biofilms that extend into the vessel (Fig. 3-1). Longitudinal sections of shoots inoculated with Ea1189 enabled us to visualize biofilms progressing within xylem tissue (Fig. 3-7A). In addition, we discovered discontinuous aggregates, suggesting that dispersal and initiation of new biofilms was occurring as a mechanism of systemic movement within individual xylem vessels.

In all mutant strains except $\Delta flg 3$, bacteria were found in high concentration in the mesophyll tissue (Fig. 3-7D). Infrequently, mutants were found inside vascular tissue, specifically the young helical xylem, in smaller populations and with little to no aggregates (Fig. 3-7C), compared to the wild type which is found more frequently and at higher populations of aggregates in both helical and developed xylem tissue (Fig. 3-7A). $\Delta flg 3$ is phenotypically similar to that of the wild type. Overall, the attachment mutants tended to be unable to localize or develop large populations within the vascular system.

DISCUSSION

We used a bioinformatics approach to identify multiple genes of *E. amylovora* encoding putative surface appendages, and we demonstrated their role in attachment, biofilm formation, and pathogenesis. These are the first reported results to indicate that type I fimbriae, flagella, type IV pili, and curli of *E. amylovora* contribute to biofilm formation in static and flowing environments, and that defects in any of these appendages result in decreased virulence *in planta*. Our previous results demonstrated that *E. amylovora* forms a biofilm *in vitro* and *in planta*. Pathogenesis and biofilm formation appear to be linked, but without identifying genes encoding traits independent of EPS production, the mechanistic role of biofilm formation in *E. amylovora* could not be studied. Interestingly, mutants with reduced biofilm formation ability appear unable to successfully establish large populations in apple xylem. Colonization of xylem is critical to the systemic movement of the pathogen through plants (5); thus biofilm-deficient mutants remain localized within an inoculated leaf and are strongly impaired in their ability to invade the rest of the plant.

This study of multiple attachment structures shows both the importance and the vast complexity of the attachment phase in biofilm establishment. This was evident when examining

the role of type IV pili using a cluster of genes identified in this study, Δhof , including the genes *ppdD*, *hofB* and *hofC*. These genes are known to encode functional type IV pili in *P. aeruginosa* (31). Type IV pili have been shown to mediate the transition from reversible to irreversible attachment in *P. aeruginosa*, and contribute to the virulence of another vascular invading plant pathogen, *R. solanacearum* (14, 34). Though timing on the transition between reversible and irreversible attachment has not been determined, it can be assumed that the transition would occur after reversible attachment (the first few hours of contact to a surface), and before or at the beginning of the expansion of the microcolony in the biofilm, or the initial growth phase of the bacteria. Under ideal situations, in *E. amylovora* this would occur between 3 and 5 h, at the end of the lag time and beginning of the growth phase (19). During the time course assay, Δhof was able to initiate attachment, however, during 4-6 h the mutant was significantly reduced in attachment to the surface compared to wild type. This implies that a deletion in the type IV pili alters irreversible attachment in *E. amylovora*. The disruption of irreversible attachment seems to stop any further significant attachment or expansion into micro- and macrocolonies.

The role of flagella in the attachment process was also examined. It is well-known that flagellar-driven motility allows several bacterial species, including *E. coli* and *Shewanella oneidensis* MR-1, to escape unfavorable environments and swim towards more favorable ones (23, 36). Flagella have also been shown to play significant roles in biofilm formation in several pathogens (7, 11, 15, 25, 38). For example, *E. coli* flagella exhibit multiple functions in biofilm formation including: motility to a surface, mediating surface contact, and expansion of the biofilm (36). In this study, we deleted two of the four gene clusters encoding the production and regulation of flagella in *E. amylovora* (32) and demonstrated varying effects on biofilm formation and virulence. One cluster, flagella gene cluster three, appears to aid in irreversible

attachment, but does not have a direct role in biofilm formation or virulence of the pathogen. Similarly, the second gene cluster does not seem to have a specific role in reversible or irreversible attachment, but contribute to biofilm formation and virulence. These results indicate that flagella production appears to be controlled by multiple gene clusters that may function independently. As a result, the flagella of *E. amylovora* seem to have multifaceted functions in the biofilm formation process.

Additional putative attachment structures were identified through our bioinformatics approach, including a regulator of curli genes, *crl*, and an invasins island, *eae*. Curli, or amyloid fibers, of *E. coli* are known to mediate in the attachment of flagella and fimbriae to surfaces, ultimately aiding in biofilm formation and virulence (2, 26, 29). Curli-like functions, including a role in pellicle formation, have been associated with the type III secretion system of *Dickeya dadantii*, an enteric plant pathogen (39). Invasins of *Yersinia* spp. or intimins of *E. coli* are outer membrane proteins known to mediate the attachment of bacteria cells to their eukaryotic hosts, but have no known function in biofilm formation (20). Our deletions in *crl* and *eae* in *E. amylovora* demonstrate that curli and invasins function in biofilm formation although no specific function during attachment was found. This implies that curli and invasins either aid in the attachment of other structures, or their role in biofilm formation does not occur during the attachment phase. The curli of *E. coli* have been shown to function in cell-to-cell contact (26). Similarly curli of *E. amylovora* could function in the building of mature biofilms. Reductions in virulence due to deletion of the curli regulator indicate not only functional attachment, but also mature biofilm formation is needed for full virulence in the host. SEM imaging of the mutants in the xylem tissue demonstrated that cells were not able to develop a mature biofilm within the xylem, supporting this hypothesis.

The final putative surface structures identified were Type I fimbriae. These were of interest because these rod-shaped surface organelles, found in most enterobacteria, have been well studied for their role in biofilm formation (36). In *E. coli*, type I fimbriae play a critical role in initial cell-to-surface contact, and are important to adhesion and biofilm formation in both static and flowing systems (4, 25). To determine if these structures play a similar role in *E. amylovora*, a time course assay of bacterial attachment was conducted. Previous studies have indicated that initial attachment of *E. amylovora* should occur within 2h of exposure to a surface, after which initial growth begins to occur (19). Our results showed that mutants with a deletion in type I fimbriae exhibited significant reductions of attachment after 2 h exposure, indicating that there is a defect in the initial attachment essential for biofilm formation.

In addition to a role in attachment, type I fimbriae are also important virulence factors in several enteric pathogens (6, 35). Even in cases where type I fimbriae are not originally present in *E. coli*; the introduction of fimbriae genes increases the severity of virulence of the pathogen (6). Similarly, in *E. amylovora*, type I fimbriae deficiencies lead to an overall reduction in virulence. Significant reductions in lesion size in immature pear fruit, as well as a reduction of disease progression within shoot tissue further indicates that initial attachment during biofilm formation contributes to virulence.

SEM imaging revealed that all mutant strains of *E. amylovora* (with the exception of Δflg 3) grow to large population size in the mesophyll. Thus, a fully functional biofilm does not seem to be required for survival and growth *in planta*. However, we also found that these mutants are unable to enter the vascular tissue like the wild type strain, indicating that biofilm formation plays a role in the entry of *E. amylovora* into the vascular tissue. This was consistent with a previous study where we found that an *lsc* mutant, deficient in biofilm formation, also remained

confined to the mesophyll (18). These findings were somewhat surprising, in that we expected a functional biofilm would be necessary to attain large population size *in planta*, and that large populations were needed to initiate entry into the xylem. Instead, it appears that biofilms play a crucial role in the actual entry into the vascular tissue. Further studies are being conducted to determine how the biofilm aids in xylem colonization. In addition, we previously found that *Δams* mutants are incapable of growth *in planta*. This seems to indicate that amylovoran, independent of a fully functional biofilm, is needed to protect *E. amylovora* from antimicrobial responses from the plant as suggested by others (3). The ability to uncouple biofilm formation from EPS biosynthesis, will now allow us to conduct future studies to examine the role of amylovoran and other extracellular polysaccharides.

In conclusion, we used a genetic approach to identify multiple structures directly or indirectly involved in the attachment phase of biofilm formation and in virulence of *E. amylovora*. Structures that appear to play a direct role in the attachment of *E. amylovora* function in the virulence of the pathogen; structures that have indirect roles in attachment do not always impact virulence. Ultimately these results demonstrate the importance of biofilm formation in the virulence and xylem entry of *E. amylovora*. Functional characterization of additional genes involved in attachment, as well as other steps in biofilm formation, may provide additional insight into the role of biofilm formation in *E. amylovora* pathogenesis.

Table 3-1. Deletion mutants constructed in chapter 3, sequence ID of the respective genes, and putative structure targeted for deletion.

Strains	Relevant characteristics	Source or reference
Ea1189	Wild type	6
Ea1189 Δ <i>ams</i>	Deletion mutant of amylovoran operon	41
Ea1189 Δ <i>hofC</i>	Deletion of EAM_0729; putative type IV pilus structure	This study
Ea1189 Δ <i>hof</i>	Deletion of EAM_0729-0731; genes <i>ppdD</i> , <i>hofB</i> , <i>hofC</i> of a putative type IV pilus structure	This study
Ea1189 Δ <i>fimD</i>	Deletion of EAM_0230; putative type I fimbriae structure	This study
Ea1189 Δ <i>fim</i>	Deletion of EAM_0230-0237; genes <i>fimAD</i> , <i>clpEF</i> , <i>fimAC</i> , <i>faeHI</i> of a putative type I fimbriae structure	This study
Ea1189 Δ <i>flg</i> 3	Deletion of EAM_2541-2562; genes <i>flhCD</i> , <i>fliADST</i> , <i>flgABCDEFGHIJKLMN</i> of a putative flagellum structure	This study
Ea1189 Δ <i>flg</i> 4	Deletion of EAM_2569-2581; genes <i>fliEFGHIJKLMNOPQ</i> of a putative flagellum structure	This study
Ea1189 Δ <i>crl</i>	Deletion of EAM_0898; putative curlin regulator	This study
Ea1189 Δ <i>eae</i>	Deletion of EAM_3759; putative invasin structure	This study

Table 3-2. Plasmids and oligonucleotide primers used in mutagenesis and complementation.

Plasmids and Primers		Source or reference
Plasmids:		41
pKD3	Plasmid utilized in λ phage recombinase mutagenesis method; Cm ^R	41
pKD46	Expresses recombinases red, β , λ , and exo for the construction of deletion mutants; Amp ^R	41
pMP2444	pBBR1MCS-5 backbone; <i>gfp</i> expressed from <i>lac</i> promoter; Gm ^R	This study
pJMK2	pBBR1MCS-3 backbone; <i>hofC</i> gene inserted as Kpn I-Sac I; Tc ^R	This study
pJMK3	pBBR1MCS-3 backbone; <i>hof</i> gene cluster inserted as Kpn I- Sac I; Tc ^R	This study
pJMK4	pBBR1MCS-3 backbone; <i>fimD</i> gene inserted as Kpn I-Sac I; Tc ^R	This study
pJMK5	pBBR1MCS-3 backbone; <i>fim</i> gene cluster inserted as Kpn I- Sac I; Tc ^R	This study
pJMK6	pBBR1MCS-3 backbone; <i>crl</i> gene inserted as Kpn I-Sac I; Tc ^R	This study
pJMK7	pBBR1MCS-3 backbone; <i>eae</i> gene inserted as Kpn I-Sac I; Tc ^R	
Primers:		
	F: 5'- ATGGGTGAACGCTTACTTTTCCG CTGGCAGGCTATTGACGATAGTGG GCAGTGTAGGCTGGAGCTGCTTC-3'	
Ea1189 Δ <i>hofC</i>	R: 5'- TTACCCAAGCGCATCTCCCA GCCTGAATACGGGCAAATACATG GCCACCACATATGAATATCCTCCTTA-3'	This study
	F: 5'-ATGGGTGAACGCTTACTTTTCCG CTGGCAGGCTATTGACGATAGTGG GCAGTGTAGGCTGGAGCTGCTTC-3'	
Ea1189 Δ <i>hof</i>	R: 5'-TCATGGCAACTGCTCCTCATCA AAACGGAACATATCCAGGCAAG CGTCCTCATATGAATATCCTCCTTA-3'	This study

Table 3-2
(cont'd)

Ea1189 Δ <i>fimD</i>	F: 5'-ATGACGCCTAAGGTGAAGAGGTAT GTGCTATTTGACGAAGCTTTCTGC CGGTGTAGGCTGGAGCTGCTTC-3' R: 5'-AATAAGTGTGCAARAGAGGACA TTGAAAAGACAGAGAACGTCGAA GCGACCATATGAATATCCTCCTTA-3'	This study
Ea1189 Δ <i>fim</i>	F: 5'-ATGAAAAAAGTAATCAACTTTAT TTTCCTGCTGCTGGCAGGTGCGGG TGAGTGTAGGCTGGAGCTGCTTC-3' R: 5'-GATGACTATGAGTTATGACTGGC CGTCACTGTGCACGGTCGCGGCC CCTTCATATGAATATCCTCCTTA-3'	This study
Ea1189 Δ <i>flg 4</i>	F: 5'-GGCAGCGGGGTGAAGTGATACA ACAGATCGGCTTAGAATCAGGCTTT ACGGTGTAGGCTGGAGCTGCTTC-3' R: 5'-TTACGAATTGAGACTAAACAGT GACAGCTTCGACATCTGCTGGAAT ACGGCATATGAATATCCTCCTTA-3'	This study
Ea1189 Δ <i>crl</i>	F: 5'-ATGACGTTACCGAGTGGACATC CTAAGAGTCGAATAATTAAGCGCT TTCAGTGTAGGCTGGAGCTGCTTC-3' R: 5'- TCAGGCGGTCAGCTTCACCGGC TGGTCAGCGAAATCCGTTGCCGGT ATCACATATGAATATCCTCCTTA-3'	This study
Ea1189 Δ <i>ea</i>	F: 5'-ATGCAGGGGGGTAAAGCGGCTC CTCCTGCAATAATCTGGGACAAAG ATGAGTGTAGGCTGGAGCTGCTTC-3' R: 5'- TTATTTTATAATATCAACATAAG GCTTGTTTATTGCGCTGCCGCTGC CAACATATGAATATCCTCCTTA-3'	This study
Δ <i>hofC</i> comp	F: 5'-GGTACCATGGGTG AACGCTTACTTTTCC-3'	This study

Table 3-2 (cont'd)		
$\Delta hofC$ comp	R: 5'- <u>GAGCTCTT</u> ACCC AAGCGCATCTCC-3'	This study
	F: 5'- <u>GGTACCAT</u> GGGTGA ACGCTTACTTTTCC-3'	
Δhof comp	R: 5'- <u>GAGCTCTC</u> ATGGC AACTGCTCCTCAT-3'	This study
	F: 5'- <u>GGTACCAT</u> GACGCCT AAGGTGAAGAGG-3'	
$\Delta fimD$ comp	R: 5'- <u>GAGCTCTT</u> ATTCACAC GTTATCTCCTGTA ACTT-3'	This study
	F: 5'- <u>GGTACCTG</u> AAATTA TTAACGAATGCCTGC-3'	
Δfim comp	R: 5'- <u>GAGCTCAT</u> GATAAAAC TTGCGGATAAATATCG-3'	This study
	F: 5'- <u>GGTACCAT</u> GACGTT ACCGAGTGGACAT-3'	
Δcrl comp	R: 5'- <u>GAGCTCTC</u> AGGC GGTCAGCTTCAC-3'	This study
	F: 5'- <u>GGTACCGG</u> TAAAG CGGCTCCTCCT-3'	
Δeae comp	R: 5'- <u>GAGCTCA</u> ATATCAAC ATAAGGCTTGTTTATTGC-3'	This study

^a restriction sites Kpn I (GGTACC) and Sac I (GAGCTC) underlined ^b Abbreviations: Amp, ampicillin; Cm, chloramphenicol; Gm, gentamicin; Tc, tetracycline;

Table 3-3. Time course assay measuring attachment of cells at 2, 4, 6, 8, 16, 24 h to glass coverslips. Each value represents the average number of cells attached within a field of view at 100x. Means within a column followed by the same letter are not significantly different according to Fisher's Protected LSD ($P \leq 0.05$).

	2 h		4 h		6 h		8 h		16 h		24 h	
Ea1189	30.6	abc	117.6	a	123.0	a	252.0	a	210.8	a	281.4	bc
$\Delta hofC$	21.1	bcd	72.2	b	28.9	d	179.2	abc	74.6	d	163.5	cd
Δhof	33.3	ab	40.3	cd	40.0	d	100.7	c	86.5	cd	142.7	cd
$\Delta fimD$	18.9	cd	65.6	bc	92.4	abc	206.7	ab	78.2	d	451.9	a
Δfim	15.1	d	101.0	a	63.1	bcd	271.3	a	80.7	cd	132.4	d
$\Delta flg 3$	42.7	a	37.6	d	51.2	cd	128.3	bc	177.7	ab	365.6	ab
$\Delta flg 4$	42.9	a	43.2	cd	52.8	cd	216.5	ab	120.6	bcd	116.5	d
Δcrl	25.9	bcd	25.9	d	100.2	ab	225.1	ab	167.6	abc	98.1	d
Δeae	29.0	bc	21.5	d	62.1	bcd	217.7	ab	145.7	abcd	86.5	d

Table 3-4. Percent lesion size on immature pear fruit inoculated with *E. amylovora* Ea1189 or various attachment mutants at 4, 6 and 8 days post inoculation. Significant differences in lesion size compared to the wild type were noted on day 8 post inoculation and are indicated with asterisks (student *t*-test; P<0.05).

	Day 4	Day 6	Day 8
Ea1189	8	51	87
<i>Δams</i>	0	0	0*
<i>ΔhofC</i>	6	46	77*
<i>Δhof</i>	4	29	72*
<i>ΔfimD</i>	3	18	57*
<i>Δfim</i>	4	41	84
<i>Δflg 3</i>	1	25	93
<i>Δflg 4</i>	2	23	85
<i>Δcrl</i>	1	21	76*
<i>Δeae</i>	2	19	80

Figure 3-1. Gene maps of genes deleted in this chapter. Genes are identified based on similarity to known attachment structures in other bacterial species. The gene *eae* encodes for invasion structures. The gene cluster *hof* encodes for type IV pili. Type I fimbriae require the *fim* gene cluster. Two of the four gene clusters encoding for genes necessary for flagellar biosynthesis and function are *flg 3* and *flg 4*.

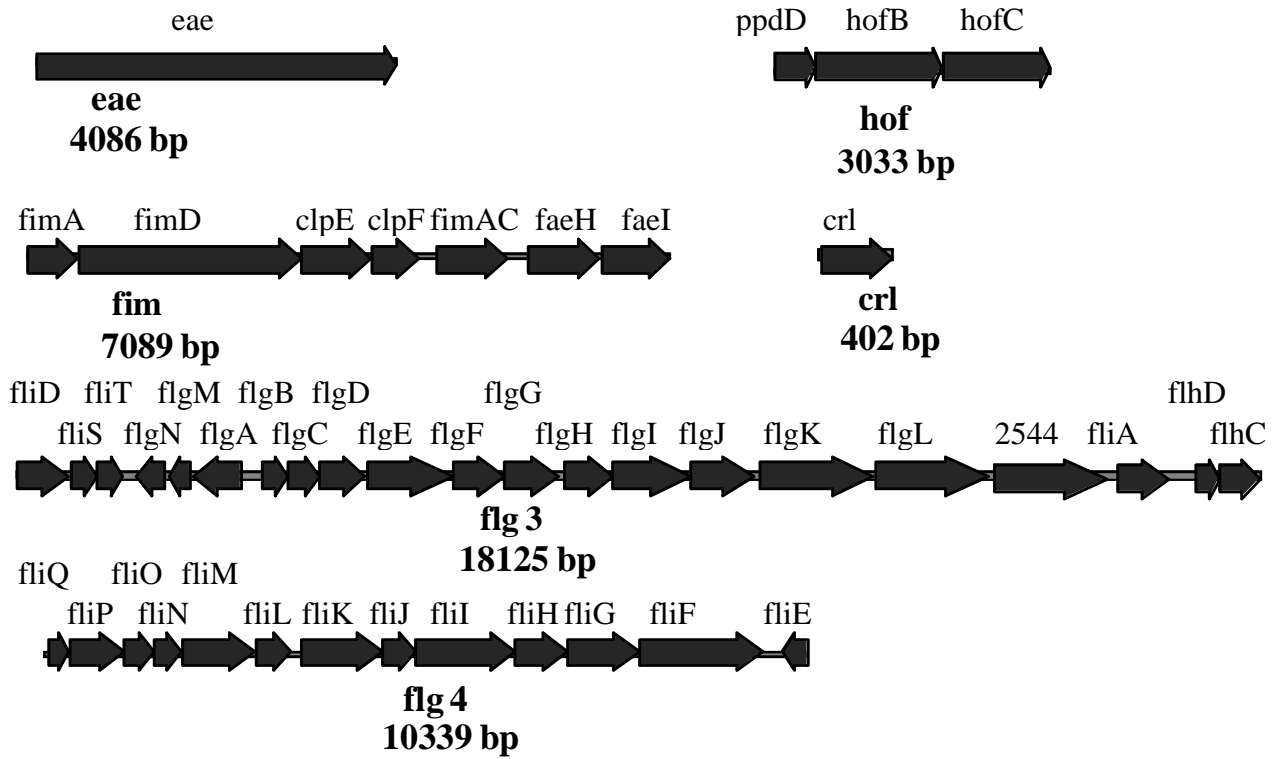


Figure 3-2. Images of putative attachment structures of *E. amylovora*. A) Transmission electron microscope imaging of a planktonic *E. amylovora* cell grown in broth culture and negatively stained. Peritrichous flagella are indicated by arrows. B) Transmission electron microscope image of *E. amylovora in planta*. Putative attachment structures connect bacterial cells to host cells C) Scanning electron image of *E. amylovora* cells attached to vascular tissue within ‘Gala’ apple tree. Imaged *E. amylovora* cells were found within a biofilm, with multiple appendages that protrude from the bacterial cell and attach to the host surface, as indicated by the arrows.

Figure 3-2 (cont'd)

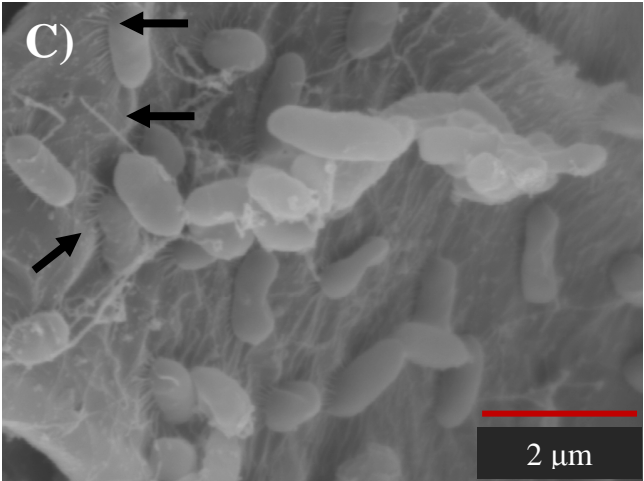
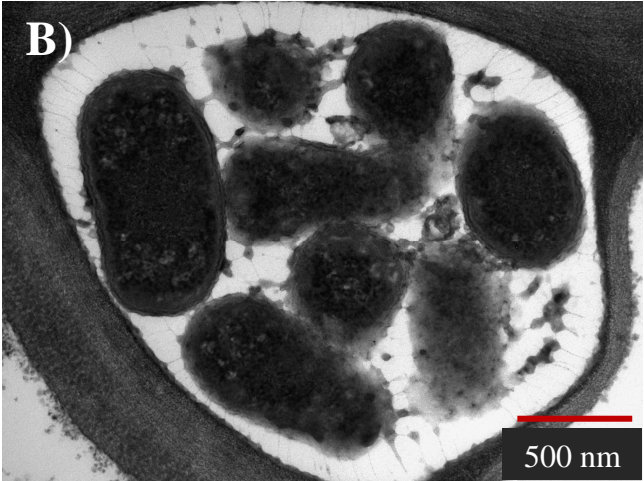
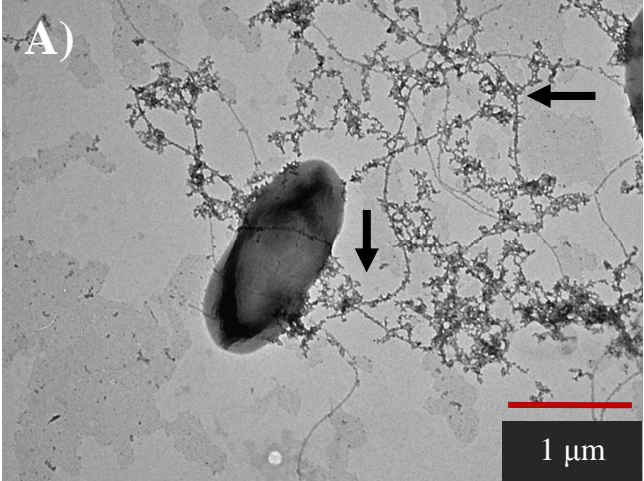


Figure 3-3. Biofilm formation of *E. amylovora*. A) Quantification of biofilm formation on glass coverslips of deletion mutants of *E. amylovora*. All mutants except $\Delta fimD$ and $\Delta flg 3$ demonstrated significant deficiencies in biofilm formation compared to Ea1189, using student *t*-test with $P < 0.05$. B) Brightfield imaging of biofilm formation on glass coverslips. All deletion mutants exhibit significant visual reduction in attachment to the glass surface after 48 h except that of $\Delta fimD$.

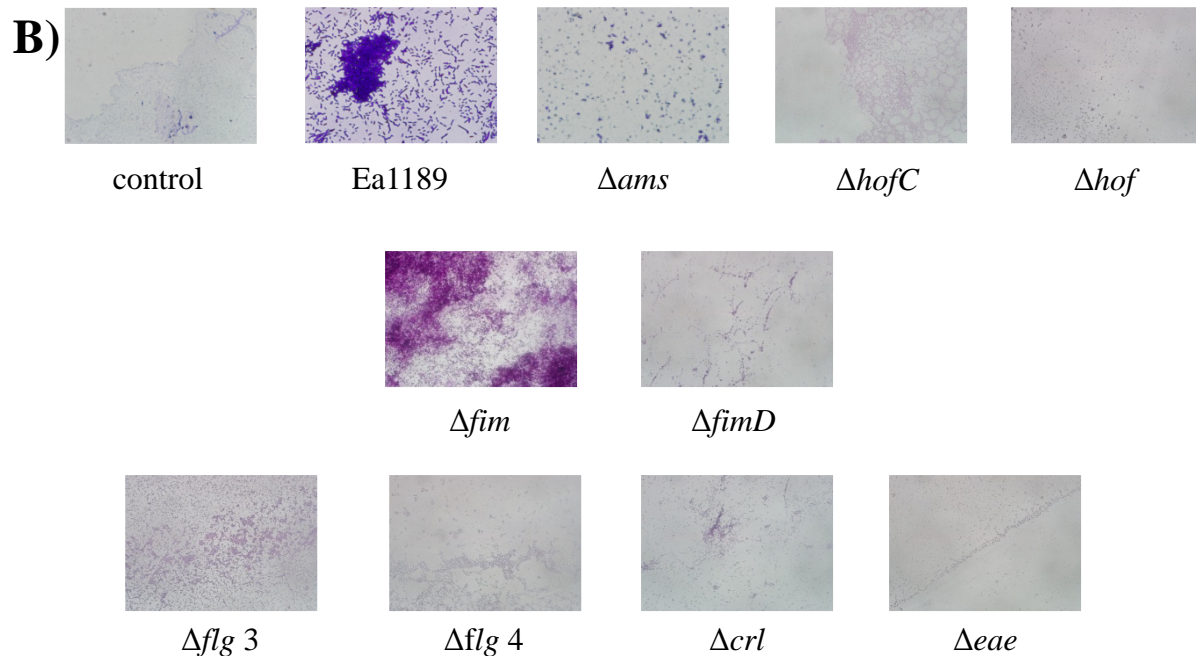
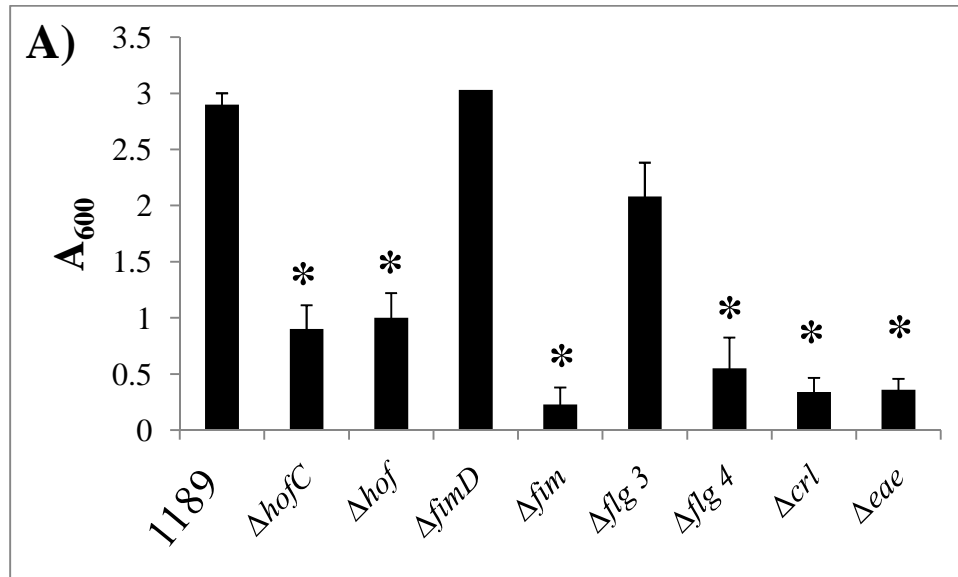


Figure 3-4. Flow cell imaging after 48 h growth measuring aggregates as brightness in fluorescence, where higher intensity (as indicated by more color layers) equals larger aggregates. A) Ea1189, exhibiting typical biofilm consisting of aggregates B) Δfim , a representative of biofilm negative behavior, including very little to no aggregates, but growth of bacteria is seen, and C) $\Delta fimD$ few aggregates are seen throughout, but not at levels that are as great as the wild type.

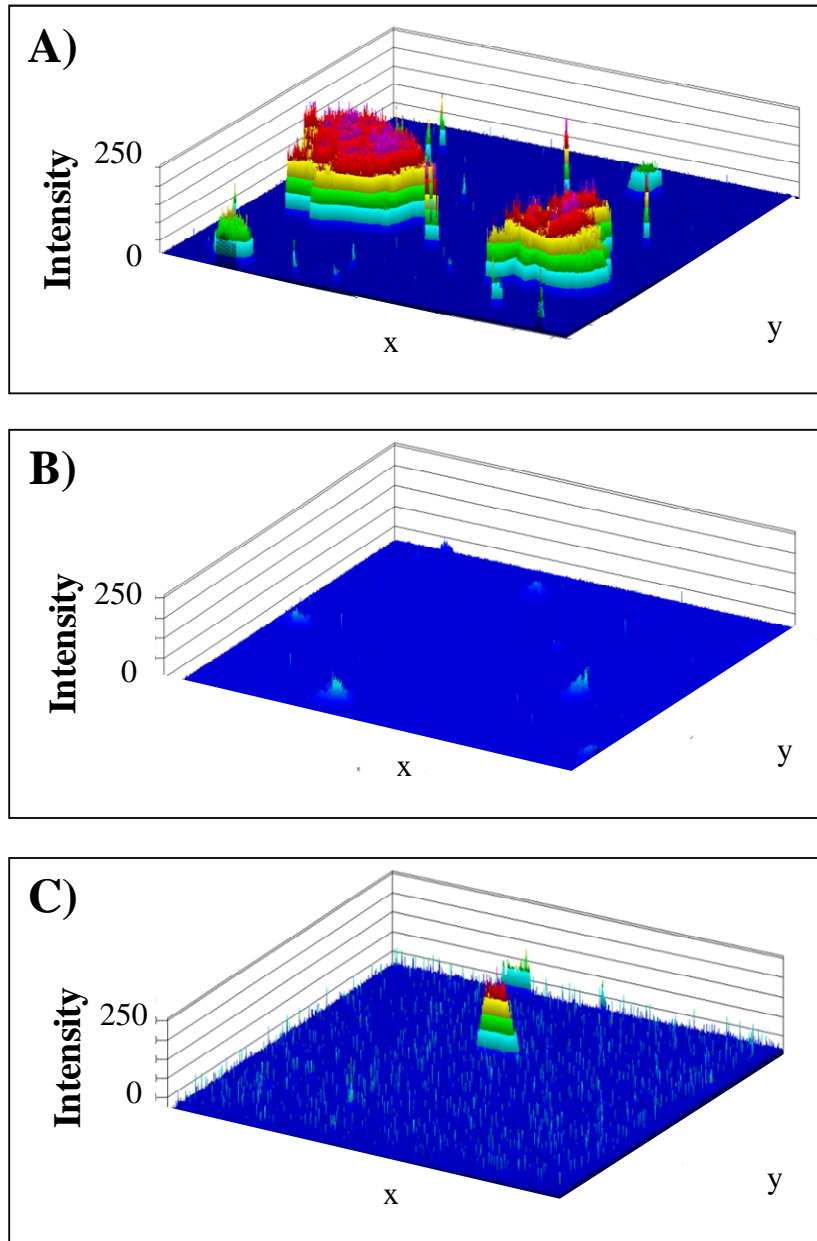


Figure 3-5. Measurement of necrosis progression in Gala apple tissue at 3 and 7 days post inoculation. Common scissor cut perpendicular to mid-vein of leaf used for inoculation demonstrates that the mutants $\Delta hofC$, $\Delta fimD$, Δfim , and $\Delta flg 4$ show significant difference in virulence using *t*-test at $P < 0.05$ at 7 days post inoculation.

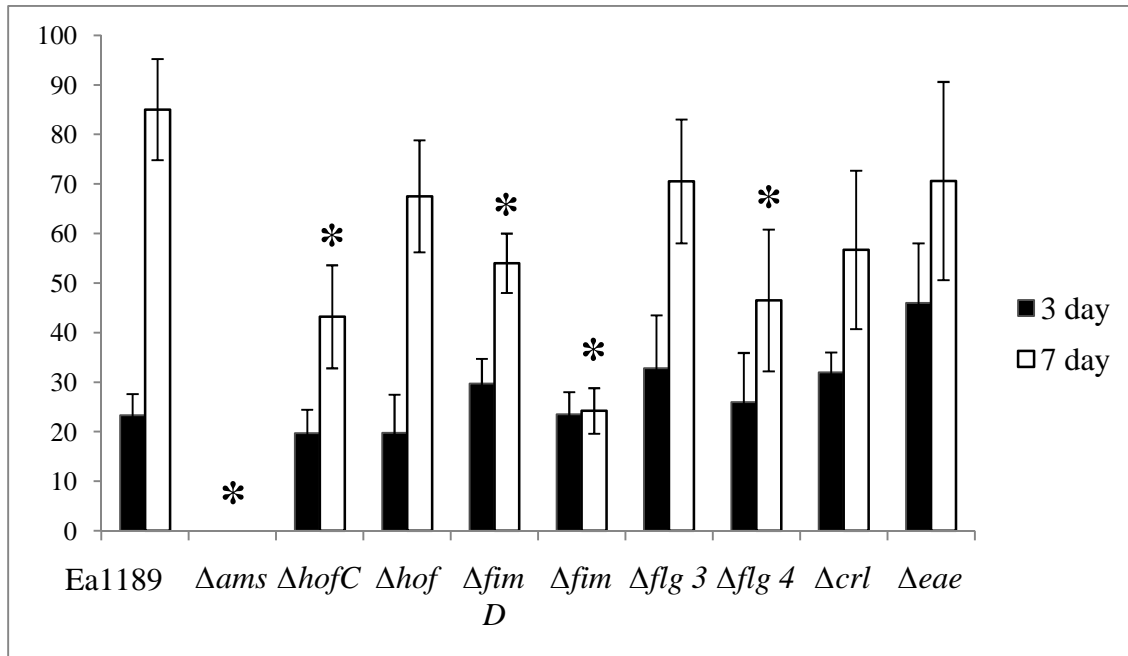


Figure 3-6. Bacterial populations in immature pear fruit over 3 days. A shift in population growth, or greater population size during earlier time points, is seen in $\Delta hofC$ and Δhof , and reductions in population size are seen in Δfim , $\Delta flg 3$ and $\Delta flg 4$. Significant changes in population indicated by asterisks, measuring significant difference using student *t*-test with $P < 0.05$.

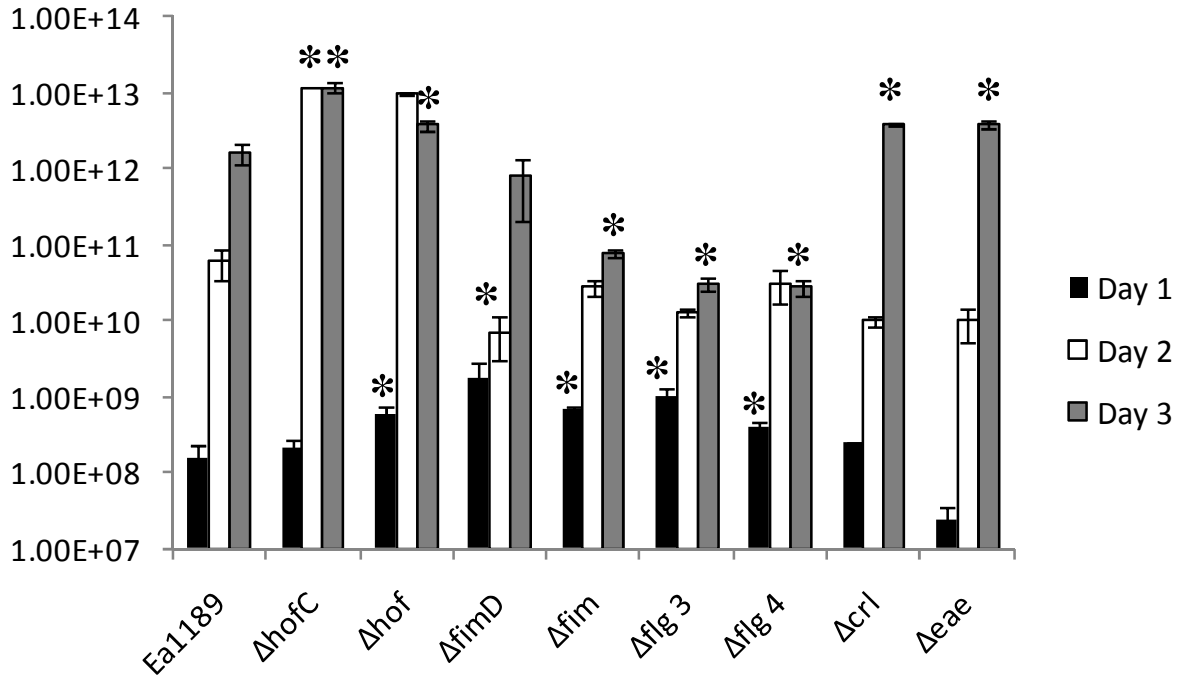
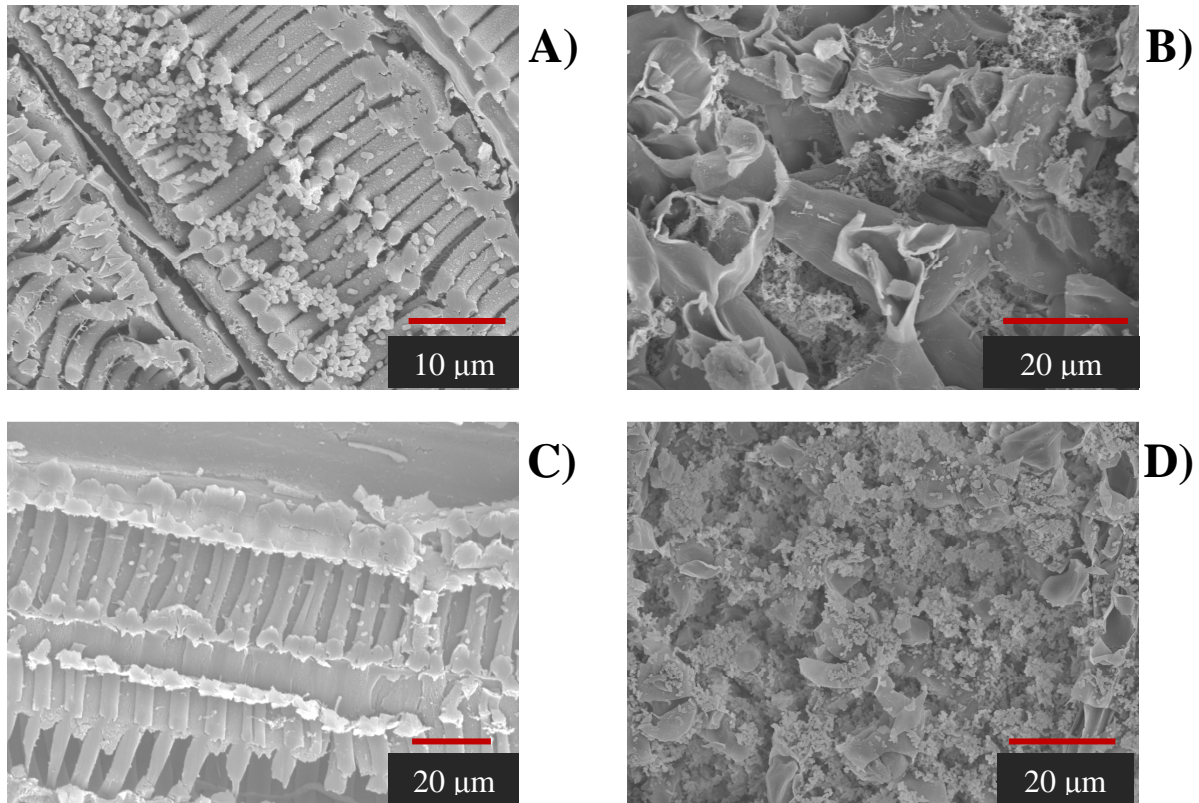


Figure 3-7. SEM images of A) Ea1189 within xylem tissue and B) mesophyll tissue. Notice distinct rings of biofilm formation within the vascular tissue, indicated by the aggregates filling the vascular space and a smaller population within the mesophyll tissue. C) Biofilm formation deficient mutant Δfim within vascular tissue and D) within mesophyll tissue, both typical of all deletion mutants, has larger population within mesophyll tissue, however few cell are able to get into xylem tissue, and unable to form a biofilm once in.



LITERATURE CITED

LITERATURE CITED

1. Bahar, O., Goffer, T., and Burdman, S. 2009. Type IV pili are required for virulence, twitching motility, and biofilm formation of *Acidovorax avenae* subsp. *citrulli*. *Mol. Plant-Microbe Interact.* 22: 909-920.
2. Barnhart, M.M., and Chapman, M.R. 2006. Curli biogenesis and function. *Annu. Rev. Microbiol.* 60: 131-147.
3. Bellemann, P., Bereswill, S., Berger, S., and Geider, K. 1994. Visualization of capsule formation by *Erwinia amylovora* and assays to determine amylovoran synthesis. *Int. J. Biol. Macromol.* 16: 290-296.
4. Beloin, C., Valle, J., Latour-Lambert, P., Faure, P., Kzreminski, M., Balestrino, D., Haagensen, J.A., Molin, S., Prensier, G., Arbeille, B., and Ghigo, J.M. 2004. Global impact of mature biofilm lifestyle on *Escherichia coli* K-12 gene expression. *Mol. Microbiol.* 51: 659-674.
5. Bogs, J., Brunchmuller, I., Erbar, C., and Geider, K. 1998. Colonization of host plants by the fire blight pathogen *Erwinia amylovora* marked with genes for bioluminescence and fluorescence. *Phytopathology* 88: 416-421.
6. Burse, A., Weingar, H., and Ullrich, M.S. 2004. NorM, an *Erwinia amylovora* multidrug efflux pump involved in *in vitro* competition with other epiphytic bacteria. *Appl. Environ. Microbiol.* 70: 693-703.
7. Connell, H., Agace, W., Klemm, P., Schembri, M., Marild, S., and Svanborg, C. 1996. Type I fimbrial expression enhances *Escherichia coli* virulence for the urinary tract. *Proc. Natl. Acad. Sci. USA* 93: 9827-9832.
8. Davey M.E., and O'Toole, G.A. 2000. Microbial biofilms: from ecology to molecular genetics. *Microbiol. Mol. Biol. Rev.* 64: 847-867.
9. Delaquis, P.J., Caldwell, D.E., Lawrence, J.R., and McCurdy, A.R. 1989. Detachment of *Pseudomonas fluorescens* from biofilms on glass surfaces in response to nutrient stress. *Microb. Ecol.* 18: 199-210.
10. Feil, H., Feil, W.S., and Lindow, S.E. 2007. Contribution of fimbrial and afimbrial adhesions of *Xylella fastidiosa* to attachment to surfaces and virulence in grape. *Phytopathology* 97: 318-324.
11. Gross, M., Geier, G., Rudolph, K., and Geider, K. 1992. Levan and levansucrase synthesized by the fireblight pathogen *Erwinia amylovora*. *Physiol. Mol. Plant Pathol.* 40: 371-381.
12. Hossain, M.M., and Tsuyumu, S. 2006. Flagella-mediated motility is required for biofilm formation by *Erwinia carotovora* subsp. *carotovora*. *J. Gen. Plant Pathol.* 72: 34-39.

13. Jahn, C.E., Willis, D.K., and Charkowski, A.O. 2008. The flagellar sigma factor FliA is required for *Dickeya dadantii* virulence. *Mol. Plant-Microbe Interact.* 21: 1431-1442.
14. Jin, Q., Hu, W., Brown, I., McGhee, G., Hart, P., Jones, A.L., and He, S.Y. 2001. Visualization of secreted Hrp and Avr proteins along the Hrp pilus during type III secretion in *Erwinia amylovora* and *Pseudomonas syringae*. *Mol. Microbiol.* 40: 1129-1139.
15. Kang, Y., Liu, H., Genin, S., Schell, M.A., and Denny, T.P. 2002. *Ralstonia solanacearum* requires type 4 pili to adhere to multiple surfaces and for natural transformation and virulence. *Mol. Microbiol.* 46: 427-437.
16. Karatan, E., and Watnick P. 2009. Signals, regulatory networks, and materials that build and break biofilm formation. *Microbiol. Mol. Biol. Rev.* 73: 310-347.
17. Kim, T., Young, B. M., and Young, G.M. 2008. Effect of flagellar mutations on *Yersinia enterocolitica* biofilm formation. *Appl. Environ. Microbiol.* 74: 5466-5474.
18. Kline K.A., Falker, S., Dahlberg, S., Normark, S., and Henriques-Normark, B. 2009. Bacterial adhesins in host-microbe interactions. *Cell Host Microbe* 5: 580-592.
19. Koczan, J.M., McGrath, M.J., Zhao, Y., and Sundin, G.W. 2009. Contribution of *Erwinia amylovora* exopolysaccharides amylovoran and levan to biofilm formation: implications in pathogenicity. *Phytopathology* 99: 1237-1244.
20. McGhee, G.C., and Sundin, G.W. 2010. Evaluation of kasugamycin for fire blight management, effect on nontarget bacteria, and assessment of kasugamycin resistance potential in *Erwinia amylovora*. *Phytopathology* 101: 192-204.
21. McGraw, E.A., Li, J., Selander, R.K., and Whittam, T.S. 1999. Molecular evolution and mosaic structure of α , β , and γ intimins of pathogenic *Escherichia coli*. *Mol. Biol. Evol.* 16: 12-22.
22. Norelli, J., Jones, A.L., and Aldwinkle, H.S. 2003. Fire blight management in the twenty-first century: using new technologies that enhance host resistance in apple. *Plant Dis.* 87: 756-765.
23. O'Toole, G., Pratt, L., Watnick, P., Newman, D., Weaver, V., and Kolter, R. 1999. Genetic approaches to study of biofilms. *Methods Enzymol.* 310: 91-107.
24. Paulick, A., Koerdt, A., Lassak, J., Huntley, S., Wilms, I., Narberhaus, F., and Thormann, K.M. 2009. Two different stator systems drive a single polar flagellum in *Shewanella oneidensis* MR-1. *Mol. Microbiol.* 71: 836-850.
25. Pizarro-Cerda, J., and Cossart, P. 2006. Bacterial adhesion and entry into the host cell. *Cell* 124: 715-727.

26. Pratt, L.A., and Kolter, R. 1998. Genetic analysis of *Escherichia coli* biofilm formation: roles of flagella, motility, chemotaxis, and type I pili. *Mol. Microbiol.* 30: 285-293.
27. Prigent-Combaret, C., Prensier, G., Thuy Le Thi, T., Vidal, O., Lejeune, P., and Dorel, C. 2000. Developmental pathway for biofilm formation in curli producing *Escherichia coli* strains: role of flagella, curli, and colanic acid. *Environ. Microbiol.* 2: 450-464.
28. Ramey, B.E., Koutsoudis, M., von Bodman, S.B., and Fuqua, C. 2004. Biofilm formation in plant-microbe associations. *Curr. Opin. Microbiol.* 7: 602-609.
29. Raymundo A.K., and Ries, S.M. 1981. Motility of *Erwinia amylovora*. *Phytopathology* 71: 45-49.
30. Saldaña, Z., Erdem, A.L., Schuller, S., Okene, I.N., Lucas, M., Sivananthan, A., Phillips, A.D., Kaper, J.B., Puente, J.L., and Giron, J.A. 2009. The *Escherichia coli* common pilus and the bundle-forming pilus act in concert during the formation of localized adherence by enteropathogenic *E. coli*. *J. Bacteriol.* 191: 3451-3461.
31. Sauer, K., Camper, A.K., Ehrlich, G.D., Costerton, J.W., Davies, D.G. 2002. *Pseudomonas aeruginosa* displays multiple phenotypes during development as a biofilm. *J. Bacteriol.* 184: 1140-1154.
32. Sauvonnet, N., Gounon, P., and Pugsley, A. 2000. PpdD type IV pilin of *Escherichia coli* K-12 can be assembled into pili in *Pseudomonas aeruginosa*. *J. Bacteriol.* 182: 848-854.
33. Sebaihia, M., Bocsanczy, A.M., Biehl, B.S., Quail, M.A., Perna, N.T., Glasner, J.D., DeClerck, G.A., Cartinhour, S., Schneider, D.J., Bentley, S.D., Parkhill, J., and Beer, S.V. 2010. Complete genome sequence of the plant pathogen *Erwinia amylovora* strain ATCC 49946. *J. Bacteriol.* 192:2020-2021.
34. Smits, T.H., Rezzonico, F., Kamber, T., Blom, J., Goesmann, A., Frey, J.E., and Duffy, B. 2010. Complete genome sequence of the fire blight pathogen *Erwinia amylovora* CFBP 1430 and comparison to other *Erwinia* spp. *Mol Plant-Microbe Interact* 24: 384-393.
35. Stoodley, P. Sauer, K., Davies, D.G., and Costerton, J.W. 2002. Biofilms as complex differentiated communities. *Annu. Rev. Microbiol.* 56: 187-209.
36. Van der Velden, A.W.M., Baumler, A.J., Tsolis, R.M., and Heffron, F. 1998. Multiple fimbrial adhesins are required for full virulence of *Salmonella typhimurium* in mice. *Infect. Immun.* 66: 2803-2808.
37. Van Houdt, R., and Michiels, C.W. 2005. Role of bacterial cell surface structures in *Escherichia coli* biofilm formation. *Res. Microbiol.* 156: 626-633.

38. Verstraeten, N., Braeken, K., Debkumari, B., Fauvart, M., Fransaer, J., Vermant, J., and Michiels, J. 2008. Living on a surface: swarming and biofilm formation. *Trends Microbiol.* 16: 496-506.
39. Wood, T.K. 2009. Insights on *Escherichia coli* biofilm formation and inhibition from whole-transcriptome profiling. *Environ. Microbiol.* 11: 1-15.
40. Yap, M.N., Yang, C.H., Barak, J.D., Jahn, C.E., and Charkowski, A.O. 2005. The *Erwinia chrysanthemi* type III secretion system is required for multicellular behavior. *J. Bacteriol.* 187: 639-648.
41. Zhao, Y., Blumer, S.E., and Sundin, G.W. 2005. Identification of *Erwinia amylovora* genes induced during infection of immature pear tissue. *J. Bacteriol.* 187: 8088-8103.
42. Zhao, Y., Sundin, G.W., and Wang, D. 2009. Construction and analysis of pathogenicity island deletion mutants of *Erwinia amylovora*. *Can. J. Microbiol.* 55: 457-464.

Chapter 4: Deletion of *Erwinia amylovora* flagellar motor protein genes alters biofilm formation and virulence in apple

ABSTRACT

Biofilm formation plays a significant role in the pathogenicity of *Erwinia amylovora* on apple. Previous research has identified important factors involved in multiple stages of the biofilm formation process, including attachment and maturation. Flagellar driven motility, which functions as a virulence factor, often contributes to biofilm formation in many pathogenic bacteria. We identified the flagellar motor stators of *E. amylovora* and generated deletion mutants. Interestingly, *E. amylovora* contains two sets of functional flagellar stators. However, deletion of single stator sets deletions did not completely eliminate function. Results presented here indicate that functional flagella and flagellar driven motility are involved in biofilm formation. Using an attachment timing assay, a lack of attachment in single flagellar motor stator mutants indicates that stators might assist in mediating contact with a surface. Reduction in virulence within both immature pear fruit and apple tree shoots demonstrates that motility is necessary for the movement of the pathogen to the vascular tissue.

INTRODUCTION

Flagellar driven motility allows several bacterial species, including *Escherichia coli* and *Shewanella oneidensis* MR-1, to escape unfavorable environments and swim towards more favorable ones (22, 32). In addition, many pathogenic bacteria need motility for full virulence. For example, deletion of flagella in *Pseudomonas aeruginosa*, an opportunistic pathogen, reduces surface infections, in turn reducing mortality (9). Flagellar motility also has been shown to play significant roles in biofilm formation in pathogens such as *Erwinia carotovora* subsp. *carotovora*, *E. coli*, *P. aeruginosa*, and *Yersinia enterocolitica* (6, 12, 13, 23, 35). Flagella have also been implicated as sensors that measure the wetness or viscosity of an environment (34). Not only are these structures multifunctional, but bacterial flagella can also come in a variety of conformations based on species: some cells have a single polar flagellum, some have multiple polar flagella, and others have peritrichous lateral flagella distributed randomly around the surface of a cell (16). In addition, a limited number of species with dual systems can express both polar and lateral flagella (17).

Bacterial flagella are long, thin filaments. Locomotion is driven by a motor at the base, both in clockwise and counter-clockwise fashion (2). These filamentous structures require a large number of genes for assembly and function; over 50 genes encode for assembly and function in *E. coli* (27). Genes encoding for the filament structure (*flg*, *flh*, and *fli*) the motor (*mot*), and directional locomotion (*che*) (7). The rotation of enteric bacterial flagella is driven by a gradient of protons across the membrane (27). This gradient is translated into energy by the flagellar motor components for physical flagella rotation (29). The flagella motor is composed of two main structures: the rotor and the stator. The rotor consists of several proteins that act as a switch, determining the rotation direction of the flagellum (29). The stator is typically

comprised of the integral membrane proteins MotA and MotB (28). MotA is suggested to form the channel that conducts the hydrogen ions across the cytoplasmic membrane and MotB is suggested to function as the anchor of MotA, attaching it to the peptidoglycan layer of the cytoplasmic membrane (10). Additionally, MotB acts as a plug that regulates the flow of protons through the membrane channel (11). To stabilize the stator and have proper function, the protein products need to form into protein complexes at a ratio of 4:2 (10, 14, 27). Protein complexes surround the rotor and are thought to generate the force for flagellum movement; thus deletions in *motA* and *motB* genes generate bacteria with paralyzed flagella (13, 22, 29).

Early studies examining the motor stators in *E. coli* and *Salmonella enteric* serovar Typhimurium demonstrated a single motor system was necessary for function of the flagellum (18). However, recent studies with *P. aeruginosa*, *S. oneidensis*, and *Bdellovibrio bacteriovorus* have identified multiple flagellar stator sets (18, 22, 28). Few species that contain multiple flagellar stators use them to power both lateral and polar flagella (17); however, many with multiple flagellar stators use them to power a single polar flagellum (30). It is suggested that multiple stators may not be functionally redundant; rather it is an energy efficient way to allow for flagellar driven motility in different environments (28). For example, *S. oneidensis* MR-1 motility primarily depends on a functional PomAB system, but under low-sodium conditions, the MotAB system is functional (22).

The arrestment of motility has been often associated with reduction in biofilm formation. The ability to form biofilms, or an aggregated network, allows single-celled organisms to act in a multi-cellular fashion which confers protection from a harsh environment, and facilitate nutrient acquisition, and is a common trait of many pathogenic bacteria (24, 26). The process of biofilm formation has distinct phases including attachment, microcolony, macrocolony, and expansion

phases (31). A number of bacterial virulence factors, such as exopolysaccharides, quorum sensing, and adhesion to a surface, have been shown to play significant roles during different stages of biofilm development (See chapters 2, 3). Flagellar driven motility functions in the transition of planktonic to attached stage in biofilm formation, as well as expansion, in *E. coli* (23). Additionally in *E. coli*, deletions in the motor stators alter biofilm formation: a deletion in the *motA* gene drastically reduces mature biofilm formation, causing flat architecture, with few aggregates (35). Those results indicate that in *E. coli* there is a strong relationship between motility, biofilm formation, and biofilm formation architecture.

Erwinia amylovora, a vascular phytopathogen, is the causal agent of fire blight on rosaceous species, particularly apples and pears. This disease is difficult to manage due to the emergence of antibiotic resistance and popularity of highly susceptible varieties (19). The pathogen is capable of rapid systemic movement within and among plants when conditions are favorable. Key pathogenicity factors including the production of the effector *dspE*, the formation of the type three secretion system and its cognate genes, as well as the production of the exopolysaccharide amylovoran have been extensively studied (1, 21). Recently it was shown that *E. amylovora* forms a biofilm during infection and that amylovoran is involved in this process, implicating biofilm formation in pathogenicity (15).

E. amylovora possesses peritrichous flagella (25). At least two of the four gene clusters involved in flagellum biosynthesis have been shown to have different roles in biofilm formation (See chapter 3). However the role of flagellum driven motility in biofilm formation has yet to be determined. Because motility has been shown in multiple instances to play a role in the virulence of *E. amylovora* (3, 5, 25), we hypothesize that motility contributes to biofilm formation, which ultimately aids in the systemic movement of the pathogen within apple. Work

presented here identifies two sets of genes encoding for flagellar motor stators *motA*₁ and *motB*₁, and *motA*₂ and *motB*₂. Mutations in these genes alter motility, biofilm formation and ultimately the virulence of *E. amylovora*. Additionally, changes in the ratio of motor stators alter the systemic movement of the pathogen.

MATERIAL AND METHODS

Bacterial strains, plasmids, and growth conditions. The bacterial strains used in this study are listed in Table 4-1. The plasmids, and oligonucleotide primers used in this study are listed in Table 4-2. All strains were grown in Luria Broth (LB) medium at 28°C, unless noted. For biofilm formation assays, including flow cell assays, strains were grown in 0.5× LB medium. Growth media were supplemented with the antibiotics ampicillin (Amp) (50 µg ml⁻¹), chloramphenicol (Cm) (20 µg ml⁻¹), gentamicin (Gm) (15 µg ml⁻¹), kanamycin (Km) (30 µg ml⁻¹), spectinomycin (Spc) (100 µg ml⁻¹) and tetracycline (Tc) (12 µg ml⁻¹) as necessary.

Deletion mutagenesis and complementation. We generated single gene deletion mutants in the flagellar motor stator genes *motA*₁ and *motB*₁, double gene deletion mutants in genes *motA*₁*B*₁ and *motB*₁*motB*₂, and quadruple gene deletion mutant in *motA*₁*B*₁*motA*₂*B*₂ of *E. amylovora* by using the λ phage recombinases as previously described (38). Single gene deletions and Δ*motA*₁*B*₁ were generated using a pKD3 backbone. To generate mutants in multiple genes, Δ*motB*₁*motB*₂ and Δ*motA*₁*B*₁*motA*₂*B*₂ pKD4 was used as well. Gene names, putative function, and annotated gene ID numbers for *E. amylovora* genes and gene clusters mutated in

this study are listed in Table 4-1. Deletion mutants $\Delta motA_1$, $\Delta motB_1$ and $\Delta motA_1B_1$ were complemented with plasmids pJMK8, pJMK9, and pJMK10 clones containing the corresponding gene from Ea1189 along with its native promoter ligated into pBBR1MCS-3. Deletion mutant $motB_1motB_2$ was complemented with plasmids pJMK8 and pJMK11, containing genes $motB_1$ and $motB_2$ respectively. Deletion mutant $\Delta motA_1B_1motA_2B_2$ was complemented with plasmids pJMK10 and pJMK12 containing the genes $motA_1B_1$ and $motA_2B_2$. Deletion mutants and complements were confirmed using PCR.

Motility assays: Swarming media was prepared as follows: 10 g tryptone, 5 g NaCl, and 3 g agar for 1 liter. For salt additive media, 10 g NaCl was added instead of 5g. For sucrose additive media, 20 g sucrose was added to the base. Overnight cultures were adjusted to a density of $\sim 2 \times 10^8$ CFU/ml. Five microliters of culture was drop plated on swarming media 20 minutes after media in plate set. Motility was evaluated after 48 h.

Pathogenicity assays. Strains were assayed for virulence using a standard immature pear fruit assay and apple shoot assay as previously described (21, 37). Briefly, for immature pear fruit assays, bacterial suspensions of strains were grown overnight in LB broth, harvested by centrifugation, and resuspended in 0.5× sterile phosphate-buffered saline (PBS) with cells adjusted to $\sim 1 \times 10^4$ CFU/ml. Immature pear fruit (*Pyrus communis* L. cv. Bartlett) were surface sterilized with 10% bleach, dried in a laminar flow hood, and wounded with a sterile needle. Wounded pear fruit were inoculated with 2 μ l of cell suspension and incubated in a humidified chamber at 28°C. Symptoms were recorded at 2, 4, 6, 7, and 8 days post inoculation. For bacterial population studies, the pear tissue surrounding the inoculation site was excised using a

no. 4 cork borer and homogenized in 0.5 ml of 0.5× PBS. Bacterial growth within the pear tissue was monitored at 0, 1, 2, and 3 days post inoculation by dilution plating of the ground material on LB medium. Fruit were assayed in triplicate, and each experiment was repeated three times.

For shoot assays, overnight cultures were washed and resuspended in 0.5× PBS at a density of $\sim 2 \times 10^8$ CFU/ml. We used 2-year-old potted apple trees (cv. Gala on M9 rootstock) obtained from Hilltop Nursery (Hartford, MI) in all experiments. The two youngest leaves of the central shoot were cut perpendicularly to midvein ~ 2.5 cm from the tip of the leaf using scissors dipped in the bacterial suspension. Inoculated shoots were bagged overnight to maintain humid conditions. Progression of disease symptoms was recorded at 3 and 7 days post inoculation.

***In vitro* crystal violet assays for biofilm formation.** We used an *in vitro* biofilm formation assay that was modified from an established crystal violet staining assay (20), as previously described (15). Biofilm formation was quantified following development on glass coverslips. Overnight cultures were adjusted to a density of $\sim 2 \times 10^8$ CFU/ml and 25 μ l of the culture was added to 2 ml of 0.5× LB in individual wells of a 24-well plate (Corning). A glass coverslip was placed at a $\sim 30^\circ$ angle in each well to maximize surface exposure to the growing culture. The plates were incubated overnight at 28°C. After 48 h, the suspension was removed and a 10% crystal violet solution was added for 1 h, after which the glass coverslip was rinsed three times with sterile water. The glass coverslips were air dried for 1 h; then, 200 μ l of 40% methanol, 10% glacial acetic acid was added to wells to resolubilize the crystal violet stain. The solubilized crystal violet was quantified through spectrophotometry at an absorbance of 600 nm using a Safire microplate reader (Tecan, Research Triangle Park, NC). Each experiment included 24 replicates and experiments were repeated three times.

Brightfield microscopy was also used to visualize biofilm formation and cell aggregation on the glass coverslips. Coverslips were processed as described above, except the crystal violet stain was not resolubilized following the sterile-water rinses. Coverslips were then examined using a brightfield microscopy Olympus IX71 inverted microscope (Olympus America Inc., New York) and images of cellular aggregation and biofilm formation were captured.

Confocal laser-scanning microscopy visualization of *E. amylovora* biofilms. Biofilm formation was further examined using a flow-cell apparatus (Stovall Life Sciences, Greensboro NC). Strains were labeled with green fluorescent protein (*gfp*) by introduction of the plasmid pMP2444 via electroporation. Cell suspensions were established in 0.5×LB medium amended with gentamicin, in the flow cell and fresh medium was passed through the flow cell chamber for 48 h at 28°C using a configuration detailed in the manufacturer’s instructions (Stovall Life Sciences). Chambers were examined using the Zeiss 510 Meta ConfoCor3 LSM confocal laser-scanning microscope (CLSM; Carl Zeiss Microimaging, GmbH) and images were captured at ×2.5, ×10, and ×20 using the LSM image browsing software (Carl Zeiss Microimaging, GmbH). Z-stacks were compiled and a three-dimensional image that measured intensity was produced by using the “2.5 dimensions” with the LSM browser.

***In vitro* ficoll attachment time course assay.** We modified a standard *in vitro* biofilm assay (20) to develop an attachment assay to measure the timing of attachment of bacterial cells to glass coverslips. Half strength LB, 0.5×LB supplemented with 3% or 30% ficoll was used in analysis; ficoll is a neutral highly branched polysaccharide used to make LB more viscous. Strains were each grown overnight in LB broth to a concentration of 2×10^8 cfu/ml. Twenty microliters of this overnight culture was then added to 2 ml of either sterile 0.5×LB, 0.5× LB

plus 3% ficoll, or 0.5× LB plus 30% ficoll medium in individual wells of a 24-well culture plate (Corning; New York), with glass coverslips (Thermo Fisher Scientific; Waltham MA) angled within wells. Glass coverslips were removed following incubation of 4, 6 and 24 h. Slides were stained with 10% crystal violet for one hour, rinsed and air dried. Bacterial cells attached to coverslips within the microscope field of view were enumerated. Ten random images of each sample from each time point were taken at 100X using an Olympus IX71 inverted microscope (Olympus America Inc.; New York). Each experiment was repeated at least four times under each condition for each strain.

Visualization of *E. amylovora* in shoot tissue using scanning electron microscopy. The two youngest leaves of three independent apple shoots (cv. Gala) were inoculated with Ea1189, deletion mutants or sterile 0.5× PBS buffer using the scissor-cut method at 1×10^{10} CFU/ml, as previously described (21). Tissue was collected at 3, 7, and 14 days postinoculation, sectioned into 1-cm sections, and fixed in paraformaldehyde/ glutaraldehyde (2.5% of each compound in 0.1 M sodium cacodylate buffer) (Electron Microscopy Sciences, Hatfield, PA) overnight. The tissue was dehydrated successively in 25, 50, 75, and 90% ethanol for 30 min each and in 100% ethanol three times for 15 min. Samples were then critical point dried using a critical point drier (Balzers CPD, Lichtenstein). Dried petiole tissue was sectioned into 1-mm latitudinal slices after critical point drying to reduce potential artifacts from the fixation process, mounted on aluminum mounting stubs (Electron Microscopy Sciences), and then coated with gold using a gold sputter coater (EMSCOPE SC500 Sputter Coater, Ashford, Kent, Great Britain). Images were captured on the scanning electron microscope (SEM) JEOL 6400V (Japan Electron Optics Laboratories) with a LaB6 emitter (Noran EDS) using analySIS software (Soft Imaging System, GmbH).

RESULTS

Identification of flagellar stators and confirmation through motility assay. Bioinformatics identified two sets of flagellum stators (Fig 4.1). In similar pathosystems, deletion of flagellar stators produces flagella, however, cells are paralyzed. Transmission electron microscopy (TEM) confirms cells still produce flagella. However, flagella of single gene deletions in *motA*₁ and *motB*₁ were entangled in the EPS (data not shown). To examine the role of the stators in flagellar motility, single gene and multiple gene deletion mutants *motA*₁, *motB*₁, *motA*₁*B*₁, *motB*₁*B*₂, and *motA*₁*B*₁*A*₂*B*₂ were assayed on a minimal agar as previously described (38). A deletion mutant in the flagellar regulator *flhC* was used as a nonmotile control, as previously determined (38). Single deletions in the genes *motA*₁, and *motB*₁, as well as the deletion in both copies of *motB*, *motB*₁*B*₂, all resulted in an arrest in motility (Table 4-3). Deletions in *motA*₁*B*₁ and *motA*₁*B*₁*A*₂*B*₂ resulted in significant reductions from the wild type, as well as each other.

Strains were also assayed on media that was supplemented with either NaCl or sucrose to determine if motility defects were due to environmental conditions. As expected, an increase in salt concentration decreased motility of the wild type, but interestingly, mutants *motA*₁*B*₁ and *motA*₁*B*₁*A*₂*B*₂ exhibited greater decreases in motility. In contrast, the addition of sucrose increased motility in strains that exhibited motility under normal conditions. Deletions in *motA*₁*B*₁ and *motA*₁*B*₁*A*₂*B*₂ still caused significant reductions in motility, however, the deletion

of both stator copies yielded motility that is not significantly different from the nonmotile mutants.

Biofilm formation *in vitro* visualization and quantification. Using a previously published, modified *in vitro* crystal violet staining method (15), we examined biofilm formation in motor stator deletion mutants. Deletions in *motA*₁, *motB*₁, and *motA*₁*B*₁ significantly reduced biofilm formation compared to Ea1189 (Fig. 4-2). Deletions in *motA*₁*B*₁ and *motA*₁*B*₁*A*₂*B*₂ resulted in biofilm formation statistically similar to that of Ea1189. Complemented *motA*₁ restores biofilm formation to wild type levels (Fig. 4-3). Complementation of *motB*₁ does not completely restore the phenotype of biofilm formation to that of wild type levels, but using Student's t-test, quantification values are not statistically different (Fig. 4-3). This could be due to plasmid copy number altering natural protein ratios. Complement mutants of *motA*₁*B*₁ also exhibits slight reduced biofilm formation compared to the wild type, but again the difference is not statistically relevant (Fig. 4-3). Visualization of attachment to coverslips after 48 h exposure was also examined (Fig. 4-4). The results are in agreement with quantification analysis.

In vitro biofilm formation was further analyzed using an *in vitro* flow cell and confocal laser scanning microscopy. Unlike the quantification method, which depends on attachment to vertical glass surface, the chamber measures overall aggregation within the chamber. Results for this assay (Fig. 4-5) were similar to the imaging and quantification assays (Figs. 4-2/4). Deletion in *motA*₁ produced zero to few aggregates but the culture did exhibit overall growth within the chamber after 48 h. Similarly, Δ *motB*₁ produced very few aggregates. Mutant Δ *motA*₁*B*₁

produced the fewest aggregates within the flow cell chamber. $\Delta motA_1B_1A_2B_2$ exhibited an aggregate phenotype similar to that of the wild type.

Ficoll time course and attachment assay. A time course assay over 4, 6 and 24 h measured attachment of cells to coverslips (Table 4-3). The medium was also supplemented with 3 and 30% Ficoll to increase the viscosity and slow down flagellum driven motility (30). At 4 h, under normal conditions, only $motA_1$ was statistically reduced in attachment compared to Ea1189, whereas $motA_1B_1A_2B_2$ was statistically increased compared to Ea1189 and other mutants.

Interestingly, the biofilm negative control containing a deletion in the operon encoding amylovoran biosynthesis (Δams) still attached to the coverslips at the early time point, slightly greater but not significantly, from the wild type Ea1189. The addition of 3% Ficoll to the growth media caused a decrease in attachment of all mutants (except control Δams) to the coverslips, with Ea1189, $motA_1$, and $motA_1B_1A_2B_2$ all exhibiting similar decreases. With the addition of 30% Ficoll only the attachment of Δams and $motA_1B_1$ exhibited an increase in attachment.

After 6 h incubation, Δams and $\Delta motA_1B_1A_2B_2$ had significantly higher attachment than Ea1189, whereas $\Delta motA_1$ and $\Delta motB_1$ were significantly reduced. Addition of 3% Ficoll increased attachment of Ea1189, and the $motA_1$, and $motB_1$ mutants. Addition of 30% Ficoll drastically increased Ea1189, $motA_1$, $motB_1$, and $motA_1B_1$ attachment.

By 24 h, attachment of the ams control was dramatically reduced. Attachment of deletions in $motA_1$ and $motB_1$ significantly increased; however, mutants were still significantly

reduced from wild type. $\Delta motA_1B_1A_2B_2$ still exhibited a marked increase in attachment.

Similar to the 6 h time point, the addition of Ficoll considerably increased attachment of all strains, except $motA_1B_1$. Attachment patterns was similar with the addition of 30%, except $motB_1$ and $motA_1B_1$ exhibited slight decreases in attachment.

Virulence assays in immature pear fruit and tree shoot tissue. At 4 days post inoculation (dpi), in immature pear fruit, the stator mutants all demonstrated changes in disease phenotypes (Fig. 4-6). Similar to the control Δams , $\Delta motB_1B_2$, and $\Delta motA_1B_1A_2B_2$ were nonpathogenic. Mutants $motA_1$, $motB_1$, and $motA_1B_1$ all had no necrosis visible on fruit surface but ooze exudated from fruit. By 8 dpi, both $motB_1B_2$, and $motA_1B_1A_2B_2$ are nonpathogenic. Similar to 4 dpi, $motA_1$ exhibited a significant decrease in necrosis, but ooze and water soaking were evident. Visible symptoms were present in $motB_1$, and $motA_1B_1$, however, they were decreased from Ea1189.

Virulence of *E. amylovora* in apple shoots was evaluated by measuring the length of wilt symptoms as disease progresses into shoot tissue. At 3 dpi, in shoot assay, shoot tissue inoculated with deletion mutants exhibited very little to no disease progression (Fig. 4-7). By 7 dpi, in shoots inoculated with $\Delta motA_1B_1$ virulence was restored. Disease progression in all other motor stator mutants at 7 dpi exhibited little to no disease.

DISCUSSION

In this study, we identified two sets of genes encoding for flagellar motor stators, generated deletion mutants, and evaluated those mutants for their biofilm formation capabilities, as well as ability to cause disease. Our results indicate that stators are needed in mediating cell contact with surfaces, an early stage of the biofilm formation process, expansion of the biofilm, and as well as the virulence of *E. amylovora*. Deletions that altered the ratio of stator proteins seemed to have more significant reductions in biofilm formation and virulence than the deletion of a complete set of stators.

Previous studies have demonstrated that deletion of the genes encoding for the flagellar stators results in paralysis of the cell; however, bacterial cells still maintain the flagellar body (7). This paralysis is a result of an inability to maintain a 4:2 ratio of the individual Mot proteins (11). Deletions that maintain the natural ratio of motor stators are still motile. For example, *P. aeruginosa* encodes two sets of motor stators, and only deletions of both significantly reduce motility to levels of the nonmotile control (30). Similarly, *S. oneidensis* MR-1, containing dual stator systems, uses both systems for motility; deletion of one set of stator genes does not completely eliminate motility (22). Bioinformatic analysis revealed that *E. amylovora* encodes for two sets of flagellar stators. Single gene deletions abolish motility as expected. Deletion of one or both stator sets did not abolish motility, deletion of a single set reduces motility by about half, and deletion of both sets reduces motility close to that of the nonmotile control.

In the case of *S. oneidensis* MR-1, it has been suggested that expression of multiple flagellar stators is influenced by environmental conditions; the pathogen is found in both fresh and salt water (22). Environmental factors, including temperature and pH, can have a significant

effect on the motility of *E. amylovora* (25). Supplementing swarming media with salt reduces the motility of any strain that exhibits motility. Stator deletion mutants have a larger percentage decrease, indicating environment may play a role in the necessity for multiple stator systems. Also, addition of sucrose increases motility of all motile strains, but deletions in motor stators are still significantly different from the wild type, with the deletion in both stators statistically similar to the nonmotile strains.

Bacterial motility has been implicated in biofilm formation as a switch from a planktonic lifestyle to a cell attached to a surface; however, it has been suggested that the flagella function in overcoming forces associated with the surface, rather than act as an adhesive for attachment (8). This would allow for attachment of other structures known to be involved in attachment (see chapter 3) regardless of changes in fluid velocity, in temperature, or nutrient concentration (8). For example, *E. coli* exhibits no difference in biofilm formation between paralyzed and nonflagellated bacteria, but the flagella still aids in the initial cell-surface contact and as well as in biofilm expansion (23). In a microarray, Wood (35) found that early steps of biofilm formation require the synthesis of different bacterial appendages including flagella that allow for reversible attachment and cell motility. For irreversible attachment, flagella synthesis is repressed and adhesive organelles are important. This microarray data then suggests that flagella may function in attachment of bacterial cells or involvement during reversible attachment is to mediate the cell-surface contact. Using an attachment timing assay, at 2 h the reduction of attachment of *E. amylovora* *motA*₁ and *motB*₁ could indicate that the stators are unable to attach; however after the addition of ficoll, shown to slow motility in other species (29), similar reductions between the mutants and the wild type are seen, indicating that the strains could not be reaching the glass surface to attach. Attachment of flagellar stator mutants at later stages in

the time course assay similarly suggest that stators are needed to get strains to surface, not in attachment of cells. Significantly decreased aggregation after 48 h suggests an inability to expand biofilms, as suggested by Pratt and Kolter (23) when examining function of stators in *E. coli*.

Interestingly, deletion of both motor stator sets significantly reduced motility, however, general biofilm formation and attachment over time were significantly increased in *E. amylovora*. Similarly, Toutain and others (30) found that deleting either stator alone causes more of a reduction in biofilm formation than deleting both sets. It is possible that in the strains with both sets of stators deleted, cells undergo the biofilm formation process, except cells not released from the biofilm at the expansion stage. A limited number of very large aggregates suggest a defect in the expansion stage of biofilm formation.

Changes in pathogen virulence indicate that motility is necessary for disease progression, not just on blossoms (25) but within the plant as well. Deletion of single stator genes causes significant reductions in virulence in shoots. Similar results were seen by Wang and others (33) when examining motility of natural variants of *E. amylovora*. Our results also indicate that *E. amylovora* may not need flagellar driven motility to cause disease in immature pear fruit: only slight reductions in virulence are exhibited on pear. It is probable that the method of inoculation located the pathogen directly to the site of disease with no need for assistance to mediate surface contact. Interestingly, deletion of both stator sets has increased biofilm capabilities; however, mutants are nonpathogenic in immature pear fruit and shoot tissue. It is possible that because these mutants are unable to stop biofilm formation, not able to transition back to the planktonic stage, they are unable to cause disease.

In conclusion, research presented here identified two sets of flagellar stators present and functional in *E. amylovora*. Flagellar driven motility is needed for biofilm formation, specifically surface-mediated contact and expansion of biofilms, as well as virulence of the fire blight pathogen. The correlation between biofilm formation and virulence, specifically in shoot tissue, suggests that motility may assist in the systemic movement of the pathogen.

Table 4-1. Bacterial strains used in this chapter.

Strains	Relevant Characteristics	Reference
Strains		
Ea1189	Wild type <i>Erwinia amylovora</i>	4
Ea1189 Δ <i>ams</i>	Deletion mutant of the <i>ams</i> operon	38
Ea1189 Δ <i>motA</i> ₁	Deletion mutant EAM_2032; mutation of putative flagellar motility protein	This study
Ea1189 Δ <i>motB</i> ₁	Deletion mutant EAM_2031; mutation of putative flagellar motility protein	This study
Ea1189 Δ <i>motA</i> ₁ <i>B</i> ₁	Deletion mutant EAM_2031-2032; mutation of putative flagellar motility proteins	This study
Ea1189 Δ <i>motA</i> ₁ <i>B</i> ₁ <i>A</i> ₂ <i>B</i> ₂	Deletion mutant EAM_; mutation of putative flagellar motility proteins	This study
Ea1189 Δ <i>flhC</i>	Deletion mutant EAM_2030; mutation of flagellar regulator	This study, 38

Table 4-2. Plasmids and primers used in this chapter.

Plasmids and Primers	Relevant Characteristics	Reference
Plasmids		
pKD3	Plasmid utilized in λ phage recombinase mutagenesis method; Cm ^R	38
pKD4	Plasmid utilized in λ phage recombinase mutagenesis method; Kan ^R	38
pKD46	Expresses recombinases red, β , λ , and exo for the construction of deletion mutants; Amp ^R	38
pMP2444	pBBR1MCS-5 backbone; <i>gfp</i> expressed from <i>lac</i> promoter; Gm ^R	15
pJMK8	pBBR1MCS-3 backbone; <i>motA</i> ₁ gene inserted from Kpn I to Sac I; Tc ^R	This study
pJMK9	pBBR1MCS-3 backbone; <i>motB</i> ₁ gene inserted from Kpn I to Sac I; Tc ^R	This study
pJMK10	pBBR1MCS-3 backbone; <i>motA</i> ₁ <i>B</i> ₁ gene cluster inserted from Kpn I to Sac I; Tc ^R	This study
pJMK11	pGB2 backbone; <i>motB</i> ₂ gene cluster inserted from Hind III to Bam HI; Spc ^R	This study
pJMK12	pGB2 backbone; <i>motA</i> ₂ <i>B</i> ₂ gene cluster inserted from Hind III to Bam HI; Spc ^R	This study
Primers		
motA ₁	F: 5'-TCATGCGTCCTGTTCCGATGTCTGTTGTGGCGATTC CGCATTGCGTACATGTGTAGGCTGGAGCTGCTTC-3' R: 5'-CAGTAGCGGCAGTGACTTCAACGTTGCTTTAATGG CTTTGCCGTTATTACCATATGAATATCCTCCTTA-3'	This study
motB ₁	F: 5'-TTACCTCGGCTGTGAGTCGCGCTCGGTCTGGGCTGA CGGAGCCGTTGCAGGTGTAGGCTGGAGCTGCTTC-3' R: 5'-CCACATCACCAAAAAAAGGCCATCATTGCCGTCAT AAAGTCGGCGTAGGCATATGAATATCCTCCTTA-3'	This study
motA ₁ B ₁	F: 5'-TCATGCGTCCTGTTCCGATGTCTGTTGTGGCGATTC GCATTGCGTACATGTGTAGGCTGGAGCTGCTTC-3' R: 5'-CCACATCACCAAAAAAAGGCCATCATTGCCGTCAT TAAAGTCGGCGTAGGCATATGAATATCCTCCTTA-3'	This study

Table 4-2 (cont'd)		Table 4-2 (cont'd)
motA ₁ B ₁ motA ₂ B ₂	R: 5'-ATGAAAGCAACCACTCCCATTATCAGGCAGCGCA AGCGCAAGCATAAAAACATATGAATATCCTCCTTA-3'	This study
motA ₁ comp	F: 5'-GGTACCTCATGCGTCCTGTTCCGAT-3' R: 5'-GAGCTCGTAATAACGGCAAAGCCATTAAAG-3'	This study
motB ₁ comp	F: 5'-GGTACCTTACCTCGGCTGTGAGTCG-3' R: 5'-GAGCTCCCTACGCCGACTTTATGACG-3'	This study
motA ₁ B ₁ comp	F: 5'-GGTACCTCATGCGTCCTGTTCCGAT-3' R: 5'-GAGCTCCCTACGCCGACTTTATGACG-3'	This study
motA ₁ B ₁ motA ₂ B ₂ comp	F: 5'-GGTACCTCATTTCAGCAGCATCCCC-3' R: 5'-GAGCTCTTTTTATGCTTGCGCTTGC-3'	This study

^a Abbreviations: Amp, ampicillin; Cm, chloramphenicol; Gm, gentamicin; Kan, kanamycin; Tc,

tetracycline, Spc, spectinomycin

Table 4-3. Swarming motility of *Erwinia amylovora* on 0.3% minimal agar medium, 0.3% minimal agar medium plus NaCl, and 0.3% minimal agar medium plus sucrose, as measured by distance travelled (in mm). Means within a column followed by the same letter are not significantly different according to Fisher's Protected LSD (P<0.05).

Strain (or mutant)	Distance travelled (mm)	Distance travelled (mm)	Distance travelled (mm)
	0.3% minimal agar medium	0.3% minimal agar medium plus NaCl	0.3% minimal agar medium plus sucrose
Ea1189	11.5 A	9.0 A	25.4 A
<i>flhC</i>	0 D	0 D	0 C
<i>motA</i> ₁	0 D	0 D	0 C
<i>motB</i> ₁	0 D	0 D	0 C
<i>motA</i> ₁ <i>B</i> ₁	5.0 B	1.7 B	18.4 B
<i>motB</i> ₁ <i>B</i> ₂	0 D	0 D	0 C
<i>motA</i> ₁ <i>B</i> ₁ <i>motA</i> ₂ <i>B</i> ₂	0.9 C	0.1 C	6.1 C

Table 4-4. Attachment of cells to glass coverslips in the presence of Ficoll to limit bacterial motility. Ficoll was added to the media at 3 or 30%. Each value represents the average number of cells attached within a field of view at 100x. Percentage values measure the change in attachment of cells of the same time point with the addition of ficoll. Means within a row followed by the same letter are not significantly different according to Fisher's Protected LSD ($P \leq 0.05$).

		Ea1189	Δams	$\Delta motA_1$	$\Delta motB_1$	$\Delta motA_1B_1$	$\Delta motA_1B_1$ $motA_2B_2$
4h	LB	47.2 BC	60.1 B	18.8 D	34.3 CD	58.6 B	98.4 A
	3% Ficoll	-58%	+6%	-58%	-37%	-15%	-51%
	30% Ficoll	-52%	+11%	-58%	-4%	+52%	-75%
6 h	LB	45.7 BC	125.8 A	12.8 D	24.2 D	58.0 B	140.9 AC
	3% Ficoll	+11%	-76%	+10%	+150%	-9%	-10%
	30% Ficoll	+150%	+31%	+73%	+91%	+143%	-59%
24 h	LB	1690.2 B	191.8 DE	813.5 CD	860.8 C	142.1 E	5310.0 A
	3% Ficoll	+228%	+392%	+27%	+109%	+182%	+2%
	30% Ficoll	+171%	+318%	+76%	-7%	+388%	+9%

Figure 4-1. Sequence alignments of A) *E. amylovora motA* genes with *E. coli*, *Y. pestis*, *P. syringae* and B) *motB* genes of *E. amylovora* with *E. coli*, *Y. pestis*, *P. syringae*. Sequence identity between *E. amylovora motA* are noted, as well as that of *motB*.

Figure 4-1 (cont'd)

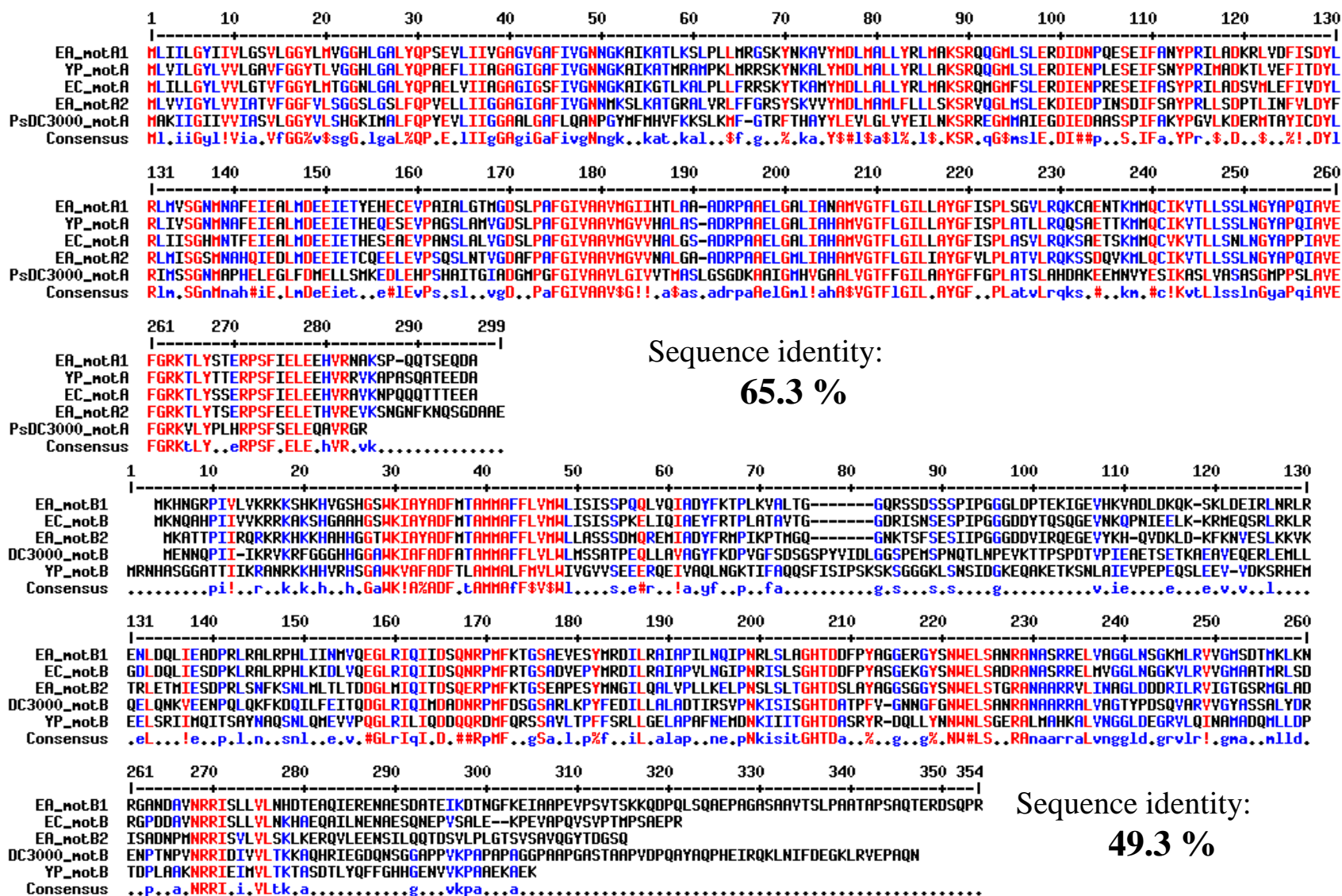


Figure 4-2. Biofilm quantification of flagellar stator mutants. Single gene and singular stator set deletions result in significantly reduced biofilm formation. Values represent mean of three replicates, 24 sample replicates from one representative experiment. Sample means were compared by an analysis of variance and separated using the Student t-test, with significant differences represented by asterisks.

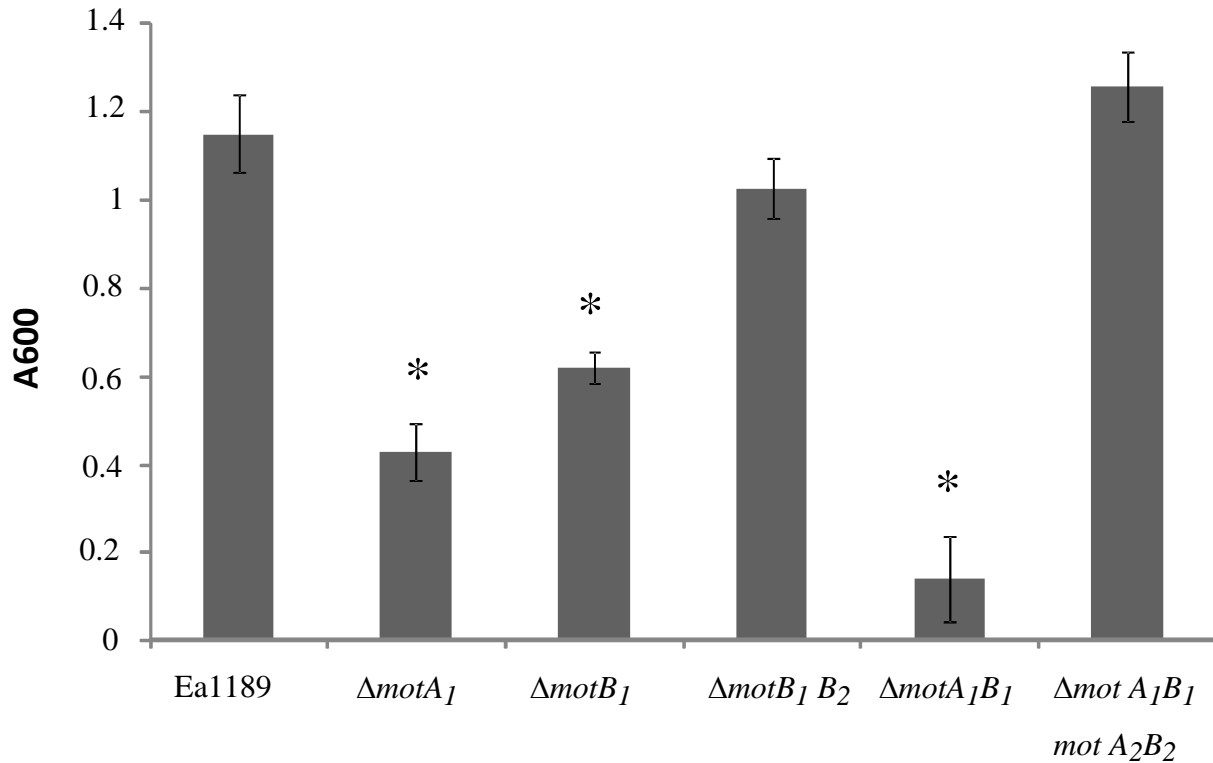


Figure 4-3. Biofilm quantification of complemented flagellar stator mutants. All exhibit biofilm formation phenotype statistically similar to Ea1189. Using Student's t-test, the difference seen in complemented *motB_I* is not of significant relevance.

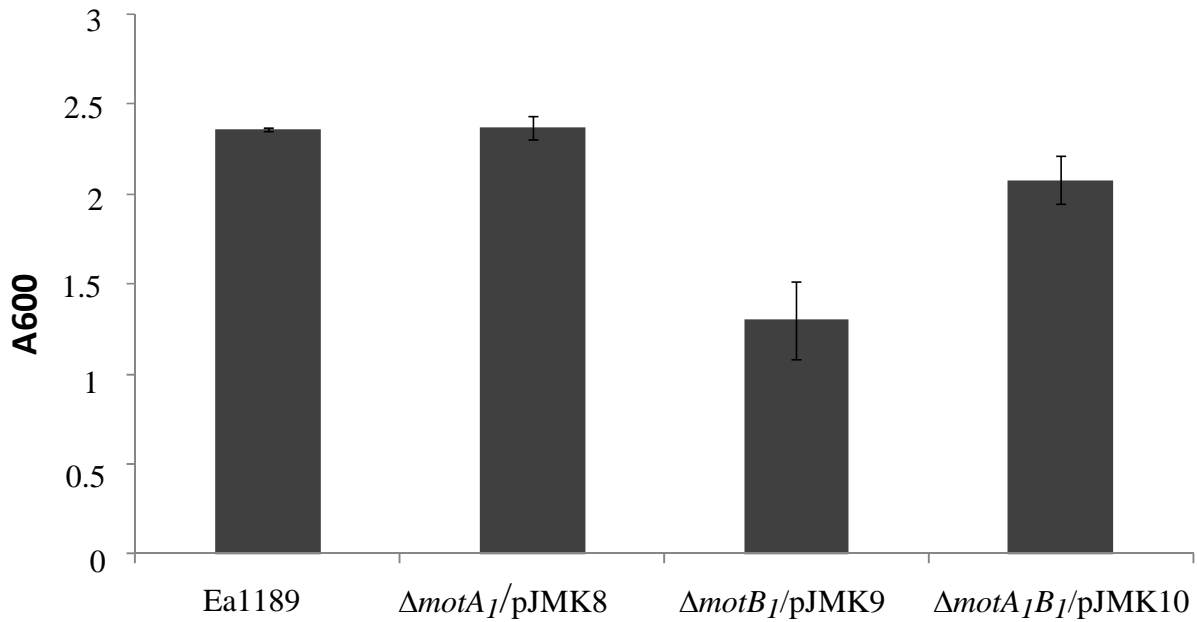


Figure 4-4. Brightfield imaging of biofilm formation of flagellar motor stator mutants on glass coverslips. Aggregation on glass is indicative of biofilm formation. Representative images of 3 independent trials of 40 images each.

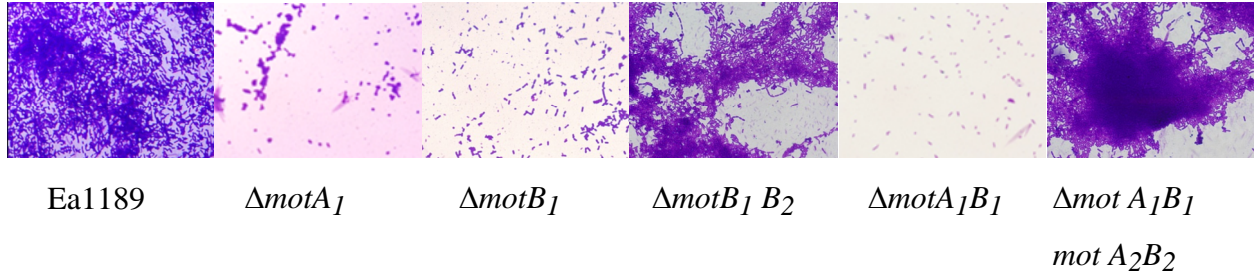


Figure 4-5. Three-dimensional view of flow-cell contents through intensity mapping after 48 h of growth. **A)** *Erwinia amylovora* Ea1189; **B)** Ea1189 Δ *motA*₁; **C)** Ea1189 Δ *motB*₁; **D)**

Ea1189 Δ *motA*₁*motB*₁ and **E)** Ea1189 Δ *motA*₁*motB*₁ Ea1189 Δ *motA*₂*motB*₂. Note: intensity mapping has set max value at 250 and maps are developed with five layers. More layers indicate greater intensity of signal and three-dimensional growth of the biofilm.

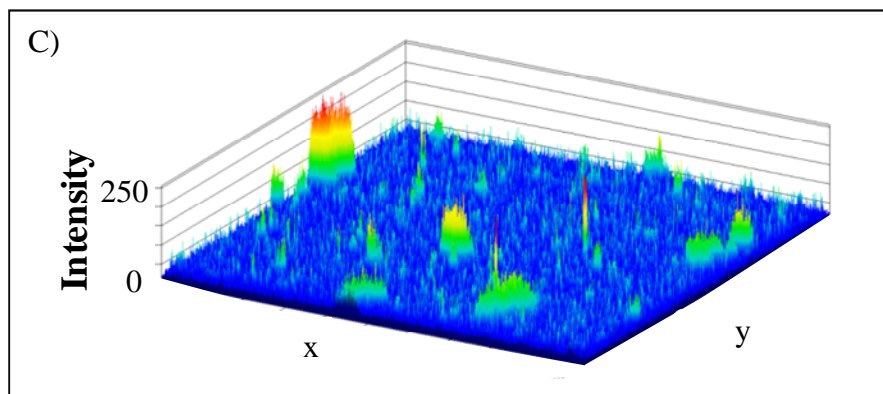
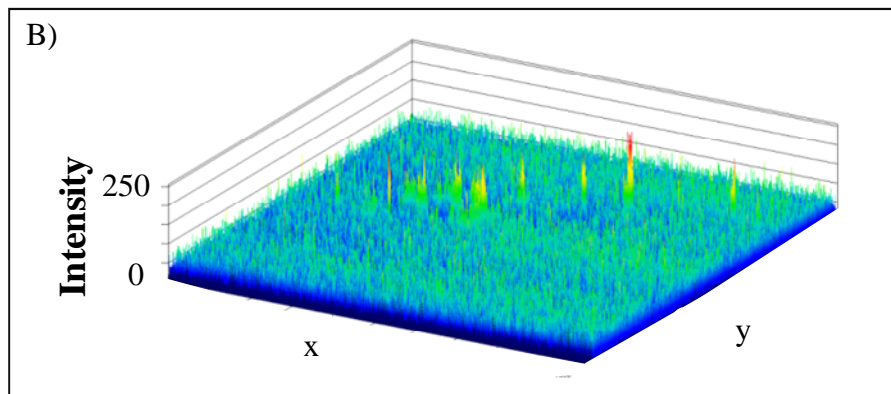
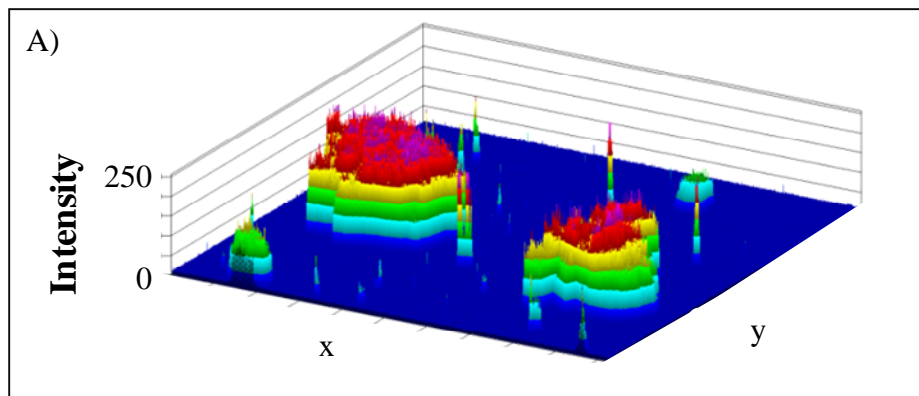


Figure 4-5 (cont'd)

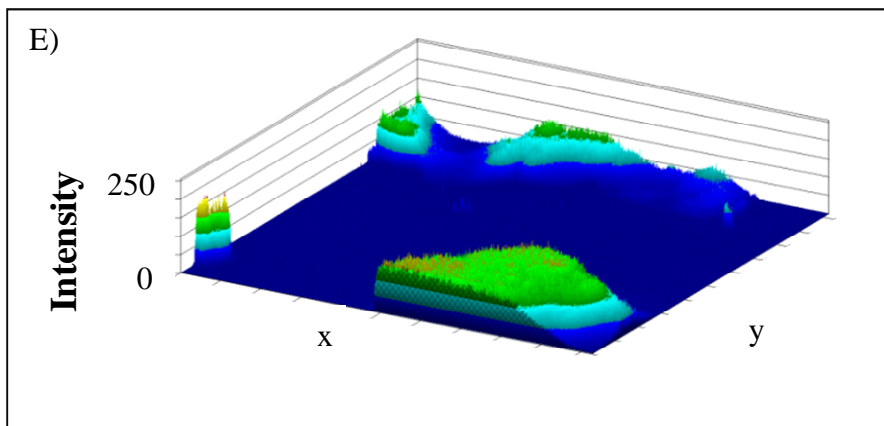
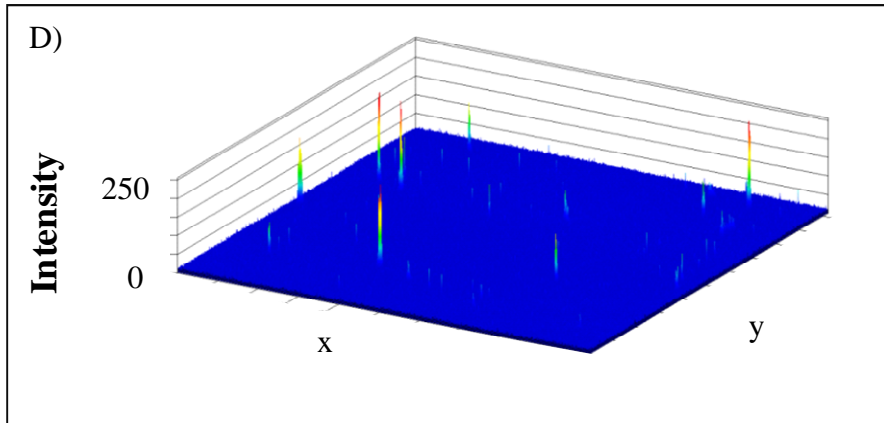


Figure 4-6. Immature pear fruit assay examining virulence of flagellar motor stator mutants at 4 days post inoculation (top row) and 8 days post inoculation (bottom row). Single gene and single stator set deletions result in reduced virulence compared to Ea1189. Deletions in both stator sets result in phenotype similar to the nonpathogenic control, Δams . Representative pears shown from three individual experiments, five pears per trial, inoculated with culture of 1×10^6 cfu/ml.

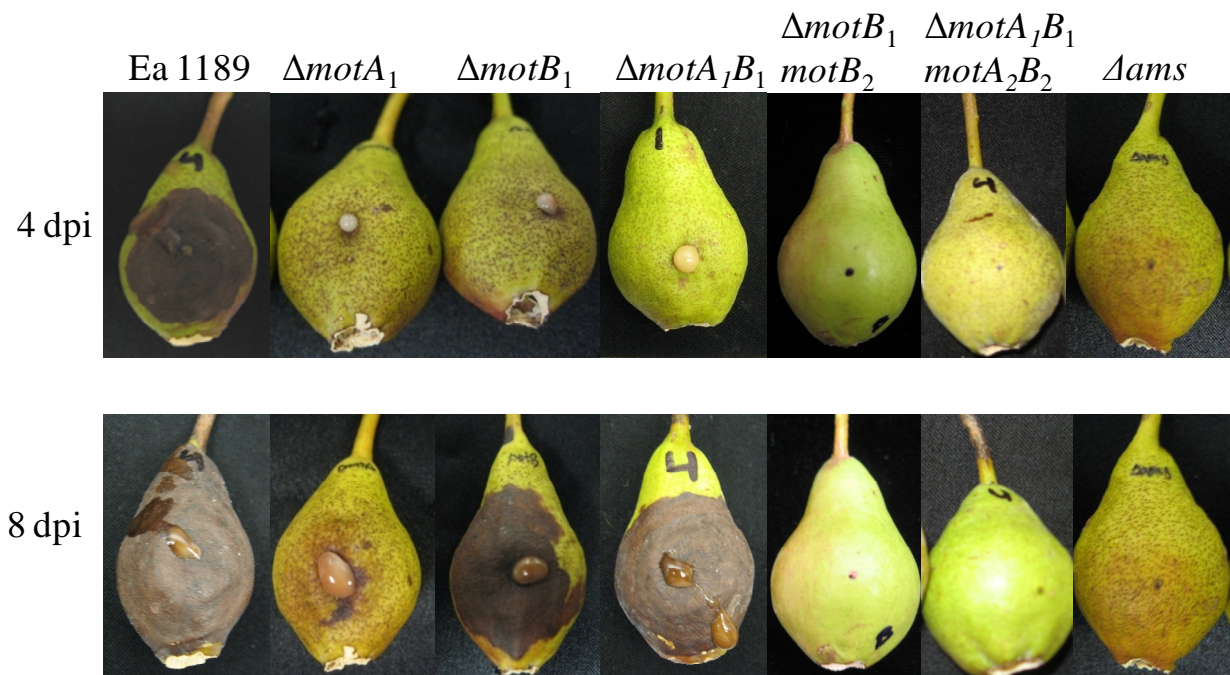
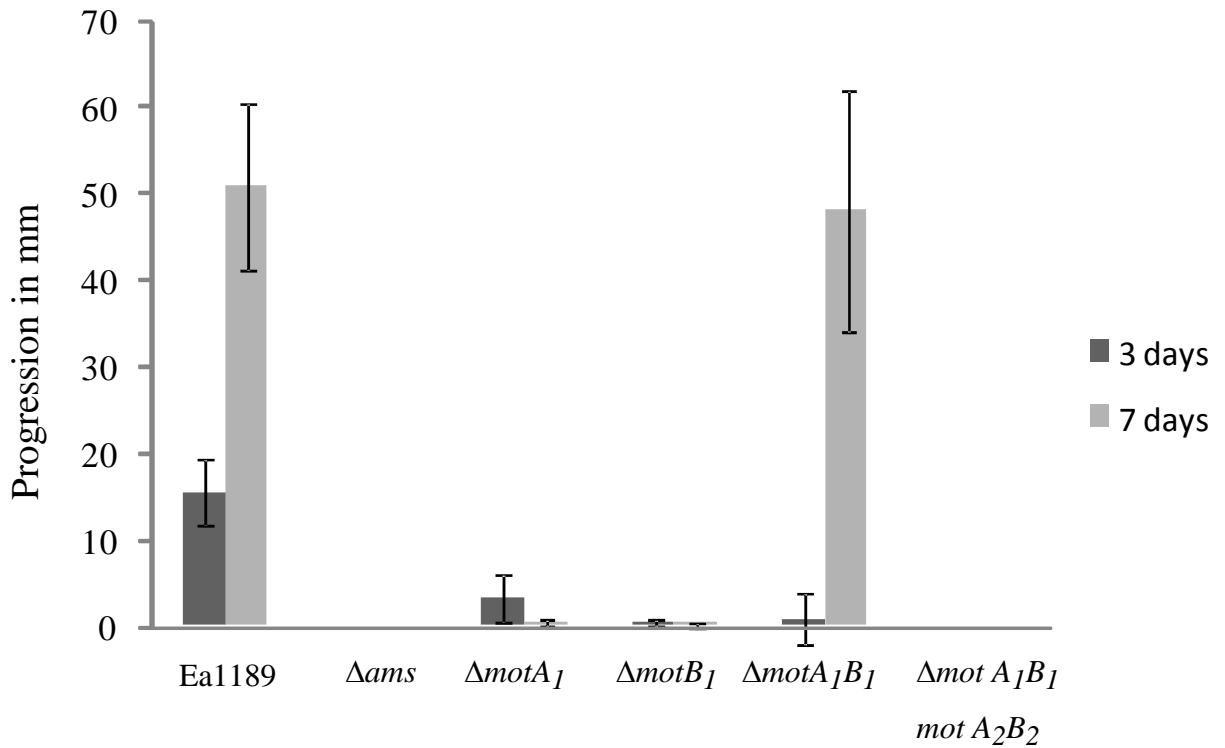


Figure 4-7. Disease progression of Ea1189 and flagellar stator mutants in apple, 3 and 7 dpi. Progression, measured in mm, was the length of visible necrosis in vascular tissue. Destructive sampling allowed for variance between 3 and 7 dpi.



LITERATURE CITED

LITERATURE CITED

1. Bellemann, P., Bereswill, S., Berger, S., and Geider, K. 1994. Visualization of capsule formation by *Erwinia amylovora* and assays to determine amylovoran synthesis. *Int. J. Biol. Macromol.* 16: 290-296.
2. Berg, H.C. 2003. The rotary motor of bacterial flagella. *Annu. Rev. Biochem.* 72: 19-51.
3. Bogs, J., and Geider, K. 2000. Molecular analysis of sucrose metabolism of *Erwinia amylovora* and influence on bacterial virulence. *J. Bacteriol.* 182: 5351-5358
4. Burse, A., Weingar, H., and Ullrich, M.S. 2004. NorM, an *Erwinia amylovora* multidrug efflux pump involved in *in vitro* competition with other epiphytic bacteria. *Appl. Environ. Microbiol.* 70: 693-703.
5. Cesbron, S., Paulin, J.P., Tharaud, M., Barny, M.A., and Brisset, M.N. 2006. The alternative σ factor *hrpL* negatively modulates the flagellar system in the phytopathogenic bacterium *Erwinia amylovora* under *hrp* inducing conditions. *FEMS Microbiol. Lett.* 257: 221-227.
6. Davey M.E., and O'Toole, G.A. 2000. Microbial biofilms: from ecology to molecular genetics. *Microbiol. Mol. Biol. Rev.* 64: 847-867.
7. DeRosier, D.M. 1998. The turn of the screw: the bacterial flagellar motor. *Cell* 93: 17-20.
8. Dolan, R.M. 2002. Biofilms: microbial life on surfaces. *Em. Infect. Dis.* 8: 881-90.
9. Drake, D., and Montie, T.C. 1988. Flagella, motility and invasive virulence of *Pseudomonas aeruginosa*. *J. Gen. Microbiol.* 134: 43-52.
10. Garza, A.G., Biran, R., Wohlschlegel, J.A., and Manson, M.D. 1996. Mutations in *motB* suppressible by changes in stator or rotor components of the bacterial motor. *J. Mol. Biol.* 258: 270-285.
11. Hosking, E.R., Vogt, C., Bakker, E.P., and Manson, M.D. 2006. The *Escherichia coli* MotAB proton channel unplugged. *J. Mol. Biol.* 364: 921-937.
12. Hossain, M.M., and Tsuyumu, S. 2006. Flagella-mediated motility is required for biofilm formation by *Erwinia carotovora* subsp. *carotovora*. *J. Gen. Plant Pathol.* 72: 34-39.
13. Kim, T., Young, B. M., and Young, G.M. 2008. Effect of flagellar mutations on *Yersinia enterocolitica* biofilm formation. *Appl. Environ. Microbiol.* 74: 5466-5474.

14. Ko, M., and Park, C. 2000. Two novel flagellar components and H-NS are involved in the motor function of *Escherichia coli*. *J. Mol. Biol.* 303: 371-382.
15. Koczan, J.M., McGrath, M.J., Zhao, Y., and Sundin, G.W. 2009. Contribution of *Erwinia amylovora* exopolysaccharides amylovoran and levan to biofilm formation: implications in pathogenicity. *Phytopathology* 99: 1237-44.
16. Macnab, R.M., and Aizawa, S.I. 1984. Bacterial motility and the bacterial flagellar motor. *Annu. Rev. Bioeng.* 13: 51-89.
17. Merino, M., Shaw, J.G., and Tomas, J.M. 2006. Bacterial lateral flagella: an inducible flagella system. *FEMS Microbiol. Lett.* 263: 127-135.
18. Morehouse, K.A., Hobley, L., Capeness, M., and Sockett, R.E. 2001. Three *motAB* stator gene products in *Bdellovibrio bacteriovorus* contribute to motility of a single flagellum during predatory and prey-independent growth. *J. Bacteriol.* 193: 932-943.
19. Norelli, J.L., Jones, A.L., and Aldwinkle, H.S. 2003. Fire blight management in the twenty-first century. *Plant Disease* 87: 756-765.
20. O'Toole, G., Pratt, L., Watnick, P., Newman, D., Weaver, V., and Kolter, R. 1999. Genetic approaches to study of biofilms. *Methods Enzymol.* 310: 91-107.
21. Oh, C.S., Kim, J.F., and Beer, S.V. 2005. The Hrp pathogenicity island of *Erwinia amylovora* and identification of three novel genes required for systemic infection. *Mol. Plant Pathol.* 6: 125-138.
22. Paulick, A., Koerdt, A., Lassak, J., Huntley, S., Wilms, I., Narberhaus, F., and Thormann, K.M. 2009. Two different stator systems drive a single polar flagellum in *Shewanella oneidensis* MR-1. *Mol. Microbiol.* 71: 836-850.
23. Pratt, L.A., and Kolter, R. 1998. Genetic analysis of *Escherichia coli* biofilm formation: roles of flagella, motility, chemotaxis and type I pili. *Mol. Microbiol.* 30: 285-293.
24. Ramey, B.E., Koutsoudis, M., von Bodman, S.B., and Fuqua, C. 2004. Biofilm formation in plant-microbe associations. *Curr. Opin. Microbiol.* 7: 602-609.
25. Raymundo, A.K. and Ries, S.M. 1981. Motility of *Erwinia amylovora*. *Phytopathology* 71: 45-49.
26. Sutherland, I.W. 2001. Biofilm exopolysaccharides: a strong and sticky framework. *Microbiology* 147:3-9.
27. Tang, H., Braun, T.F., and Blair, D.F. 1996. Motility protein complexes in the bacterial flagellar stator. *J. Mol. Biol.* 261: 209-221.

28. Thormann, K.M., and Paulick, A. 2010. Tuning the flagellar motor. *Microbiology* 156: 1275-1283.
29. Toutain, C.M., Caizza, N.C., Zegans, M.E., and O'Toole, G.A. 2007. Roles for flagellar stators in biofilm formation by *Pseudomonas aeruginosa*. *Res. Microbiol.* 158: 471-477.
30. Toutain, C.M., Zegans, M.E., and O'Toole, G.A. 2005. Evidence of two flagellar stators and their role in the motility of *Pseudomonas aeruginosa*. *J. Bacteriol.* 187: 771-777.
31. Van Houdt, R., and Michiels, C.W. 2005. Role of bacterial cell surface structures in *Escherichia coli* biofilm formation. *Res. Microbiol.* 156: 626-633.
32. Verstraeten, N., Braeken, K., Debkumari, B., Fauvart, M., Fransaer, J., Vermant, J., and Michiels, J. 2008. Living on a surface: swarming and biofilm formation. *Trends in Microbiol.* 16: 496-506.
33. Wang, D., Korban, S.S., and Zhao, Y. 2010. Molecular signature of differential virulence in natural isolates of *Erwinia amylovora*. *Phytopathology* 100: 192-198.
34. Wang, Q., Suzuki, A., Mariconda, S., Porwollik, S., and Harshey, R.M. 2005. Sensing wetness: a new role for bacterial flagellum. *EMBO J.* 24: 2034-2042.
35. Wood, T.K. 2009. Insights on *Escherichia coli* biofilm formation and inhibition from whole-transcriptome profiling. *Environ. Microbiol.* 11: 1-15.
36. Wood, T.K., Gonzalez Barrios, A.F., Herzberg, M., and Lee, J. 2006. Motility influences biofilm architecture in *Escherichia coli*. *Appl. Microbiol. Biotechnol.* 72: 361-367.
37. Zhao, Y., Blumer, S.E., and Sundin, G.W. 2005. Identification of *Erwinia amylovora* genes induced during infection of immature pear tissue. *J. Bacteriol.* 187: 8088-8103.
38. Zhao, Y., Sundin, G.W., and Wang, D. 2009. Construction and analysis of pathogenicity island deletion mutants of *Erwinia amylovora*. *Can. J. Microbiol.* 55: 457-64.

CONCLUDING REMARKS AND FUTURE DIRECTIONS:

Summary of work

The fire blight pathogen *Erwinia amylovora* is capable of rapid systemic movement in host tissue. However, the mechanism behind this movement is poorly understood. Previous research indicated that *E. amylovora* mutants deficient in the EPS amylovoran are unable to move past the site of inoculation (3). Additionally, the movement of several mutants deleted in virulence factors, such as the production of the EPS levan, is delayed (3). In other vascular pathogens, biofilm formation correlates with the movement of the pathogen. For example, *P. stewartii* strains that are deficient in biofilm formation are significantly reduced in movement from the site of inoculation in susceptible sweet corn (8). A mutation in an adhesin-like protein in *X. oryzae* caused reduction in biofilm formation, and reduced in movement to or growth within xylem vessels (4).

The work presented here demonstrates that *E. amylovora* is capable of biofilm formation (chapter 2). Using deletion mutants in the EPSs amylovoran and levan, I was able to demonstrate a correlation between virulence and biofilm production. Mutants deficient in either EPS exhibited significant reductions in *in vitro* biofilm formation. Initial experiments from chapter 2 indicated that amylovoran deficient mutants are unable to undergo biofilm formation. Results from the time course assay in chapter 4, which examined biofilm over earlier and more frequent time points, indicated that amylovoran deficient cells are still able to attach to surfaces but never able to develop into mature biofilms. Together, these results suggest that in biofilm formation, amylovoran functions in the development of micro-and macrocolonies on a surface. The functional characterization of amylovoran in pathogenicity is more complex. It is well

known amylovoran mutants do not move past the site of inoculation. However, it is difficult to determine if systemic movement is arrested by a lack of biofilm formation or if amylovoran-deficient cells are more susceptible to host defenses.

Bacterial cells deficient in levan production produced significantly reduced biofilms compared to the wild type. Closer examinations of the levan mutants showed bacterial colonies were unable to establish large aggregates. The role in virulence for levan is mostly undefined. It has been suggested that levan provides additional protection from host defenses (7), which is also the primary suspected function of amylovoran. Interestingly, those mutants, known to be delayed in virulence, were found growing primarily in the intercellular space of apple leaves using SEM imaging; few cells could be found in the xylem and never in characteristic biofilm formation fashion. This implies that levan may function in the development of macrocolonies, which ultimately may be needed for the entry of the pathogen into xylem tissue.

To further demonstrate the importance of biofilm formation in the systemic movement of the pathogen, I needed to separate the formation of biofilms from EPS production. To do this, I used a genetic approach to identify additional bacterial factors known to contribute to biofilm formation. Chapter 3 addressed the role of bacterial surface structures, including type I fimbriae, flagella, type IV pili, and curli, which have been demonstrated to function in the biofilm formation of other pathogens such as *X. fastidiosa* (6) and *D. dadantii* (12). Other than peritrichous flagella, no other surface attachment structures have been identified in *E. amylovora*. Deletions in genes encoding for such structures demonstrated that bacterial surface structures are important in biofilm formation. Additionally, the time course assay separated the function of the structures into reversible and irreversible attachment. Fimbriae seem to be necessary for reversible attachment. Type IV pili are needed for irreversible attachment. Under

both situations attachment is necessary for mature biofilm formation. Virulence assays in immature pear fruit indicate that the type IV pili, or irreversible attachment are needed to establish full virulence. However, in shoot tissue, fimbriae or reversible attachment is important as well. Immature pear fruit and shoot tissue are very different tissue types. It is possible that the different stages of biofilm formation contribute differently to the spread of disease in the various tissue types. Alternatively, additional bacterial factors that contribute to biofilm formation suggest redundant functionality. Interestingly, in shoots inoculated with structure deficient mutants which display reduced virulence, bacterial cells were mostly not found within the xylem tissue. These results further implicate the importance of biofilm formation in the movement of the pathogen to the xylem.

Flagella have been suggested to function in mediating contact with surfaces and the expansion of biofilms (9). In chapter 3, I generated deletion mutants in two of the four gene clusters encoding for flagellar production and function. Deletion of one of them demonstrated no significant change in biofilm formation, nor any change in virulence. The deletion of a different cluster produced cells that were reduced in biofilm formation and reduced in their capability to cause disease in shoots. A time course attachment assay could not identify a specific function in reversible or irreversible attachment, indicating that the function of the flagella may be as previously speculated: mediating surface contact and expansion. A lack of clarity in function, or even a role in biofilm formation for the other gene cluster could be attributed to redundancy of function among the clusters.

In *P. aeruginosa* it has been demonstrated that functional flagellar stators are necessary for bacterial motility and biofilm formation (11). In *E. amylovora*, I identified two sets of flagellar motor stators necessary for flagellar driven motility. I generated deletion mutants in

single genes, and in one and both sets of motor stators. Not unexpectedly, mutants that altered the ratio of stator protein production eliminated motility of the pathogen. However, deletion of a single set of stators only reduced motility. A correlation between motility and virulence in shoots can be made: cells that are nonmotile are nonpathogenic in shoot tissue and cells that retain partial motility are reduced in virulence at early time points. In pear tissue, similar correlations can be seen, except only the deletion mutant in both sets of stators is nonpathogenic. Additionally, when deleted in single genes or in one stator set, mutants are reduced in biofilm formation. In a time course attachment assay, with the addition of ficoll to slow motility of the wild type, it appears that motility is needed for initial biofilm formation. It is possible this is because cells altered in motility are not able to mediate contact with the surface. Interestingly, mutants deleted in both stator sets exhibit increased biofilm formation, even at early time points. However, based on similar results seen *P. aeruginosa* these results are to be expected (11). Additional results from later time points indicate that motility may be needed for the release of cells to form new biofilms.

The goal of research presented here was to examine the role of biofilm formation in the systemic movement of *E. amylovora*. I identified several factors involved in the formation of biofilms. Ultimately, these results indicate that biofilm formation is important in systemic movement, but some stages are more dispensable than others. For instance, initial attachment is needed by the pathogen for entry into the vascular tissue. Additionally the formation of macrocolonies, with the help of levan, is also needed for the pathogen to localize to the xylem. Overall, my results suggest that biofilm formation is needed for rapid, systemic movement of the pathogen.

Future directions

Biofilm formation contributes to the systemic movement of *E. amylovora* in apple. Work presented here identified a number of factors involved in the biofilm formation process. However, even with the deletion of these factors, biofilm formation was never entirely eliminated. Moreover, only in the case of amylovoran is disease abolished. This suggests that factors that contribute to biofilm formation may function in a redundant or additive fashion. Alternatively, regulatory triggers that mediate the transition between biofilm formation stages could be critical. In addition, work presented here only examined biofilm formation of *E. amylovora* in a susceptible cultivar of apple. It is probable that there is variation among cultivars, specifically more resistant varieties, that inhibits pathogen biofilm formation, either chemically or anatomically.

Biofilm formation has been shown to be an integral process for many pathogenic bacteria. Identifying additional factors that contribute to biofilm formation, as well as generating mutants that are deleted in multiple factors could completely abolish biofilm formation and disease. In chapter 4, I identified two sets of flagellar stators. However, I was unable to determine if the stators have redundant functionality. Making deletions in the other set of individual stators, and cross-complementing the stators could determine if the stators function redundantly. Additionally, a search of the sequence of the *E. amylovora* genome revealed several genes that have the potential to act in a redundant fashion with attachment structures presented in chapter 3. Additional mutational studies examining single and multiple gene deletions encoding for homologous genes could resolve if bacterial surface factors such as type I fimbriae have multiple gene clusters that encode for redundant function. However, if biofilm

formation factors act in an additive fashion, a slightly different approach to mutational studies is needed. Deletion mutants in differing biofilm factors will need to be generated and evaluated.

Alternatively, it may not be the stages of biofilm formation that are integral for pathogenicity, but the transition between each stage. Though those factors are largely unknown, it is speculated that environmental signals, including pH, temperature and moisture, population density, or mineral and nutrient availability could act as switches. Interestingly, iron acts as a critical signal to trigger macrocolony formation in *P. aeruginosa* (2). In that study, deletion of siderophores, known for sequestering iron, significantly altered biofilm formation. *E. amylovora* produces a siderophore known to be involved in virulence (5). It is possible that this factor could assist in regulation of biofilm formation. By eliminating transition signals, there is the potential to halt the systemic movement of the pathogen.

A number of groups have identified host defense responses that have the potential to halt disease. However, all have identified host defenses that are overcome by the pathogen. Despite this, the existence of more resistant cultivars suggests that some varieties of apple can defend against the fire blight pathogen. If *E. amylovora* uses biofilm formation in systemic movement, it is possible that resistant hosts prevent the establishment of biofilm formation. Interestingly, the blocking of iron availability using lactoferrin, which is produced by the human innate immune system to chelate iron, restricts biofilm formation by *P. aeruginosa* (10). The production of lactoferrin suggests that host innate immune systems may already have some level of protection against biofilm formation. Perhaps resistant fire blight hosts have the potential to produce secretions that could inhibit biofilm formation.

Alternatively, more resistant trees could simply be anatomically different enough to prevent the progression of disease. Host resistance to *X. fastidiosa* can be attributed to differences in size of the pitted vessels within the xylem tissue (1). In apple, the application of Apogee®, a shoot growth regulator, thickens xylem cell walls of the susceptible varieties (appendix). Results from this study suggest that this can inhibit the pathogen from entering vascular tissue. It is possible that more resistant trees have slight differences in host anatomy that prevents the invasion of the pathogen.

Ultimately, disruption of *E. amylovora* biofilm formation has the potential to provide a novel method of control, whether it is through disruption of various stages of biofilm formation, or fine tuning host defenses to prevent biofilm formation.

LITERATURE CITED

LITERATURE CITED:

1. Alves, E. Marucci, C.R., Lopes, J.R.S., and Leite, B. 2004. Leaf symptom on plum, coffee and citrus and the relationship with the extent of xylem vessels colonized by *Xylella fastidiosa*. J. Phytopathol. 152: 291-297.
2. Banin, E., Vasil, M.L., and Greenberg, E.P. 2005. Iron and *Pseudomonas aeruginosa* biofilm formation. Proc. Natl. Sci. Acad. USA 102: 11076-11081.
3. Bogs, J., Richter, K., Kim, W.S., Jock, S., and Geider, K. 2004. Alternative methods to describe virulence of *Erwinia amylovora* and host-plant resistance against fireblight. Plant Pathol. 53: 80-89.
4. Das, A. Rangaraj, N., and Sonti, R.V. 2009. Multiple adhesin-like functions of *Xanthomonas oryzae* pv. *oryzae* are involved in promoting leaf attachment, entry, and virulence on rice. Mol. Plant-Microbe Interact. 22: 73-85.
5. Dellagi, A., Brisset, M.N., Paulin, J.P., and Expert, D. 1998. Dual role of desferrioxamine in *Erwinia amylovora* pathogenicity. Mol. Plant-Microbe Interact. 11: 734-742.
6. Feil, H., Feil, W.S., and Lindow, S.E. 2007. Contribution of fimbrial and afimbrial adhesins of *Xylella fastidiosa* to attachment to surfaces and virulence in grape. Phytopathology 97: 318-324.
7. Geier, G. and Geider, K. 1993. Characterization and influences on virulence of the levansucrase gene from the fire blight pathogen *Erwinia amylovora*. Physiol. Mol. Plant Pathol. 42: 387-404.
8. Koutsoudis, M.D., Tsaltas, D., Minogue, T.D., and von Bodman, S.B. 2006. Quorum-sensing regulation governs bacterial adhesion, biofilm development, and host colonization in *Pantoea stewartii* subspecies *stewartii*. Proc. Natl. Sci. Acad. USA 103: 5983-5988.
9. Pratt, L.A., and Kolter, R. 1998. Genetic analysis of *Escherichia coli* biofilm formation: roles of flagella, motility, chemotaxis and type I pili. Mol. Microbiol. 30: 285-293.
10. Singh, P.K., Parsek, M.R., Greenberg, E.P., and Welsh, M.J. 2002. A component of innate immunity prevents bacterial biofilm development. Nature 417: 552-555.
11. Toutain, C.M., Caizza, N.C., Zegans, M.E., and O'Toole, G.A. 2007. Roles for flagellar stators in biofilm formation by *Pseudomonas aeruginosa*. Res. Microbiol. 158: 471-477.

12. Yap, M.N., Yang, C.H., Barak, J.D., Jahn, C.E., and Charkowski, A.O. 2005. The *Erwinia chrysanthemi* type III secretion system is required for multicellular behavior. *J. Bacteriol.* 187: 639-648.

APPENDICES

Appendix 1: Investigating mechanisms of fire blight control by prohexadione-calcium.

This appendix was published as follows: McGrath, M.J, Koczan, J.M., Kennelly, M.M., and Sundin, G.W. 2009. Investigating mechanisms of fire blight control by prohexadione-calcium. *Phytopathology* 99: 591-596.

ABSTRACT

Mechanisms of fire blight control by the shoot-growth regulator prohexadione-calcium (ProCa) were investigated by comparing disease development in ProCa-treated potted apple trees (cv. Gala) to paclobutrazol (another shoot-growth regulator)-treated and nontreated trees and in ProCa-treated cv. McIntosh trees in the field. Twenty-eight days after inoculation with *Erwinia amylovora* Ea110, disease incidence on ProCa and paclobutrazol-treated shoots was significantly reduced compared with that on nontreated shoots. Disease severity (percent shoot length infected) was also significantly lower on both ProCa- and paclobutrazol-treated shoots than on nontreated shoots. However, bacterial populations within inoculated shoots were high and bacterial growth occurred in all treatments. In addition, the mean cell wall width of the cortical parenchyma midvein tissue of the first and second youngest unfolded leaves of ProCa and paclobutrazol-treated shoots was significantly wider both 0.5 and 2 cm from the leaf tips compared with the cell walls of the nontreated tissue. Taken together, these results suggest that reduction of fire blight symptoms by ProCa and paclobutrazol is not the result of reduced populations of *E. amylovora* in shoots. Moreover, because paclobutrazol also reduced disease severity and incidence, changes in flavonoid metabolism induced by ProCa but not paclobutrazol

does not appear to be responsible for disease control as suggested in recent literature. Finally, although this study did not directly link disease control to the observed cell wall changes, the possibility that an increase in cell wall width impedes the spread of *E. amylovora* should be investigated in more depth.

INTRODUCTION

Fire blight, caused by the bacterium *Erwinia amylovora*, is a destructive and economically important disease of apple and pear. There are several distinct phases of the disease, including blossom blight, shoot blight, and rootstock blight (21). The diversity of susceptible host tissues, combined with the limited number of management tools available to control the disease, has made it difficult to stop or slow the progress of fire blight epidemics. Streptomycin has been the primary material for the effective control of blossom blight but resistance to streptomycin occurs widely in the western United States and has developed in some regions of Michigan (2, 14, 16, 18). The blossom blight phase of fire blight is initiated in the spring following the epiphytic colonization of blossom stigmas (10, 32). Surface-associated populations of *E. amylovora* on blossoms remain the only effective target for control attempts utilizing bactericides (25). Alternative blossom blight control materials such as the antibiotic oxytetracycline or biological control agents, including Serenade MAX, BlightBan A506, and Bloomtime E325, are typically less effective than streptomycin (18, 31).

After bloom, blossom blight infections and active limb cankers provide the inoculum for shoot blight infections, which are most severe on actively growing shoots. Succulent new growth is vulnerable to damage during storms, especially those with wind driven rain (17). Wounding is an important predisposition factor for fire blight infection (1, 4), and trauma events such as wind or hail storms not only wound trees but also introduce *E. amylovora* cells to internal tissues. These internalized populations are not affected by streptomycin unless applications are made optimally within 4 to 6 h of the trauma event (22, 33). Antibiotics are not recommended for shoot blight control due to antibiotic resistance concerns (11). Thus, the lack of tools available

for shoot blight management is a critical limiting factor in overall fire blight management, and alternate tools for shoot blight management would be beneficial for growers.

A number of chemicals have been developed to regulate growth in apple (24), including prohexadione-calcium (ProCa) (6). ProCa is a plant growth regulator that acts as a structural mimic of 2-oxoglutaric acid and inhibits late steps of gibberellin biosynthesis, resulting in reduced shoot growth (6, 26). In addition to growth control, ProCa has been observed to reduce the incidence of shoot blight in apple (19–21, 34) and pear (3). ProCa reduced both disease incidence and severity on inoculated shoots and secondary spread from the inoculated shoots to noninoculated shoots (7).

The mechanism by which ProCa reduces fire blight infection is unknown, although there is a correlation between disease control and growth control (21). However, reductions in fire blight have been observed without any concomitant reduction in shoot growth (7). There are many potential mechanisms of control; however, one possible mechanism that has been proposed is that ProCa induces resistance in the host by triggering alternate biosynthetic pathways leading to the production of flavonoid antimicrobial compounds such as luteoflavin and luteoforol (8, 9, 29). Luteoforol is a transiently occurring flavonoid that is not normally produced in rosaceous species but is apparently produced in apple treated with ProCa (8, 27, 29). This compound has been shown to inhibit *E. amylovora* in vitro (29). Another growth regulator, paclobutrazol, blocks earlier steps (compared with ProCa) in the gibberellins biosynthesis pathway, and is not known to induce the production of luteoflavin or luteoforol (8). As a result, if the antimicrobial activity of luteoforol is responsible for the control of shoot blight, reductions in disease incidence and severity would not be expected with the application of paclobutrazol.

Other possible mechanisms for ProCa-mediated fire blight control center on effects related to reductions in tree vigor. For example, the sorbitol content of young, actively growing apple tissue is significantly reduced compared with nongrowing tissue (13), and lower sorbitol content in shoots is associated with increased fire blight susceptibility (30). Another possibility is through the occurrence of anatomical changes in plant tissue associated with reduced growth. Young, expanding shoot tissue is characterized by the formation of protoxylem; as tissue expansion stops, protoxylem is converted to metaxylem elements which contain uniformly thickened cell walls that are more lignified (5). Paclobutrazol has been shown to cause structural changes in the leaf tissue of rape (36), maize (28), and Chinese potato (12). Changes in the cellular anatomy of apple shoot tissue could potentially impede the movement of *E. amylovora* through shoot tissue.

Our overall goal in this study was to investigate the potential mechanism of shoot blight control by ProCa. Our first objective was to compare symptom development and *E. amylovora* population growth in ProCa-, paclobutrazol-, and nontreated trees. Our second objective was to use scanning electron microscopy to compare the width of cell walls from midvein cortical tissue from ProCa-, paclobutrazol-, and nontreated leaves.

MATERIALS AND METHODS

Bacterial strain and growth conditions. The virulent, rifampicin-resistant strain *E. amylovora* Ea 110 (15) was used for all experiments. The bacterium was cultured on Luria-Bertani agar medium amended with rifampicin at 100 g/ml (LB+rif) at 28°C. For inoculations and bacterial enumeration, cells were diluted in 0.5X phosphate buffered saline (PBS).

Plant material. Experiments with potted apple trees were conducted using 2-year-old apple cv. Gala on M-9 rootstock (Hilltop Fruit Trees, Hartford, MI). These trees were potted in 11.3- liter

pots in a 3:1 mixture of Bacto Hi-porosity soil mix (Michigan Peat Company) to field soil. Trees were placed in a Michigan State University (East Lansing, MI) greenhouse and watered and pruned (experiments conducted ~6 weeks after pruning, on actively growing tissue) as necessary until experiments were conducted. Trees selected to study disease development were randomized and placed outside the greenhouse. Trees used for microscopy studies were placed in a growth chamber (12 h of light and 12 h of dark conditions maintained at 25°C). Field experiments were conducted using 26-year-old apple cv. McIntosh trees located in a Michigan State University orchard.

Application of shoot-growth regulators. ProCa (formulated as Apogee, 27.5% a.i. prohexadione calcium, BASF) and paclobutrazol (Cambistat Rainbow Treecare Scientific Advancements, 22.3% a.i. paclobutrazol) were applied to eight potted apple trees on 7 July 2006. The ProCa treatment was applied at 0.9 g of Apogee with 1.2 ml of Regulaid (Kalo Inc.) and 0.9 g of ammonium sulfate per 946.1 ml of water (0.26 mg a.i./ml). Leaves and shoots were sprayed to run-off with this mixture. The paclobutrazol treatment was applied to the soil of each potted tree (basal drench) at 12.5 ml of Cambistat with 0.18 ml of Regulaid and 0.14 g of ammonium sulfate per 137.5 ml of water (21.7 mg a.i./ml). Eight additional trees were left untreated. This was repeated on both 7 July and 7 September 2007 with ProCa and paclobutrazol applied to 10 and 8 trees/treatment, respectively. On 6 November 2007, ProCa and paclobutrazol were applied to four potted apple trees each, with three trees left untreated. These trees were used to generate tissue for microscopy.

ProCa treatments for field experiments were assigned in a completely randomized design, and ProCa was applied to trees to run-off using a handgun sprayer. The high-concentration ProCa treatment was applied to six trees with Apogee at 250 mg/liter on 23 May 2005. The low-

concentration treatment was applied to six trees as a split application, with Apogee at 125 mg/liter applied on 23 May and a second application on 2 June 2005. Regulaid (1.25 ml/liter) and ammonium sulfate (0.9 g/liter) were mixed with Apogee prior to application. Six trees were left untreated.

Bacterial inoculation. Potted apple tree shoots were inoculated with *E. amylovora* Ea110 or 0.5× PBS (control) by cutting 1 cm from the tips of the two newest unfolded leaves on each shoot using a scissors dipped in the bacterial suspension (10^8 CFU/ml) before each cut (scissor-cut inoculation method). Shoots were inoculated on 17 July 2006, 23 July 2007, and 21 September 2007. Following inoculation, plastic bags were placed over shoots and removed the following day.

On 17 June 2005, six randomly selected shoots from each field tree were inoculated with Ea110 (3×10^5 CFU/ml) and six additional shoots/tree were inoculated with a higher concentration of Ea110 (3×10^5 CFU/ml). All shoots were inoculated by the scissor-cut inoculation method.

Disease evaluation and recovery of bacteria from sampled leaves. Shoot length, disease incidence (presence or absence of a shoot lesion), severity (length of lesion/current season's growth \times 100), and conditional severity (assessed by determining severity of diseased shoots only) were assessed over the course of each potted tree experiment.

CFU were determined by destructively sampling 5 randomly chosen shoots/treatment in the first potted tree experiment, 10 shoots/treatment in the final potted tree experiments, and 2 shoots/treatment in the field tree experiments. For each shoot, the inoculated leaf, its petiole, and 2 cm of shoot basal to the petiole were homogenized with a Polytron PT 10-35 blender

(Brinkmann Instruments, Inc.) in 10 ml of chilled 0.5× PBS, and 10-fold serial dilutions were plated on LB+rif+cycloheximide. After 72 h, bacterial populations in inoculated shoots were determined using dilution plating.

Determination of cell wall widths in midvein cortical tissue. On 13, 19, and 27 November 2007, five shoots per treatment were randomly selected and the first, second, and seventh youngest unfolded leaves of each shoot were removed. Leaf sections (1 by 1 cm, bisected by the midvein) 0.5 and 2 cm from each leaf tip were removed and fixed in paraformaldehyde/glutaraldehyde, 2.5% each in 0.1 M sodium cacodylate buffer (Electron Microscopy Sciences, Hatfield, PA) overnight. Tissue was then dehydrated successively in 25, 50, 75, and 90% ethanol for 30 min each, and 100% ethanol three times for 15 min. Samples were subsequently dried with a critical point drier (Balzers CPD, Lichtenstein). One 0.5-mm cross-section of the midvein was removed from the center of each block of tissue and mounted on aluminum mounting stubs (Electron Microscopy Sciences, Hatfield, PA), which were coated with gold using a gold sputter coater (EMSCOPE SC500 Sputter coater, Ashford, Kent, Great Britain). Images were captured using a scanning electron microscope (JEOL 6400V; Japan Electron Optics Laboratories) with a LaB6 emitter (Noran EDS) using analySIS software (Soft Imaging System, GmbH). Fifty random cell-wall measurements per section of the cortical parenchyma were made using analySIS software.

Statistical analysis. In order to conduct statistical analyses, all data sets were assessed for normality and equality of variance. *E. amylovora* population data were log (x + 1) transformed prior to analysis. Differences among treatments in populations (CFU/ shoot) from field experiments were assessed using a one-way analysis of variance (ANOVA) followed by Tukey's multiple comparison test (with $P \leq 0.05$). In the potted tree experiments, differences among

treatments in CFU/shoot, severity, and conditional severity were assessed via the Kruskal-Wallis (nonparametric) ANOVA test followed by the post-hoc Tukey's multiple comparison test.

Disease incidence was compared among treatments using Fisher's exact test. Differences in cell wall width among treatments were assessed via the Kruskal-Wallis ANOVA test followed by the post-hoc Games-Howell multiple comparison test. The Mann-Whitney rank sum test was used to compare shoot length at the beginning and conclusion of all trials for each treatment. All statistical analyses were conducted with SYSTAT (v.12.02.00; SYSTAT Software, Inc., San Jose, CA).

RESULTS

Effect of ProCa on disease development and bacterial populations in potted apple trees.

Potted apple trees were used to compare the effects of the two shoot-growth regulators on disease development. The size of these trees allowed for full coverage of ProCa, which was applied by spray to trees, and for even application of paclobutrazol, which was applied via basal drench to pots containing each tree. In addition, the size of these trees allowed for shoots to be inoculated uniformly and for accurate assessment of incidence and severity over time. Results from the three potted tree trials were consistent; therefore, only the results from the final trial are presented. Mean shoot length increased significantly only in nontreated shoots (4.4 ± 0.7 cm at 0 days postinoculation to 10.4 ± 2.4 cm at 28 days postinoculation). Mean shoot lengths at 28 days postinoculation in ProCa-treated (3.7 ± 1.1 to 5.1 ± 1.4 cm) and paclobutrazol-treated trees (5.1 ± 1.4 to 7.3 ± 1.9 cm) were not significantly different ($P \leq 0.05$) from 0 days postinoculation.

Disease incidence at 28 days postinoculation was significantly reduced on both ProCa- and paclobutrazol-treated shoots compared with nontreated shoots (Fig. A-1A). There were no significant differences in disease incidence between the paclobutrazol-treated shoots and the

ProCa-treated shoots. Disease severity at 14, 21, and 28 days postinoculation was lower on both ProCa- and paclobutrazol- treated shoots compared with nontreated shoots (Fig. A-1B). When conditional severity was assessed, there were no significant differences among treatments at 7, 21, and 28 days postinoculation (Fig. A-1C). Mean *E. amylovora* populations increased after inoculation in shoots of all treatments (Fig. A-2) with no significant differences at 0 or 28 days postinoculation. *E. amylovora* cells were distributed throughout ProCa-, paclobutrazol-, and nontreated shoots as detected by sampling and plating excised tissue (data not shown).

Effect of ProCa on bacterial populations in apple shoots in the field. Shoot-growth regulators are commonly applied to mature trees; therefore, bacterial populations were also assessed on field trees to determine whether results were comparable with potted apple trees. Similar results were obtained when the mature trees treated once with Apogee at 250 mg/liter and twice with Apogee at 125 mg/liter were compared with nontreated trees inoculated with *E. amylovora* at 3×10^5 CFU/ml or 3×10^7 CFU/ml (Fig. A-3A and B) in that, by the third day after inoculation, growth of *E. amylovora* was observed in all treatments and, by the conclusion of the experiment, populations of *E. amylovora* were extremely high in all treatments. In shoots inoculated with 3×10^7 CFU/ml, there were significant differences in subsequent population size only on day 7 (Fig. A-3A). On day 7, the nontreated control shoots had significantly higher populations than shoots treated with high doses of ProCa (Fig. A-3A). In shoots inoculated with 3×10^5 CFU/ml, the shoots treated with Apogee at 250 mg/liter supported slightly lower populations than the untreated shoots (Fig. A-3B), and nontreated control shoots had significantly higher populations than shoots treated with Apogee at 250 mg/liter at two sampling dates.

Determination of cell wall width in midvein cortical tissue. Microscopy was used to assess whether anatomical changes occurred after the application of shoot-growth regulators. At 7, 13, and 21 days after treatment, the mean midvein cell wall width (cortical parenchyma tissue) of the first and second unfolded leaves of ProCa- and paclobutrazol-treated shoots was significantly wider both 0.5 and 2 cm from the leaf tips compared with the cell walls of the nontreated tissue (Fig. A-4 A to C; Table A-1). However, the thickened walls were not uniform across the tissue viewed. The cell wall widths of the seventh leaf at 7 days after application were not significantly different among treatments. At 13 days after treatment, the cell walls (seventh unfolded leaves) of the ProCa- and paclobutrazol-treated shoots were significantly thicker both 0.5 and 2 cm from the leaf tips. At 21 days after treatment, there were no differences among treatments 0.5 cm from the leaf tip but, at 2 cm, the cells walls of the ProCa- and paclobutrazol-treated tissue were thicker than the nontreated cell walls. Finally, the cell walls of the seventh leaves were compared with the first and second unfolded leaves of the nontreated tissue over time. The cell walls of the seventh leaf were significantly thicker than the first and second leaves at both 0.5 and 2 cm from the leaf tip at each sampling date, with the exception of the first leaf at 13 days (after treatment), 2 cm of the leaf tip, where the cell walls did not significantly differ from the seventh leaf.

DISCUSSION

Recent studies have suggested that ProCa triggers the production of flavanoids, not normally found in rosaceous species, that provide antimicrobial activity against *E. amylovora*, and that it is this activity that is the primary mechanism of fire blight control by ProCa (8, 29). Since luteoforol can be neither measured nor extracted from apple tissue due to its high reactivity (8), the results of this study provide strong support against this hypothesis. Although disease

incidence and severity were lowest in the ProCa-treated shoots compared with paclobutrazol- and nontreated shoots, significant reductions in incidence and severity were also found with the paclobutrazol treatment. It is highly unlikely that these reductions are due to luteoforol, because the paclobutrazol treatment is not known to trigger luteoforol production in apple shoots. It is possible that the ProCa treatment induces luteoforol production and the paclobutrazol treatment induces other novel flavanoids that result in disease control. However, this seems unlikely because *E. amylovora* populations were similarly high in ProCa-, paclobutrazol-, and nontreated tissue. Thus, even though luteoforol cannot be directly measured and we did not attempt to compare flavanoid content of ProCa-treated apple shoots, our results suggest that ProCa treatment of apple shoots does not induce the production of chemicals with significant antimicrobial activity against *E. amylovora*.

Although studies detailing reductions in disease incidence and severity after application with ProCa (7, 19, 20, 21, 34) are numerous, these studies did not examine *E. amylovora* population size following inoculation. Moreover, studies examining the phytoalexin-like properties of luteoforol (8, 29) did not assess effects on population size in planta. Examinations of populations of *E. amylovora* pathogenicity mutants in immature pear assays have shown that the mutant strains do not grow following inoculation (35). However, assessments of *E. amylovora* pathogenicity or virulence mutants following inoculations into apple shoots have typically focused on the percentage of blighted shoot, similar to our data presented in Figure A-1B, instead of on reduced population size in shoots. We have determined that populations of an amylovoran-deficient pathogenicity mutant of *E. amylovora* are rapidly reduced over 10⁶-fold compared with a wild-type strain following apple shoot inoculation (J. M. Koczan and G. W. Sundin, *unpublished information*). Thus, the observation of extensive growth following

inoculation and the finding of similar large populations of *E. amylovora* in symptomless shoots treated with growth regulators and symptomatic nontreated tissue was surprising.

These findings led us to investigate the alternate possibility that ProCa treatment would induce anatomical changes in apple tissue that affected fire blight control. One such observed change was the thickening of the cell walls of the midvein in the treated tissue of the youngest unfolded leaves compared with nontreated tissue. It is possible that these thickened cell walls of the parenchyma serve as a physical barrier that *E. amylovora* must breach in order to enter the xylem from interveinal tissue. The systemic migration of *E. amylovora* in plants is dependent in part upon a functional type III secretion system (23), and we hypothesize that the pathogen is incapable of successful interaction with host cells that have thickened cell walls.

Interestingly, it was also found that the mature seventh unfolded leaves of the nontreated tissue tended to have thicker cell walls than the first and second leaves. Often, the youngest leaves are more susceptible to fire blight infection (4, 30). In our preliminary studies, inoculations of the sixth leaf and beyond did not lead to shoot infections in mature apple tree cvs. Fuji and Gala (data not shown). Suleman and Steiner (30) found that sorbitol concentrations increased and solute potentials decreased with apple leaf age. They speculated that this helps maintain the turgidity of the host cells because the solute potential of *E. amylovora* in the intercellular spaces needs to be more negative than the surrounding cells of the host for plasmolysis to occur.

The reduced susceptibility of older leaves may be due to increased cell wall thickness, increased solute potential, or other physiological changes as the leaf matures and shoot elongation ceases. The inhibition of gibberellin biosynthesis and shoot elongation by ProCa and paclobutrazol may trigger analogous physiological changes leading to similar reductions in susceptibility.

It is evident that migration of *E. amylovora* through leaf tissue, into the leaf midvein, and from leaves into stem tissue needs to be studied in more depth to determine whether cell wall changes impede movement. Our results demonstrated that when *E. amylovora* was (presumably) introduced directly into the xylem by the scissor-cut method, disease incidence was reduced in ProCa-treated compared with nontreated tissue. However, if lesions developed, they continued to expand along the shoot regardless of treatment with ProCa or paclobutrazol. This could be explained if ProCa or paclobutrazol treatment did not lead to a uniform thickening of cell walls in all cases, which would allow sporadic pathogenesis and further casts doubt on the possible induction of antimicrobial substances by ProCa. In order to determine the mechanism of control, a comprehensive study to determine the role that migration (both to the xylem and through the xylem) plays in fire blight disease development is required. In summary, our results have led us to hypothesize that ProCa treatment leads to a decrease in apple shoot infection by *E. amylovora* through an alteration in tree physiology resulting in thickened cell walls in the cortical parenchyma, creating a physical barrier capable of stopping infection and systemic spread of the pathogen. ProCa has become an important tool for fire blight control, especially for apple growers dealing with *E. amylovora* strains that are resistant to streptomycin and in regions where trauma conditions are prevalent. If we are able to understand the mechanism of control by ProCa, it could aid in the development of additional materials for fire blight control.

Table A-1. Effect of prohexadione-calcium and paclobutrazol on the width of cell walls widths of the mid-vein cortical parenchyma tissue of apple cv ‘Gala’.

		Mid-vein cell wall widths (μm) with standard error					
		Location of veinal section from leaf tip					
		0.5 cm			2 cm		
		Sampling date (days after treatment) ^a					
Leaf ^b	Treatment ^c	7 d	13 d	21 d	7 d	13 d	21 d
1 st	Non-trt	0.90 \pm 0.10 a ^d	1.17 \pm 0.11 a	1.29 \pm 0.12 a	1.64 \pm 0.11 a	2.04 \pm 0.16 a	1.65 \pm 0.09 a
	ProCa	1.67 \pm 0.07 b	2.36 \pm 0.07 b	1.81 \pm 0.11 b	2.26 \pm 0.30 b	2.97 \pm 0.18 b	2.35 \pm 0.09 b
	Paclobutrazol	1.18 \pm 0.10 c	1.90 \pm 0.18 c	1.70 \pm 0.19 b	2.57 \pm 0.17 c	2.45 \pm 0.15 c	2.19 \pm 0.18 c
2 nd	Non-trt	0.97 \pm 0.02 a	1.82 \pm 0.12 a	1.35 \pm 0.19 a	1.65 \pm 0.13 a	1.92 \pm 0.03 a	1.75 \pm 0.13 a
	ProCa	1.85 \pm 0.05 b	2.56 \pm 0.08 b	2.22 \pm 0.25 b	1.91 \pm 0.06 b	2.90 \pm 0.06 b	3.13 \pm 0.13 b
	Paclobutrazol	1.53 \pm 0.13 c	2.75 \pm 0.19 c	2.54 \pm 0.13 c	2.07 \pm 0.15 c	2.68 \pm 0.06 c	2.79 \pm 0.20 c
7 th	Non-trt	1.89 \pm 0.03 a	2.04 \pm 0.01 a	2.32 \pm 0.04 a	2.51 \pm 0.05 a	2.22 \pm 0.02 a	2.46 \pm 0.05 a
	ProCa	1.92 \pm 0.08 a	2.49 \pm 0.19 b	2.37 \pm 0.20 a	2.59 \pm 0.06 a	2.82 \pm 0.05 b	2.94 \pm 0.06 b
	Paclobutrazol	1.94 \pm 0.11 a	2.34 \pm 0.17 c	2.44 \pm 0.09 a	2.52 \pm 0.04 a	2.86 \pm 0.11 b	2.93 \pm 0.14 b

Table A-1 (cont'd)

^aTrees were treated on 6 November 2007.

^bThe 1st, 2nd, and 7th newest unfolded leaves were sampled from shoots.

^cProCa was applied at 0.9 g Apogee® with 1.2 ml Regulaid® and 0.9 g ammonium sulfate/946.1 ml water. Paclobutrazol was applied

(basal drench) at 86.0 ml Cambistat® with 1.2 ml Regulaid® and 1.0 g ammonium sulfate/946.1 ml water.

^dMeans among treatments/leaf/sampling date/location from leaf tip were separated using the Kruskal-Wallis test followed by the post-hoc Games-Howell multiple comparison test when $P \leq 0.05$. Different letters indicate significant differences ($P \leq 0.05$).

Figure A-1. Disease incidence on non-treated apple shoots \boxtimes , and shoots treated with prohexadione-Ca \blacksquare , or paclobutrazol \square . Incidence was determined by the presence of a lesion on individual shoots. Different letters indicate statistical differences ($P \leq 0.05$). All shoots were inoculated the virulent strain *Erwinia amylovora* Ea 110 using the scissor dip method.

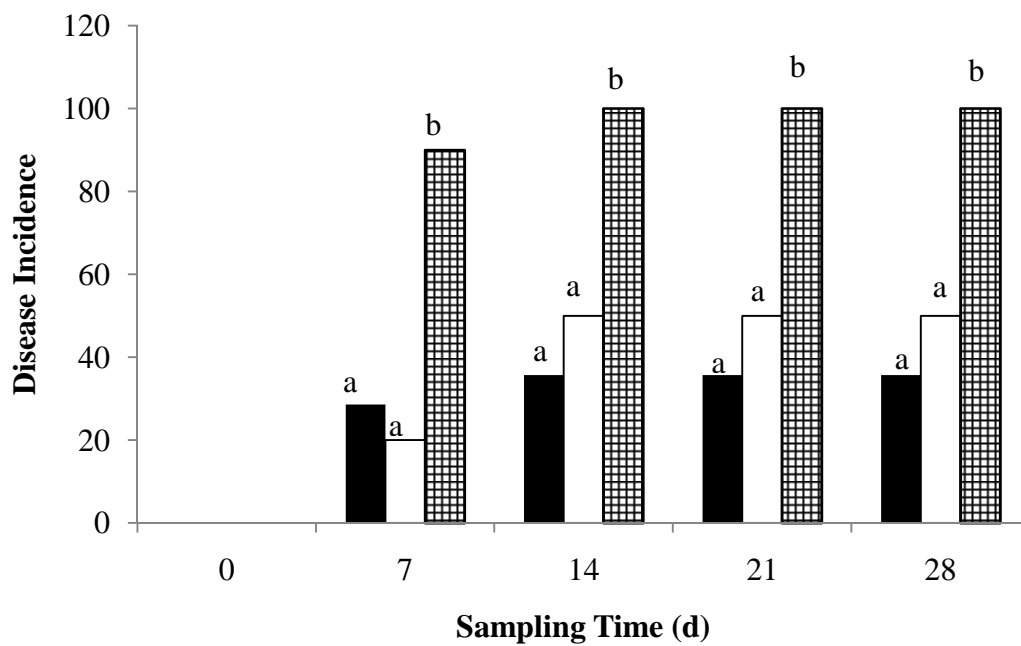


Figure A-2. Disease severity (with S.E.) on non-treated apple shoots , and shoots treated with prohexadione-Ca , or paclobutrazol . Severity was determined by taking the length of lesion/current season's growth x 100. Different letters indicate statistical differences ($P \leq 0.05$). All shoots were inoculated the virulent strain *Erwinia amylovora* Ea 110 using the scissor dip method.

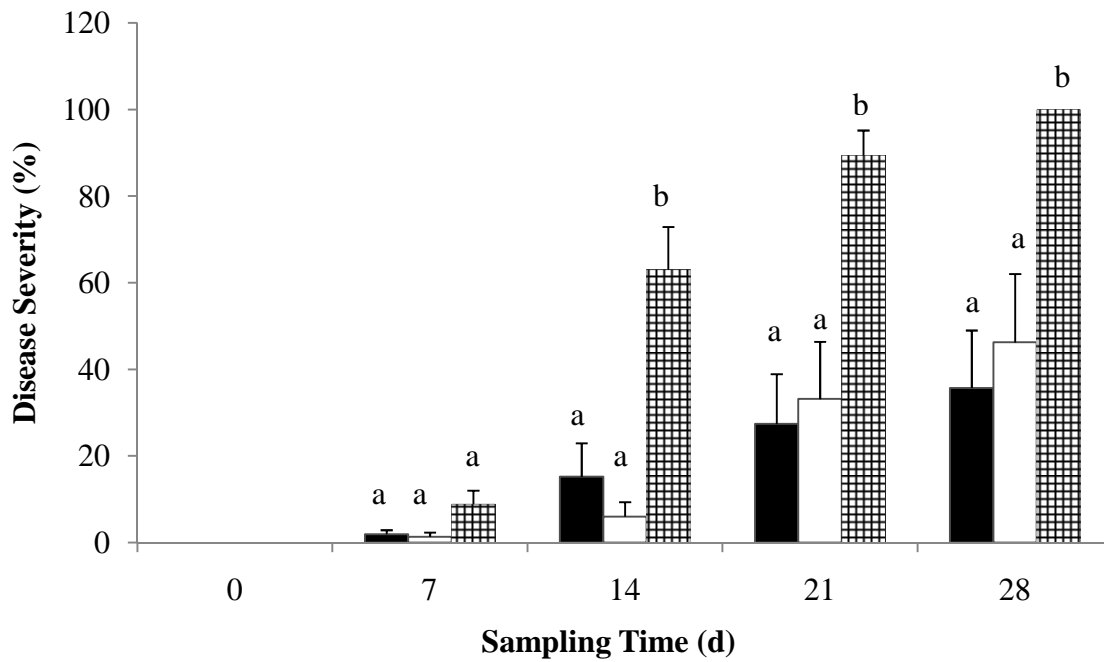


Figure A-3. Conditional severity (with S.E.) on non-treated apple shoots , and shoots treated with prohexadione-Ca , or paclobutrazol . Conditional severity was determined by taking the length of lesion/current season's growth x 100 on diseased shoots only. Different letters indicate statistical differences ($P \leq 0.05$). All shoots were inoculated the virulent strain *Erwinia amylovora* Ea 110 using the scissor dip method.

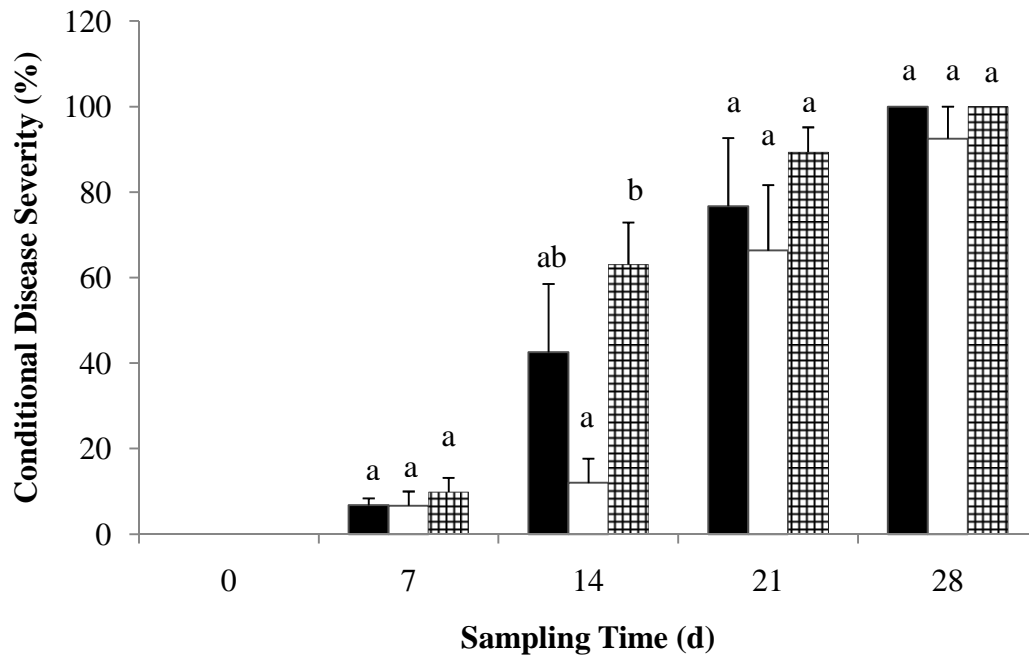


Figure A-4. Mean log (x+1) CFU/shoot (with S.E.) on non-treated apple shoots, and shoots treated with prohexadione-Ca or paclobutrazol at 0 d (initial inoculation) ■, and 28 d □ after inoculation with the virulent strain *Erwinia amylovora* Ea 110 using the scissor dip method. No significant differences ($P \leq 0.05$) among treatments at 0 or 28 d were found.

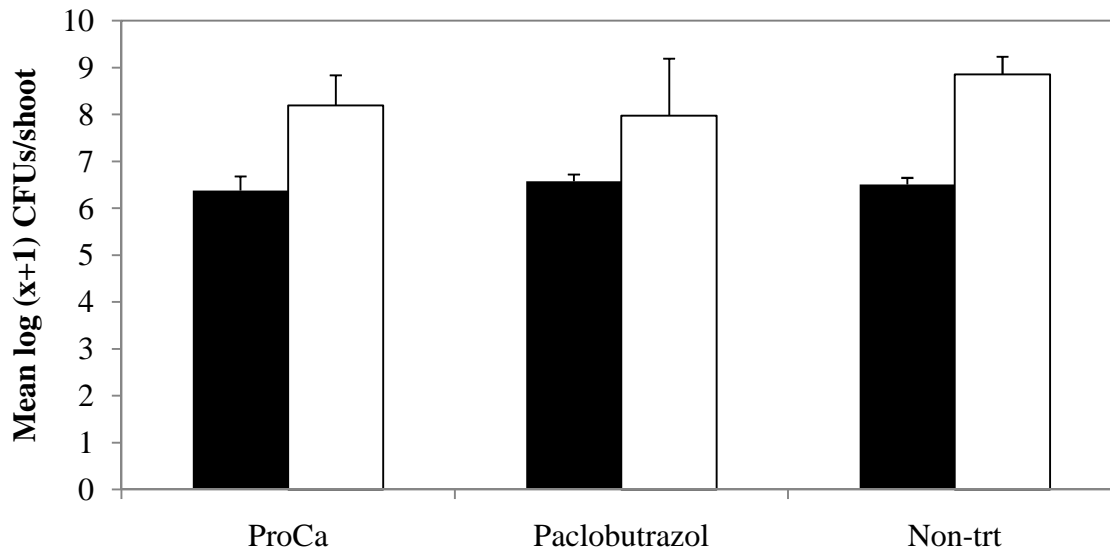


Figure A-5. Mean log CFU/g in shoots of cv. ‘McIntosh’ treated with high doses of ProCa (250 mg/l Apogee®), low doses of ProCa (125 mg/l Apogee® applied twice), or shoots left untreated after inoculation with the virulent strain *Erwinia amylovora* Ea 110. Shoots were inoculated with either 3×10^5 CFU/ml (low Ea) or 3×10^7 CFU/ml (high Ea) using the scissor dip method.

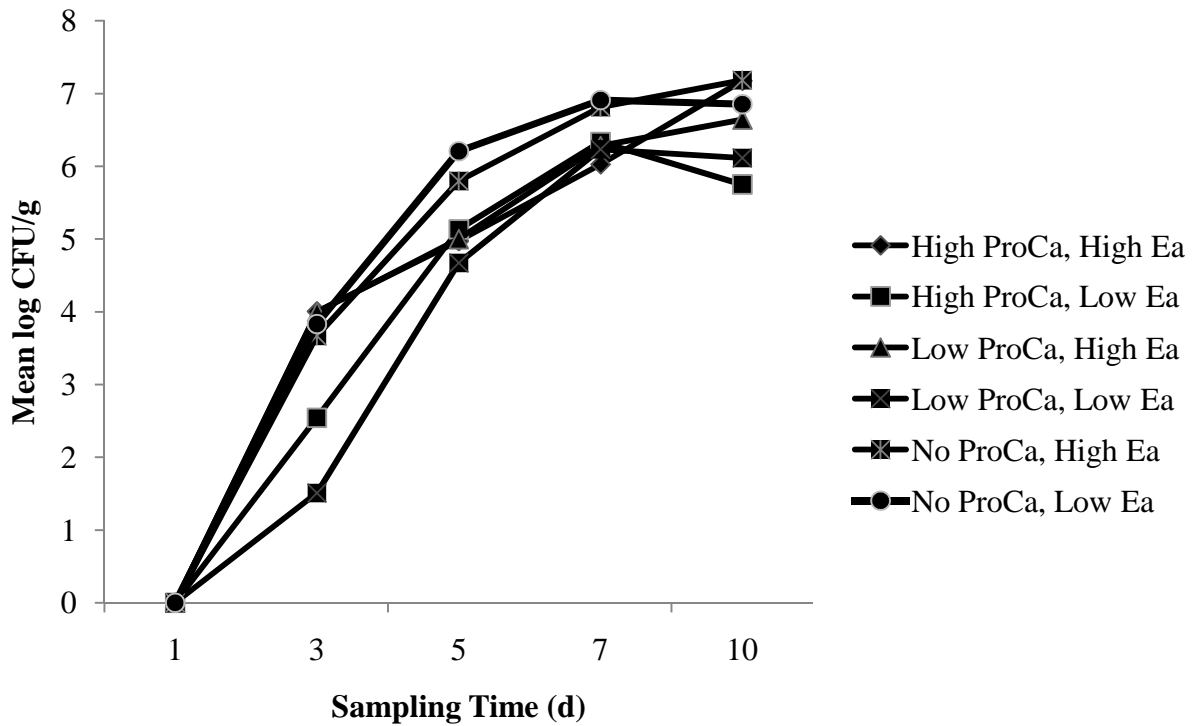
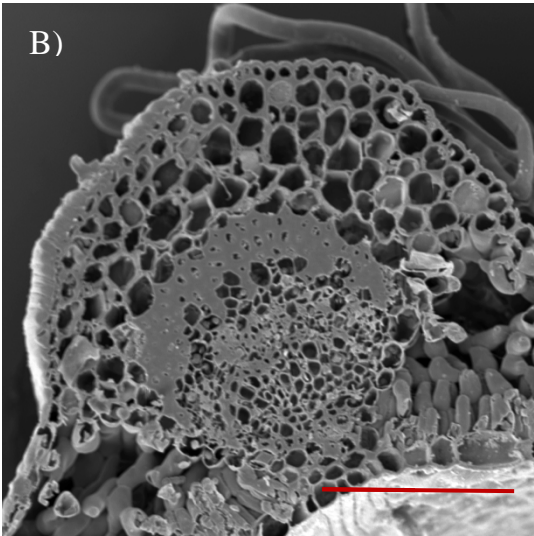
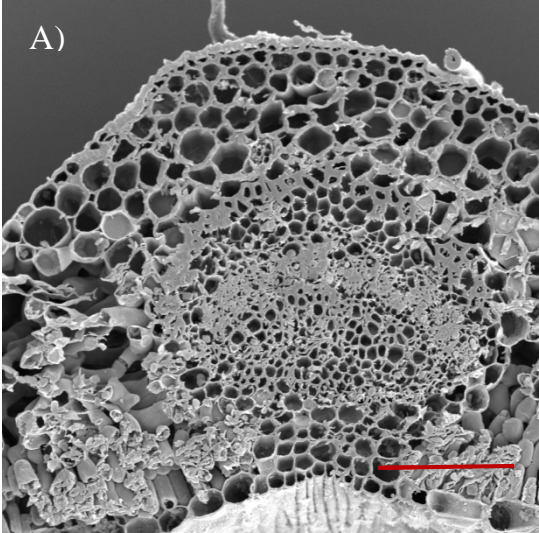


Figure A-6. Apple mid-vein tissue 2 cm from the leaf tip of the 2nd newest unfolded leaves, 13 d after treatment with ProCa (A), paclobutrazol (B), or trees left untreated (C). Scale bars (in red) are 100 μ m in length.

Figure A-6 (cont'd)



LITERATURE CITED

LITERATURE CITED

1. Brooks, A.N. 1926. Studies of the epidemiology and control of fire blight on apple. *Phytopathology* 16: 665-669.
2. Chiou, C.S., and Jones, A.L. 1993. Nucleotide sequence analysis of a transposon (TN5393) carrying streptomycin resistance genes in *Erwinia amylovora* and other gram-negative bacteria. *J. Bacteriol.* 175: 732-740.
3. Costa, G., Andreotti, C., Bucchi, F., Sabatini, E., Bazzi, C., Malaguti, S., and Rademacher, W. 2001. Prohexadione-Ca (Apogee): Growth regulation and reduced fireblight incidence in pear. *HortScience* 36: 931-933.
4. Crosse, J.E., Goodman, R.N., and Shaffer, W.H., Jr. 1972. Leaf damage as a predisposing factor in the infection of apple shoots by *Erwinia amylovora*. *Phytopathology* 62: 176-182.
5. Dickson, W.C. 2000. Integrative plant anatomy. Academic Press, San Diego, CA.
6. Evans, J. R., Evans, R. R., Regusi, C. L., and Rademacher, W. 1999. Mode of action, metabolism, and uptake of BAS 125w, Prohexadione-calcium. *HortScience* 34: 1200-1201.
7. Fernando, W.G.D., and Jones, A.L. 1999. Prohexadione calcium – a tool for reducing secondary fire blight infection. *Acta Horticulturae* 590: 299-307.
8. Halbwirth, H., Kampan, W., Stich, K., Fischer, T.C., Meisel, B., Forkmann, G., and Rademacher, W. 2002. Biochemical and molecular biological investigations with respect to induction of fire blight resistance in apple and pear by transiently altering the flavonoid metabolism with specific enzyme inhibitors. *Acta Horticulturae* 590: 485-492.
9. Halbwirth, H., Martens, S., Wienand, U., Forkmann, G., and Stich, K. 2003. Biochemical formation of anthocyanins in silk tissue of *Zea mays*. *Plant Sci.* 164: 489-495.
10. Hattingh, M.J., Beer, S.V., and Lawson, E.W. 1986. Scanning electron microscopy of apple blossoms colonized by *Erwinia amylovora* and *E. herbicola*. *Phytopathology* 76: 900-904.
11. Jones, A.L. 2001. Challenges of controlling fire blight. *The Compact Fruit Tree* 34: 86-91.
12. Kishorekumar, A., Abdul Jaleel, C., Manivannan, P., Sankar B., Sridharan, R., Somasundaram, R., and Panneerselvam, R. 2006. Differential effects of hexaconazole of Chinese potato (*Solenostemon rotundifolius* Poir., J.K. Morton). *Acta Biol. Szegediensis* 50: 127-129.

13. Li, T., H., and Li, S.H. 2005. Leaf responses of micropropagated apple plants to water stress: nonstructural carbohydrate composition and regulatory role of metabolic enzymes. *Tree Physiol.* 25: 495-504.
14. Loper, J.E., Henkels, M.D., Roberts, R.G., Grove, G.G., Willett, M.J., and Smith, T.J. 1991. Evaluation of streptomycin, oxytetracycline, and copper resistance in *Erwinia amylovora* isolated from pear orchards in Washington State. *Plant Dis.* 75: 287– 90.
15. Maxson-Stein, K., McGhee, G. C., Smith, J. J., Jones, A. L., and Sundin, G. W. 2003. Genetic analysis of a pathogenic *Erwinia* sp. isolated from pear in Japan. *Phytopathology* 93: 1393-1399.
16. McManus, P. S., and Jones, A. L. 1994. Epidemiology and genetic analysis of streptomycin-resistant *Erwinia amylovora* from Michigan and evaluation of oxytetracycline for control. *Phytopathology* 84: 627-633.
17. McManus, P. S., and Jones, A. L. 1994. Role of wind-driven rain, aerosols, and contaminated budwood in incidence and spatial pattern of fire blight in an apple nursery. *Plant Dis.* 78: 1059-1066.
18. McManus, P. S., Stockwell, V. O., Sundin, G. W., and Jones, A. L. 2002. Antibiotic use in agriculture. *Annual Review of Phytopathology* 40: 443-465.
19. Momol, M. T., Ugine, J. D., Norelli, J. L., and Aldwinckle, H. S. 1999. The effect of prohexadione calcium, SAR inducers and calcium on the control of shoot blight caused by *Erwinia amylovora* on apple. *Acta Hort.* 489: 601-605.
20. Norelli, J. L., Jones, A. L., and Aldwinckle, H. S. 2003. Fire blight management in the twenty-first century: using new technologies that enhance host resistance in apple. *Plant Dis.* 87: 756-765.
21. Norelli, J. L., and Miller, S. S. 2004. Effect of prohexadione-calcium dose level on shoot growth and fire blight in young apple trees. *Plant Dis.* 88: 1099-1106.
22. Ockey, S. C., and Thomson, S. V. 2006. Preventing shoot blight of apple with streptomycin applications following simulated hail injury. *Acta Hort.* 704: 211-216.
23. Oh, C. S., and Beer, S. V. 2005. Molecular genetics of *Erwinia amylovora* involved in the development of fire blight. *FEMS Microbiol. Lett.* 253: 185-192.
24. Petracek, P. D., Silverman, F. P., and Greene, D. W. 2003. A history of commercial plant growth regulators in apple production. *HortScience* 38: 937-942.
25. Psallidas, P. G., and Tsiantos, J. 2000. Chemical control of fire blight. Pages 199-234 in: *Fire Blight: The Disease and Its Causative Agent, Erwinia amylovora*. J. L. Vanneste, ed. CABI Publishing, Wallingford, Oxon, UK.

26. Rademacher, W. 2000. Growth retardants: Effects on gibberellin biosynthesis and other metabolic pathways. *Annu. Rev. Plant Physiol. Plant Mol. Biol.* 51: 501-531.
27. Römmelt, S., Treutter, D., Speakman, J. B., and Rademacher, W. 1999. Effects of prohexadione-Ca on the flavonoid metabolism of apple with respect to plant resistance against fire blight. *Acta Hort.* 489: 359-363.
28. Sopher, R. C., Krol, M., Huner, N. P. A., and Fletcher, R. A. 1999. Chloroplastic changes associated with paclobutrazol induced stress protection in maize seedling. *Can. J. Bot.* 77: 1-12.
29. Spinelli, F., Speakman, J., Rademacher, W., Halbwirth, H., Stich, K., and Costa, G. 2005. Luteoforol, a flavan 4-ol, is induced in pome fruits by prohexadione-calcium and shows phytoalexin-like properties against *Erwinia amylovora* and other plant pathogens. *Eur. J. Plant Pathol.* 112: 133-142.
30. Suleman, P., and Steiner, P. W. 1994. Relationship between sorbitol and solute potential in apple shoots relative to fire blight symptom development after infection by *Erwinia amylovora*. *Phytopathology* 84: 1244-1250.
31. Sundin, G. W., Werner, N. A., Yoder, K. S., and Aldwinckle, H. S. 2009. Field evaluation of biological control of fire blight in the eastern United States. *Plant Dis.* 93: 386-394.
32. Thomson, S. V. 1986. The role of the stigma in fire blight infections. *Phytopathology* 76: 476-482.
33. van der Zwet, T., and Keil, H. L. 1972. Importance of pear-tissue injury to infection by *Erwinia amylovora* and control with streptomycin. *Can. J. Microbiol.* 18: 893-900.
34. Yoder, K. S., Miller, S. S., and Byers, R. E. 1999. Suppression of fire blight in apple shoots by prohexadione-calcium following experimental and natural inoculation. *HortScience* 34: 1202-1204.
35. Zhao, Y., Blumer, S. E., and Sundin, G. W. 2005. Identification of *Erwinia amylovora* genes induced during infection of immature pear tissue. *J. Bacteriol.* 187: 8088-8103.
36. Zhou, W. J., Shen, H. C., Xi, H. F., and Ye, Q. F. 1993. Studies on the regulation mechanism of paclobutrazol to the growth of rape plant. *Acta Agric. Zhejiang* 19: 316-320.